AWARD NUMBER: W81XWH-15-1-0347

TITLE: REPOSITIONING ANTIMALARIAL DRUG QUINACRINE TO ENHANCE CARBOPLATIN
SENSITIVITY IN OVARIAN CANCER

PRINCIPAL INVESTIGATOR: VIJI SHRIDHAR, PHD

CONTRACTING ORGANIZATION: MAYO CLINIC

REPORT DATE: NOVEMBER 2019

TYPE OF REPORT: FINAL

PREPARED FOR: U.S. Army Medical Research and Materiel Command
                Fort Detrick, Maryland 21702-5012

REPORT DOCUMENTATION PAGE

Form Approved
OMB No. 0704-0188

Public reporting burden for this collection of information is estimated to average 1 hour per response, including the time for reviewing instructions, searching existing data sources, gathering and maintaining the data needed, and completing and reviewing this collection of information. Send comments regarding this burden estimate or any other aspect of this collection of information, including suggestions for reducing this burden to Department of Defense, Washington Headquarters Services, Directorate for Information Operations and Reports (0704-0188), 1215 Jefferson Davis Highway, Suite 1204, Arlington, VA 22202-4302. Respondents should be aware that notwithstanding any other provision of law, no person shall be subject to any penalty for failing to comply with a collection of information if it does not display a currently valid OMB control number. **PLEASE DO NOT RETURN YOUR FORM TO THE ABOVE ADDRESS.**

1. REPORT DATE Nov 2019	2. REPORT TYPE Final	3. DATES COVERED 08/15/2015 - 08/14/2019

4. TITLE AND SUBTITLE

REPOSITIONING ANTIMALARIAL DRUG QUINACRINE TO ENHANCE CARBOPLATIN SENSITIVITY IN OVARIAN CANCER

5a. CONTRACT NUMBER

5b. GRANT NUMBER
W81XWH-15-1-0347

5c. PROGRAM ELEMENT NUMBER

6. AUTHOR(S)

VIJAYALAKSHMI (VIJI) SHRIDHAR, PHD

E-Mail: Shridhar.vijayalakshmi@mayo.edu

5d. PROJECT NUMBER

5e. TASK NUMBER

5f. WORK UNIT NUMBER

7. PERFORMING ORGANIZATION NAME(S) AND ADDRESS(ES)

MAYO CLINIC
200 1ST STREET SW
ROCHESTER, MN 55905

8. PERFORMING ORGANIZATION REPORT NUMBER

9. SPONSORING / MONITORING AGENCY NAME(S) AND ADDRESS(ES)

U.S. Army Medical Research and Materiel Command
Fort Detrick, Maryland 21702-5012

10. SPONSOR/MONITOR'S ACRONYM(S)

11. SPONSOR/MONITOR'S REPORT NUMBER(S)

12. DISTRIBUTION / AVAILABILITY STATEMENT

Approved for Public Release; Distribution Unlimited

13. SUPPLEMENTARY NOTES

14. ABSTRACT

Based preliminary data and additional data generated by this project, we have determined that the antimalarial drug Quinacrine (QC) reduces cell viability and promotes chemotherapy-induced cell death in an autophagy-dependent manner more extensively in chemoresistant cells compared to their isogenic chemosensitive control cells as quantified by the Chou-Talalay methodology. Overall, our results show for the first time that synergy with QC and carboplatin involves a complex interplay between AV and apoptosis in OVCa cells and is associated with upregulation of INP2, downregulation of p62, and simultaneous upregulation of CTSL only in resistant cells.

15. SUBJECT TERMS

16. SECURITY CLASSIFICATION OF:			17. LIMITATION OF ABSTRACT	18. NUMBER OF PAGES	19a. NAME OF RESPONSIBLE PERSON USAMRMC
a. REPORT Unclassified	**b. ABSTRACT** Unclassified	**c. THIS PAGE** Unclassified	Unclassified		19b. TELEPHONE NUMBER (include area code)

Standard Form 298 (Rev. 8-98)
Prescribed by ANSI Std. Z39.18

Table of Contents

1. **INTRODUCTION:** Resistance to chemotherapy is a contributing factor to mortality associated with ovarian cancer (OVCa). Drugs that synergize with cisplatin/paclitaxel in recurrent tumors will have a potential impact in prolonging the survival of OVCa patients[1]. Currently, designing and discovering new drugs to treat cancer remains a laborious and expensive process. In contrast, "Drug repositioning" is a promising approach, whereby existing FDA-approved drugs are used to treat a different and new disease. *Preliminary studies from my group show that an established anti-malarial drug, Quinacrine (QC) has anti-cancer effects, specifically, against ovarian cancer (OVCa)*. QC, an acridine derivative, is an inexpensive ($30/month) oral drug that was discovered in the 1920s and was initially used widely as an antimalarial drug. With almost a century's worth of experience and safety record, it is extensively studied and recognized as a potential chemotherapeutic agent to treat malignant pleural effusions [2]. **Overall, our results show for the first time that synergy with QC and carboplatin involves a complex interplay between Autophagy (AV) and apoptosis in OVCa cells and is associated with upregulation of TP53INP2, downregulation of p62, and simultaneous upregulation of Cathepsin L (CTSL) only in resistant cells.** *The synergy that we see between QC and carboplatin in resistant cells could be used in clinical treatment to overcome the resistance as well as lower the therapeutic dose, thus avoiding the toxic side effects of carboplatin/paclitaxel in OVCa treatment.*

2. **KEYWORDS:** Quinacrine, P62/SQSTM1-sequestosome, SCID-Severe combined immunodeficiency, LC3-Microtubule associated light chain 3, TEM- Transmission Electron Microscopy, SKOV3/DDP-SKOV3 cisplatin resistant cells, SKOV3TR-Taxol resistant SKOV3 cells, HeyA8MDR-HeyA8 multidrug resistant, PI-Propidium iodide, PARP-Poly ADP Ribose Polymerase, P62-PB1 domain-Phox and Bem1p domain, P62-UBA domain-P62 ubiquitin associated domain, CTSB-Cathepsin B, CTSL-Cathepsin L

3. **OVERALL PROJECT SUMMARY:** Based on the preliminary data presented in the original proposal and continuation of additional data generated proposed in the grant, we determined that the antimalarial drug Quinacrine (QC) reduces cell viability and promotes chemotherapy-induced cell death in an autophagy-dependent manner more extensively in chemoresistant cells compared to their isogenic chemosensitive control cells as quantified by the Chou-Talalay methodology. Our preliminary data, *in vitro* and *in vivo*, indicate that QC induces autophagy by downregulating p62/SQSTM1 to sensitize chemoresistant cells to autophagic-and caspase-mediated cell death in a p53-independent manner. QC promotes autophagosome accumulation and enhances autophagic flux by clearance of p62 in chemoresistant ovarian cancer (OvCa) cell lines to a greater extent compared to their chemosensitive controls. Notably, p62 levels were elevated in chemoresistant OvCa cell lines and knockdown of p62 in these cells resulted in a greater response to QC treatment. Bafilomycin A, an autophagy inhibitor, restored p62 levels and reversed QC-mediated cell death and thus chemosensitization. Importantly, our *in vivo* data shows that QC alone and in combination with carboplatin suppresses tumor growth and ascites in the highly chemoresistant HeyA8MDR OvCa model compared to carboplatin treatment alone. Collectively, our preclinical data suggest that QC in combination with carboplatin can be an effective treatment for patients with chemoresistant OvCa. Overall, our results show for the first time that synergy with QC and carboplatin involves a complex interplay between AV and apoptosis in OVCa cells and is associated with upregulation of INP2, downregulation of p62, and simultaneous upregulation of CTSL only in resistant cells. **The manuscript [3] resulting from this study was published in the journal Oncotarget in 2015 and attached in the Appendix section.**

Hypothesis: Based on our studies, our hypothesis is that *INP2* induced by QC regulates AV and sensitizes chemoresistant cancer cells to cis/carboplatin by downregulating p62 and enhancing AV and cathepsin- and caspase-mediated cell death. We proposed the following Specific Aims to test our hypothesis:

Aim 1: **Determine the contribution of autophagy in sensitizing resistant cells to carboplatin.** We will determine the role of TP53INP2 and p62 in QC-induced AV and define the mechanism by which QC synergizes with carboplatin to sensitize chemoresistant cancer cells.

Aim 2: Identify additional novel or known markers that could contribute towards QC-induced synergy with carboplatin in resistant cells.
In this Aim, we propose to identify additional novel or known markers that may contribute towards QC induced synergy in resistant cells by performing RNA sequencing of all three sensitive and resistant isogenic cell lines with and without QC treatment to mechanistically define the differential transcriptional response.

Aim 3*: **Examine the role of QC in chemoresponse using *in vivo* avatar models.** In this aim, we proposed to examine the role of QC in chemoresistance *in vivo* in preclinical "Avatar model" of ovarian cancer using QC alone and in combination with conventional chemotherapy (carboplatin/paclitaxel) using 3 different chemoresistant avatar models that mimic patient response. Three chemosensitive Avatar models will be used as controls to determine if addition of QC will prolong the duration of response.

ACCOMPLISHMENTS:
Aim 1: **To determine the contribution of autophagy in sensitizing resistant cells to carboplatin.**
 We will determine the role of TP53INP2 and p62 in QC-induced AV and define the mechanism by which QC synergizes with carboplatin to sensitize chemoresistant cancer cells.

Aim 1: <u>Determine the contribution of autophagy in sensitizing resistant cells to carboplatin (Months 1-36).</u>
Autophagy: Depending on the cellular context, autophagy that involves cellular degradation of damaged organelles, long lived proteins and aggregates could play a pro-survival or a pro-death role.[4] Autophagy is also implicated as a factor contributing to the anticancer efficacy of drugs as well as drug resistance.[5] However, the underlying mechanisms that result in apoptosis or survival remain to be determined. This context dependent status of autophagy has clinical implications and needs to be clearly established to understand how the specific status of autophagy can influence tumorigenesis and treatment response.

Role of TP53INP2 in Autophagy Induction: Previous studies have shown that the gene, *TP53INP2* (hereafter referred to as *INP2)* is <u>essential for **induction of autophagy**</u> and upon autophagic induction, the protein product INP2 translocates from the nucleus to autophagosomes where it colocalizes with LC3 and LC3 related proteins and Beclin1[6]. Furthermore, downregulation of *INP2* inhibits autophagy induction most likely through autophagosome formation since this process is also completely inhibited. Surprisingly, our gene expression profiling studies also showed an upregulation of *INP2* by 2.0 and 2.4 fold (p= 4.52×10^{-10} and 5.81×10^{-11}) in OV207 (mutant p53, R273H) and C13* (wild type p53) cancer cell lines, respectively when treated for 6 hrs with 8µM QC compared to untreated controls. Our studies show for the first time in OVCa cell lines that *an essential* autophagy *inducing protein, INP2 is induced very early on by QC treatment.* Although our studies show increased QC-mediated *INP2* expression by Q-PCR, *it is not clear whether INP2 is essential* for *autophagy induction by QC. We are proposing to test this unknown in this proposal.*

Aim 1A : <u>Determine the contribution of TP53INP2 in QC induced autophagy in OVCA cells.</u>
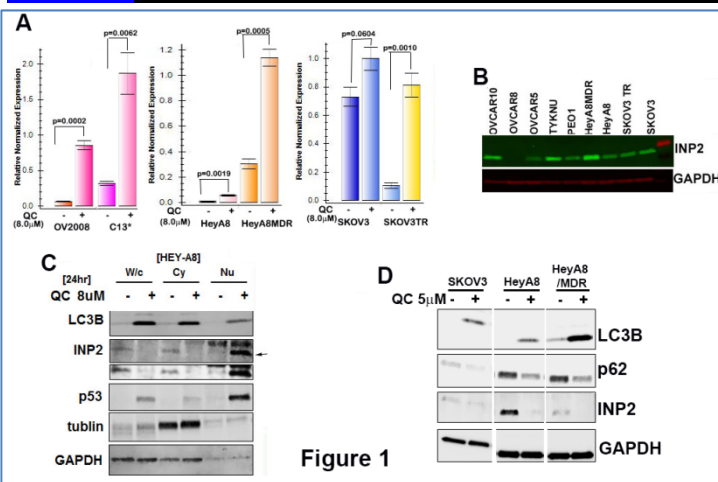

Figure 1

Previous studies have shown that the gene, *TP53INP2* (hereafter referred to as *INP2)* is essential for induction of autophagy**.** Upon autophagic induction, INP2 protein product translocates from the nucleus and interacts with transmembrane protein vacuole membrane protein 1 (VMP1) in the cytoplasm and colocalizes with LC3, LC3 related proteins and Beclin1 in the autophagosomes (47). Furthermore, siRNA mediated downregulation of *INP2* showed that INP2 expression is necessary for autophagosome development. Surprisingly, our gene expression profiling studies also showed an upregulation of *INP2* by 2.0 and 2.4 fold (p= 4.52x10-10 and 5.81x10-11) in OV207 (mutant p53, R273H) and C13* (wild type p53) cancer cell lines, respectively when treated for 6 hrs with 8µM QC compared to untreated controls (Figure 1 A). Our studies show for the first time in OVCa cell lines that *an* AV *inducing protein, INP2 is induced very early on by QC treatment.* Although our studies show increased QC-mediated *INP2* expression by Q-PCR, *it is not clear whether INP2 is essential* for *AV induction by QC to promote cisplatin sensitivity.* Initially, we determined INP2 expression in several ovarian cancer cell lines by western blot analysis as shown in figure 1 B. <u>To determine if INP2 translocates from the nucleus into the cytoplasm upon QC treatment</u>, we did cell fractionation of HeyA8 cells treated with 8µM QC for 24 hrs. In contrast to what we anticipated, we saw a tremendous upregulation of INP2 in the nuclear (Nu) compartment but not in the cytoplasm. Indeed at this time point and QC

concentration, <u>we saw downregulation of INP2 in the cytoplasmic (Cy) compartment as well as in the whole cell lysate (W/c).</u> Coinciding with this downregulation there is an increase in LC3B levels (Figure 1C). This phenomenon was not unique to HeyA8 cells since QC treatment also downregulated INP2 at the protein level in several ovarian cancer cell lines (Panel 3 in Figure 1D with QC treatment). This is in contrast to what we observed at the RNA level (Figure 1A).

These data suggests two things. 1. INP2 may be degraded under QC induced autophagy in the cytoplasm or 2. INP2 has no role in QC induced autophagy since it is downregulated at the protein level upon QC treatment. We surmised that if genetic downregulation of INP2 in C13 and HeyA8MDR cells also show that shRNA downregulated clones also display QC-induced autophagy- this will provide additional evidence of <u>INP2 not playing a role in QC-induced autophagy</u>. To determine if QC- induced downregulation of INP2 protein could be autophagy mediated by QC, we pretreated HeyA8 and HeyA8 MDR cells with Bafilomycin A.

To further understand the role of INP2 in autophagy induction or in chemoresponse, we generated two different shRNA downregulated clones both in C13 and HayA8 MDR cells with non-targeted control shRNA transduced cells (NTC). Efficient downregulation of INP2 expression in sh1 and sh2 cells is shown by western blot analysis in Figures 2A and B-right most panels). We used immunoflourescence analysis to detect AV in the INP2 sh clonal lines As shown in figures 2A and B, to our surprise, we saw significantly more LC3B stating by IFC in INP2 shRNA downregulated clones both in C13 and HeyA8MDR cells at the basal level and even more in these clones upon 10μM QC treatment for 24 hrs compared to NTC cells.

Western blot analysis of C13 and HeyA8MDR shINP2 clones showed that 10μM QC treatment induced autophagy by downregulating p62 (red stars) and upregulating LC3BII (Blue stars) in both the NTC and shRNA downregulated cells in both these cell lines independent of genetic downregulation of INP2 (Figures 2C and D).
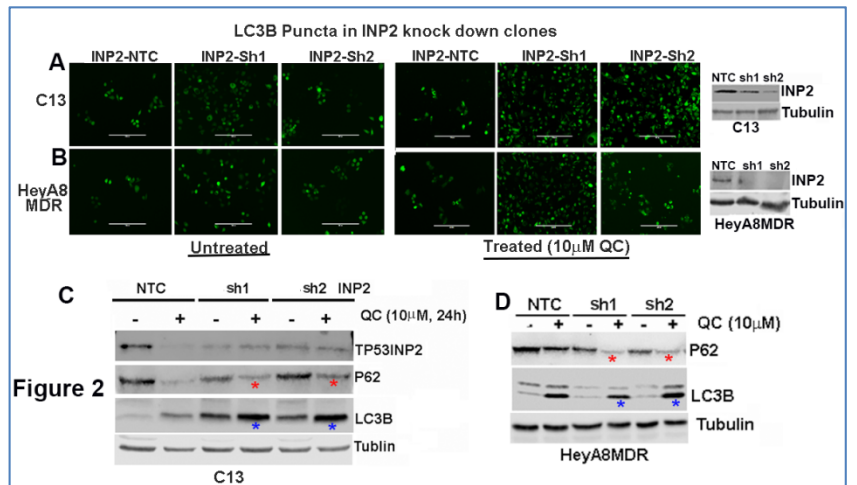
Collectively, these data provide strong support to our current finding that both QC-induced INP2 protein downregulation and genetic downregulation of INP2 followed by QC treatment induces autophagy independent of INP2.
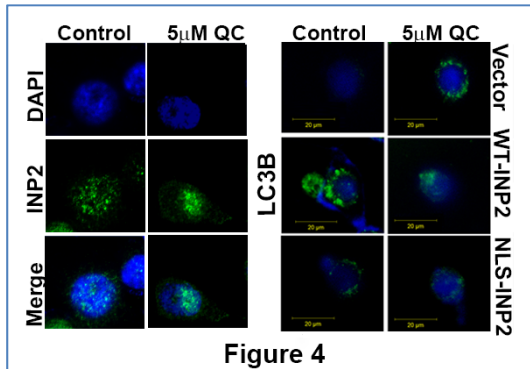

To determine if QC- induced downregulation of INP2 protein could be autophagy mediated by QC, we pretreated HeyA8 and HeyA8 MDR cells with Bafilomycin A. As shown in figure 3 (red stars), pretreatment with Bafilomycin A rescued the expression of INP2 in HeyA8 and HeyA8 MDR cells (Blue stars in figure 3). As we had previously reported Baf A1 treatment also rescued p62 levels and inhibited apoptosis as evidenced by the absence of cleaved PARP.
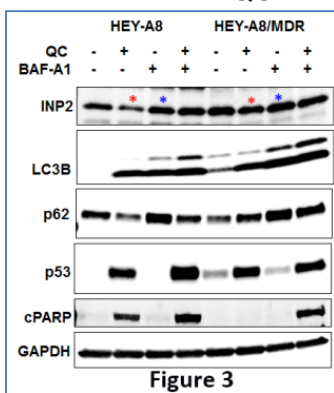
Our cell fractionation experiments in HeyA8 cells treated with 8μM QC for 24 hrs showed <u>a tremendous upregulation of INP2 in the nuclear (Nu) compartment and downregulation of INP2 in the cytoplasm (Figure 2B)</u>. Consistent with this data, our IFC analysis of endogenous INP2 localization upon QC treatment also showed that INP2 is for the most part is located in the nuclear region in the untreated cells and after QC treatment increases INP2 levels are seen shifted to one corner of the nucleus (Figure 4A, middle panel). This is similar to what has been reported as nucleolar cap formation by fibrillar center proteins upstream binding factor (UBF) and fibrillarin (FBL) and indicative of rRNA transcription block [7]. Additional findings from this study indicate that the nucleolar caps represent stalled transcription sites. To understand the mechanism by which QC promotes nuclear upregulation of INP2 to promote autophagy, we transfected WT-INP2 and nuclear export signal mutated INP2 (INP2-NLS) into HeyA8 cells with vector

transfected cells as control and determined the localization of LC3B after treating the cells with 5.0µM QC for 24hrs as shown in figure 4B. While LC3B was solely localized in the cytoplasm of vector transfected, enhanced expression of wildtype INP2 the cytoplasmic LC3B was translocated to the nucleus (Figure 4B, midd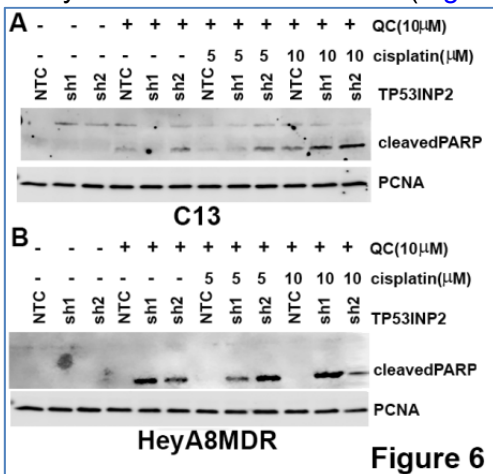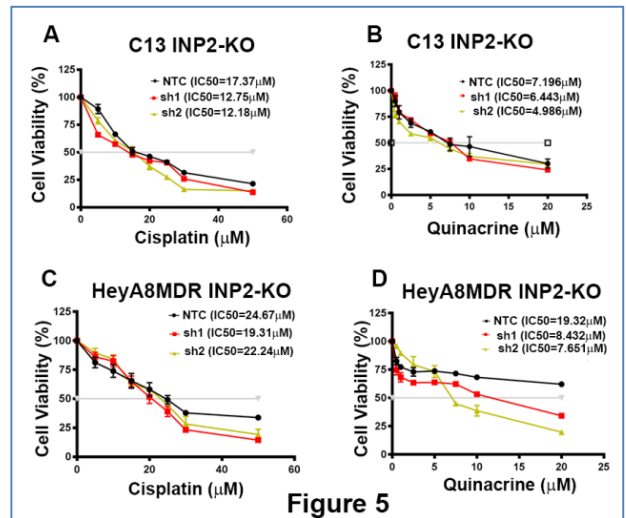le panel) in a manner similar to endogenous INP2 in QC treated parental cells shown in figure 4A. Whether this shift in localization is in the nucleolar region is not currently known. This could be a distinct possibility based on the studies by Xu et al., where the authors have shown that INP2 promotes rDNA transcription and that repression of INP2 rDNA promoter activity and the production of ribosomal RNA (rRNA) and proteins [8]. An alternate possibility is that nuclear INP2 may promote the initiation of autophagy by associating with de-acetylated nuclear LC3B under nutrient deprived (in this context by QC treatment) as shown by Huang and Liu et al in 2015 [9]. Similar results were obtained with NER mutated INP2 transfected cells except the LC3B was evenly distributed in the nucleus as opposed to one corner of the nucleus (Data not shown).

Figure 4

We next asked the question is QC-induced INP2 critical for sensitizing cis/carboplatin-mediated cell death more in the resistant cells? We did MTT based proliferation assays with QC alone and in combination with increasing cisplatin concentration to determine if downregulation of INP2 sensitized C13 and HeyA8MDR cells to drug induced cytotoxicity.

As shown in Figures 5 A-D genetic downregulation of INP2 with shRNAs shifted the IC50 values for both QC and cisplatin. IC50 values for QC for C13 and HeyA8MDR cells were 7.29 to 6.4 and 5.0µM and for HeyA8MDR were 19.3 to 8.47 and 7.6µM for NTC vs sh1 and sh2 cells respectively. However, QC did not modulate cisplatin induced cytotoxicity upon INP2 downregulation. Indeed the IC50 for cisplatin shifted from 17.37 to 12.95 and 12.18 µM for C13 cells and 24.67 to 19.3 and 22.9 µM for Heya8MDR cells respectively suggesting that downregulation of INP2 sensitizes the cells to cisplatin mediated cytotoxicity to a minimal extent.

Figure 5

Under similar conditions, to determine the extent of apoptosis, apoptotic markers- cleaved PARP (and caspase 3 levels-data not shown) were determined by immunoblot analysis in these clonal lines (Figures 6A and B). C13 and HeyA8MDR NTC, INP2sh1 and sh2 cells were treated with 10.0µM QC alone and in combination with 5.0 and or 10µM cisplatin for 24 hrs. Cell lysates were extracted and run on western blots and probed with cleaved PARP and PCNA asa control antibody. While QC alone treatment induced PARP cleavage in the INP2 downregulated clones in the C13 cells more than in the NTC cells the combination of QC with cisplatin was more effective in inducing apoptosis in the shINP2 cells (Figure 6A). In HeyA8MDR cells QC alone was as effective as the combination of QC with cisplatin in the shINP2 cells compared to NTC cells (Figure 6B). These results are consistent with what we observed with our data shown in Figure 5 using MTT assays. Collectively, in contrast to what was expected based on the literature, these data suggest that QC induced cisplatin sensitivity is independent of INP2 in these cells.


Figure 6

Collectively, our data indicate that TP53INP2 does not play a role in QC-induced autophagy and is minimally involved in chemoresponse.

Aim 1B: <u>Determine the role of p62 in QC mediated synergy with carboplatin in chemoresistant OVCA cells.</u>

Role of P62 in sensitizing chemoresistant OVCa to Pt based cytotoxicity: The p62 protein, also called sequestosome 1 (SQSTM1), is an ubiquitin-binding scaffold protein that colocalizes with ubiquitinated protein aggregates and is required both for the formation and the degradation of polyubiquitin-containing bodies by autophagy. P62 binds to LC3B through the LIR (LC3 interacting region) domain and in itself degraded during the autophagic process. Other studies have shown that that the elimination of p62 by autophagy suppresses tumorigenesis[10] in vivo and growth of several human carcinoma cell lines in vitro[11]. Since p62 accumulates when autophagy is inhibited, and decreased levels can be observed when autophagy is induced, p62 may be used as a marker to study autophagic flux. Selective degradation of P62 is physiologically relevant since high levels of P62 in various tumor types are associated with poor prognosis and survival[12]. Studies show that cisplatin resistant OVCa cells SKOV3/DDP express higher levels of P62 and siRNA downregulation of P62 in these cells sensitized these cells to cisplatin mediated cytotoxicity[13].

Based on the preliminary data presented in the original proposal and continuation of additional data generated proposed in the grant, we determined that the QC reduced cell viability and promoted chemotherapy-induced cell death in an autophagy-dependent manner considerably more in chemoresistant cells compared to their isogenic chemosensitive control cells as quantified by the Chou-Talalay methodology. Our preliminary data, *in vitro* and *in vivo*, indicate that QC induces autophagy by downregulating p62/SQSTM1 to sensitize chemoresistant cells to autophagic-and caspase-mediated cell death in a p53-independent manner. QC promoted autophagosome accumulation and enhanced autophagic flux by clearance of p62 in chemoresistant OvCa cell lines to a greater extent compared to their chemosensitive controls. Notably, p62 levels were elevated in chemoresistant OvCa cell lines and knockdown of p62 in these cells resulted in a greater response to QC treatment. Bafilomycin A, an autophagy inhibitor, restored p62 levels and reversed QC-mediated cell death and thus chemosensitization. Importantly, our *in vivo* data shows that QC alone and in combination with carboplatin suppresses tumor growth and ascites in the highly chemoresistant HeyA8MDR OvCa model compared to carboplatin treatment alone. Collectively, our preclinical data suggest that QC in combination with carboplatin can be an effective treatment for patients with chemoresistant OvCa. **The manuscript [3] resulting from this study was published in the journal Oncotarget in 2015 and attached in the Appendix section.**

Based on the publication, we hypothesized that p62 knock down (KD) may enhance **sensitivity to carboplatin**
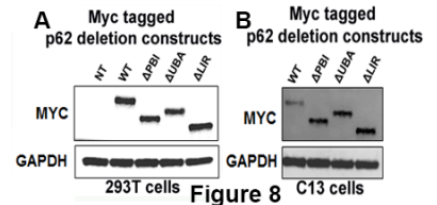

Figure 7
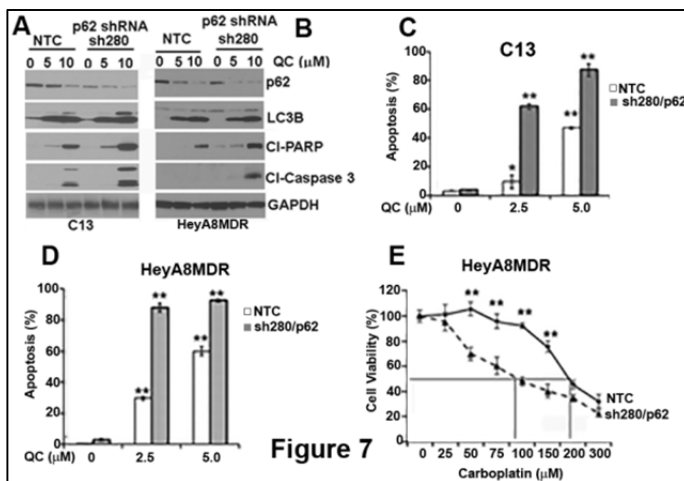
treatment in HeyA8MDR and C13 ovarian cancer cells. Elevated level of p62 has been previously shown to be critical in imparting chemoresistance in OvCA cells [43]. Our data indicate that QC treatment downregulated p62 levels preferentially in the chemoresistant C13 and HeyA8MDR cells (Figure 2A in the attached manuscript). Previous studies have shown that p62 downregulation sensitizes cells to cisplatin-mediated cytotoxicity [23]. To determine whether p62 plays role in QC- and carboplatin-mediated apoptosis, we generated two different p62 knockdown shRNA clones in HeyA8MDR and C13 cells as described in Materials and methods section with non-targeted control transduced cells (NTC) as controls. Efficient knockdown of p62 was confirmed in

C13 and HeyA8MDR cells by western blot analysis using anti-p62 antibody (Figures 7A and B). To further evaluate the effect of QC in inducing apoptosis in NTC and p62-depleted cell s, we treated C13 NTC and p62 shRNA clones with 0, 5.0, 10.0 µM of QC for 24 hours. Evaluation of apoptotic marker proteins by western blot analysis revealed that p62 knockdown cells exhibited higher degree of cleaved PARP and caspase 3 whereas no significant change was observed in LC3B II induction upon QC treatment in C13 NTC as well as p62shRNA cells (Figure 7A). Consistent with this data, QC treatment in HeyA8MDR p62shRNA cells showed increased degree of caspase 3 and PARP cleavage while no change was detected in LC3B II induction (Figure 7B). This data suggests that p62 downregulation in C13 and HeyA8MDR sensitizes the cells to QC treatment. Similarly, annexin/PI staining of these cells after treatment with QC revealed that C13 and HeyA8MDR p62 knockdown cells were more sensitive to QC-induced cell death when compared to NTC cells (Figures. 7C and 7D). More

importantly, genetic downregulation of p62 in HeyA8MDR cells enhanced carboplatin sensitivity (please note the reduction in carboplatin IC50 from 176 µM in NTC cells to 110 µM in p62 knockdown cells) (Figure 7E). Collectively, these findings indicate that p62 downregulation sensitizes cells to QC-mediated cell death.

In order to map the domain within p62 that is critical for conferring synergy in OVCa cell, we generated deletion constructs of p62 starting with Myc p62 full length construct and validated it by immunoblot.as shown in Figures 8 A and B which shows the expression of the Myc tagged p62 deletion constructs in 293T and C13 cells by transient transfections.


Figure 8

We also generated clonal lines of the deletion constructs in C13/CAS9-p62g cells as shown in Figure 9B. For comparison, in Figure 9A the levels of endogenous p62 is shown in non-transfected (NT) and in p62 deletion constructs including the full length WT control. Expression levels of these constructs in the clonal lines are shown by using both P62-Lck and anti-Myc antibody. Since the p62-lck immunogen does not recognize the PB1 domain the expression level of this construct was not detected with this antibody.

Figure 9
• p62-lck :ImmunogenHuman p62 lck ligand aa. 257-437 BD Transduction Laboratories™ (Catalog No.610832)

We wanted to determine if QC mediates downregulation of exogenously expressed deletion constructs. While 10µM QC treatment downregulated the expression of the exogenously expressed HA-tagged and p62 WT construct in C13 cells, the Myc tagged construct did not show a similar profile (Compare HA and Myc levels with increasing QC treatment). As expected, the endogenous p62 levels were consistently down in all three cell lines including the vector transfected controls. Consistent with this down regulation there was increase in LC3BII, p53 and cleaved PARP levels (Figu re 10). However the Myc-tagged deletion constructs expressed in C13-Cas9-p62g cells did not show any downregulation of p62. It is not clear if the Myc tag confers a different conformation of p62 compared to HA-tag at this point.

Figure 10   C13
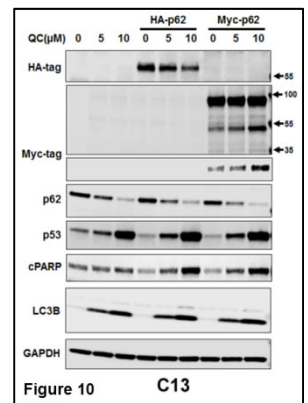
We tested the effect of carboplatin and QC in the clonal lines with specific deletion constructs. Figure 11 shows the response of C13 cells (CRIPR-Cas9 Scg and CRISPR-Cas9p62g) to QC and/or carboplatin at 72hrs. Each point represents the mean value of 6 replicates (error bars show + 2 standard errors of the mean). To our surprise, re-expression of p62WT construct into the C13-Cas9-p62g cells conferred sensitivity to carboplatin (Figure 11A). The IC50 for carboplatin decreased from 90µM in the p62g cells to 50µM in theP62WT transfected cells. The difference in the IC50 for QC was comparable in these two cell lines (Figure 11B). Similarly, deletion of specific domains, specifically deletion of LIR domain conferred slightly more sensitivity to carboplatin and to a limited extent to QC compared to full length construct (Figures 11C and D respectively). Based on the literature, we anticipated that the presence of p62 would confer resistance to chemotherapy. In contrast, we see that

the deletion and or full length p62 when re-expressed in p62 deleted cells conferred some sensitivity to carboplatin compared to vector transfected cells.
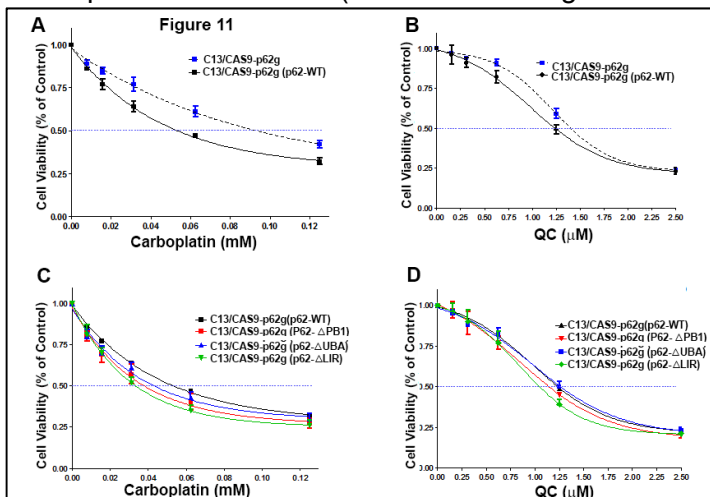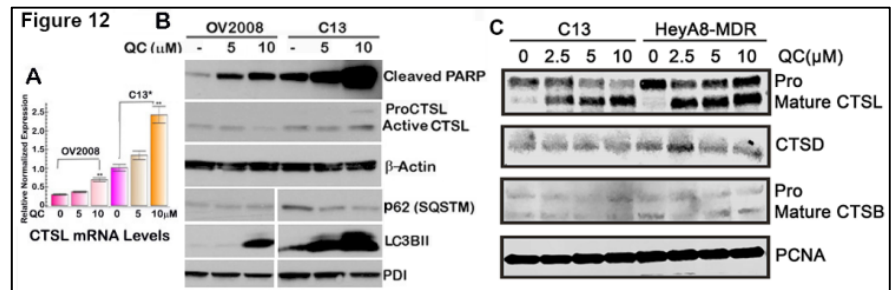
Collectively, these data suggest that downregulation of p62 seen with QC probably plays a more significant role in promoting autophagy than chemosensitivity.

Aim 1C: *Next we asked the question what is the mechanistic basis for QC's differential response in modulating the expression of p62 in sensitive vs resistant cells.*

It is well established that cancer cells can undergo caspase dependent (Type 1) or apoptotic like autophagic death (Type 2) by recruiting lysosomal proteases to induce cell death. Lysosomes are acidic organelles involved in several cellular functions, including repair of the plasma membrane, degradation of macromolecules, antigen and recycling of cell surface receptors and apoptosis signaling [1]. More importantly, lipophilic, cationic drugs such as quinacrine, partition into lipid bilayers and cause increased lysosomal membrane permeabilization (LMP) and this results in the release of lysosomal content to the cytosol. Among the lysosomal proteases, the cysteine Cathepsins B (CTSB) and L

Figure 12

(CTSL) have been implicated in promoting caspase-dependent programmed cell death [14,15] or mitochondrial membrane permeabilization [16,17]. Our data shown in figures 12 A and B clearly shows that QC induced autophagy also upregulated the lysosomal protease CTSL and to a lesser extent CTSB but not CTSD (Fig.12C) in OC cells. One of the unanswered questions is whether QC-induced upregulation of CTSL more in resistant cells compared to its isogenic sensitive cells is involved in the degradation of p62 in resistant cells? To ascertain whether QC-mediated sensitizing effect on C13 cells but not on OV2008 cells could be attributed to the differential modulation of cathepsin expression/activity we performed q-PCR to detect CTSL in these cells. q-PCR analysis showed that the basal CTSL mRNA was 3.2 fold higher in C13 compared to OV2008 cells (Fig.12A). Further, the, expression of active form of CTSL protein was higher in C13 than in OV2008 upon QC treatment (Fig.12B, lane 6 compared to lane 3). These results suggest a possibility that p62 degradation may in part may also be mediated by CTSL since we had previously reported that QC treatment promoted p62 downregulation, induced LC3B expression and increased apoptosis as indicated by increased PARP cleavage in ATG5 WT MEFs but not in ATG5 null MEFs, as shown in Fig.3b in[18,] and now
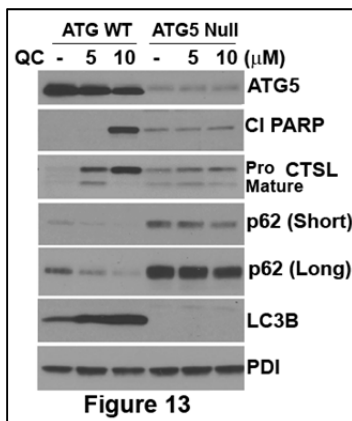
Figure 13

shown here as Figure 13. In autophagy deficient ATG5 null cells, QC still activates CTSL albeit it is more pronounced in autophagy proficient ATG5WT cells. Consistent with this, we see that p62 is undergoing a more pronounced degradation in ATG5 WT cells compared to ATG5 null cells, suggesting a role for both autophagy and CTSL mediated degradation of p62. In ATG5 null cells, despite the lack of autophagy, p62 still is downregulated by QC treatment (panel 4, p62 short time exposure) where CTSL is activated minimally by QC treatment compared to ATG5WT cells. In our ongoing studies, we have explored the possibility that p62 could be a substrate of CTSL (Figure 20).

Next, to determine if the increase in PARP cleavage is mediated by the increase in the CTSL activity levels
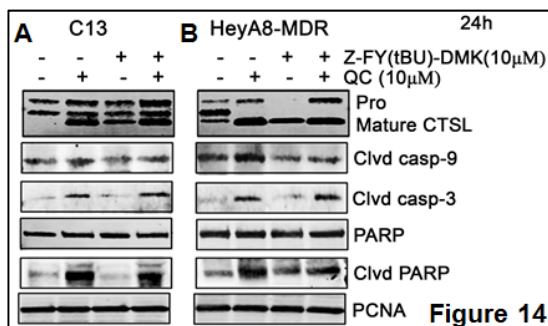
Figure 14

(Lanes 2 and 4 in both cell lines), C13* and HeyA8MDR cells were treated with various concentrations of cathepsin L specific inhibitor Z-Phe-Tyr-CHO for 24 hrs to inhibit CTSL activity in the presence and absence of QC as shown in figures 14 A and B respectively. Inhibiting CTSL activity with Z-Phe-Tyr-CHO treatment alone reduced the levels of cleaved caspases 3, 9 and cleaved PARP in both cell lines (Lane 3 in Figures 14 A and B). QC alone treatment (that potentially upregulates CTSL activity) resulted in significant upregulation of these 3 apoptotic markers. Co-treatment of QC + Z-Phe-Tyr-CHO resulted in slight downregulation of cleaved caspase 9 and PARP (Lane 4, panels 2 and 5 in Figs. 14 and B). Collectively, these results suggest that inhibiting CTSL activity results in the attenuation of QC-induced apoptosis.

To further elucidate the specific cathepsin involved in QC mediated cytotoxicity and cell death, C13 cells were treated with pepstatin A (CTSD inhibitor), CA-74me (CTSB inhibitor) and Z-FY(tBU)-DMK (CTSL inhibitor) at indicated concentrations in the presence and absence of 5µM QC for 24 hrs. Cell survival was assessed by clonogenic assays and the levels of cleaved PARP by western blot analysis.as shown in figures 15A/B, D/E and G/H respectively. The colony forming ability of cells treated with QC alone in the absence of the 3

cathepsin inhibitors was significantly inhibited compared to untreated cells. However, inhibiting Cathepsin B, D and L activities promoted clonogenic survival. In contrast to CTSL inhibitor treatment, QC- induced clonogenic death was rescued by co-treatment with CTSB and D inhibitors compared to CTSB and CTSD treatment alone. In contrast, inhibiting CTSL activity did not overcome the cytotoxic effect of QC, suggesting that QC-induced cytotoxicity is CTSL dependent. This was reflected in cleaved PARP levels in the combination treatment with CTSD and B inhibitors with QC compared to QC alone treated cells (Comparable densitometric levels of cleaved PARP [3.93 to 3.63 for CTSD and 3.79 to 4.26 for CTSB inhibitor respectively] in Figures 15 C and F-lane 4 compared to lane 2. However in the QC+ CTSL inhibitor treatment group, the levels of cleaved PARP were significantly less (Densitometric values in Fig 15I Lane 4 compared to lane 2 –1.04 to 3.74).

Figure 15

Additionally, the role of CTSL in QC-induced cell death was assessed by FACS- PS externalization assay. The change in movement of the normal inward-facing phosphatidylserine of the cell's lipid bilayer expression to outer layer of the plasma membrane indicates the early stages of apop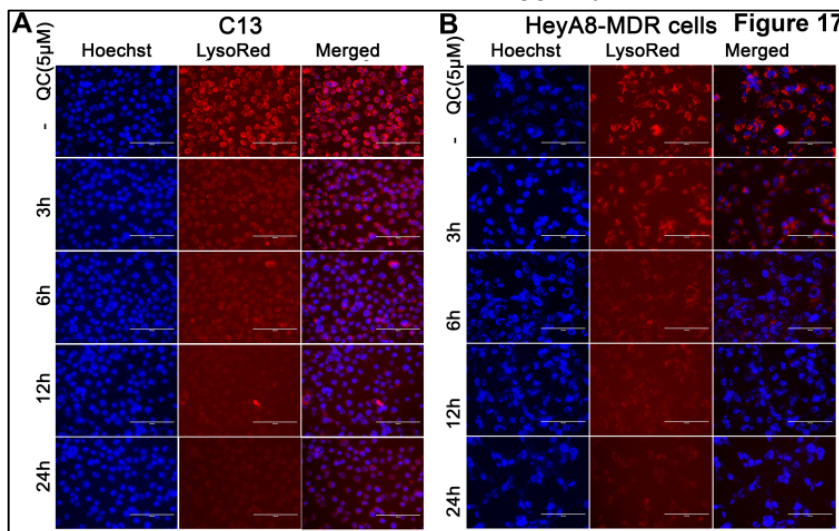tosis. As verified by Annexin V–pacific blue and PI staining (Figure 16), QC alone treated cells exhibited 30.3% (23.5+6.9) and 36.4% (32.8+3.6) of early and late apoptotic cells in both C13 and HeyA8-MDR cells respectively (Fig.16 Panels 2). However, in the cells treated with QC and Z-FY(tBU)-DMK, QC-induced apoptotic cells death was arrested and decreased to 10.8% 3.1+7.6 and 15.2% 11.4+3.1 of apoptotic cells in C13 and HeyA8-MDR cells

respectively (Fig.16 panels 4). Also, inhibition of CTSL activity with Z-FY(tBU)-DMK alone completely blocked apoptosis to the levels in control untreated cells (Fig16. panels 3 compared to panel1, 7% and 6.4% in C13 and1.12 to 0.64 in HeyA8MDR cells). Collectively, these results highlight the role of CTSL in QC- apoptotic cell death.
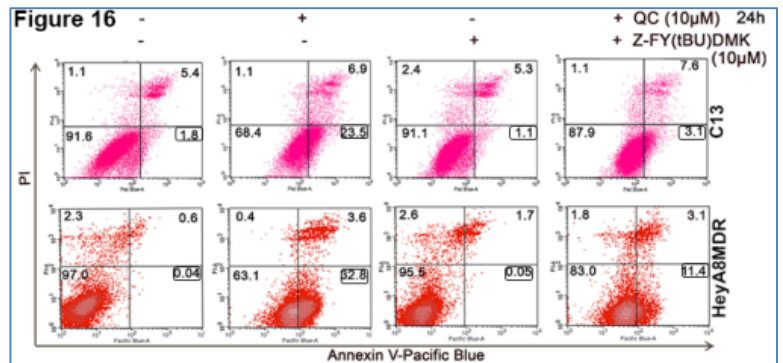
Apoptotic stimuli have been shown to trigger lysosomal membrane permeability (LMP), leading to the release of cathepsins, which activate death signaling pathways in the cytosol. To determine if QC treatment promotes LMP, C13 cells were initially exposed to 5.0 and 10 µM QC (data not shown) for 3, 6, 12 and 24 hrs at incubated with and treated with 50nM Lyso Tracker Red for 1hr at 37°C and loss of lysotracker staining indicative of LMP was visualized using confocal microscopy. Since 5 µM QC was effective in inducing LMP in C13 cells, HeyA8 MDR cells were also tested for QC-induced LMP under similar conditions as shown in figures 17 A and B (Middle and merged panels) respectively. QC induced LMP was evident as early as 3hrs and 6

hrs in C13 and HeyA8MDR cells respectively.

Whilst the data shown in figures 12 and 14 confirm that the mature form of CTSL is generated after QC treatment- it does not necessarily reflect the levels of CTSL activity. Therefore we determined CTSL activity with increasing concentrations of QC in the presence and absence of 10 µM CTSL inhibitor for 24 hr in a cell based assay Magic Red® Cathepsin L Assay Kit from (Immunochemistry Technologies LLC, Bloomington, MN) following manufacturer's instruction. If cathepsin enzymes are active, the Magic Red substrate MR-FR2 enters the cell in a non-flourescent state and is cleaved and the cresyl violet fluorophone will become fluorescent upon excitation. The more Magic Red substrate is cleaved the signal will intensify reflecting the increased activity of CTSL in the cell.
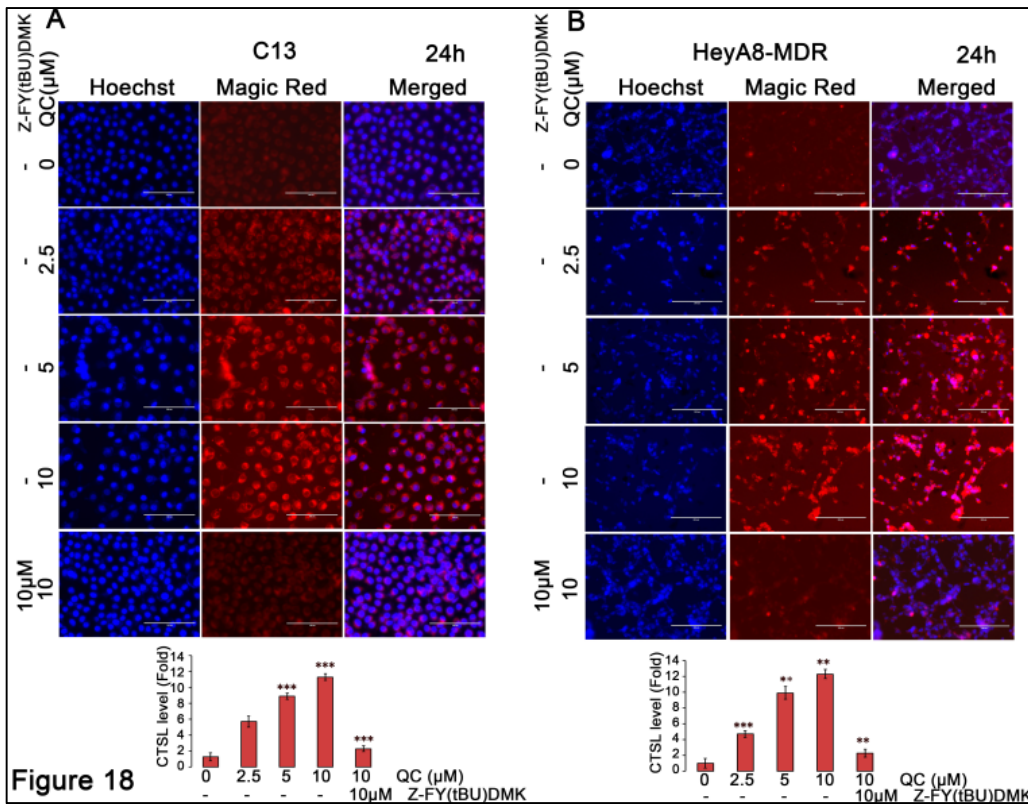
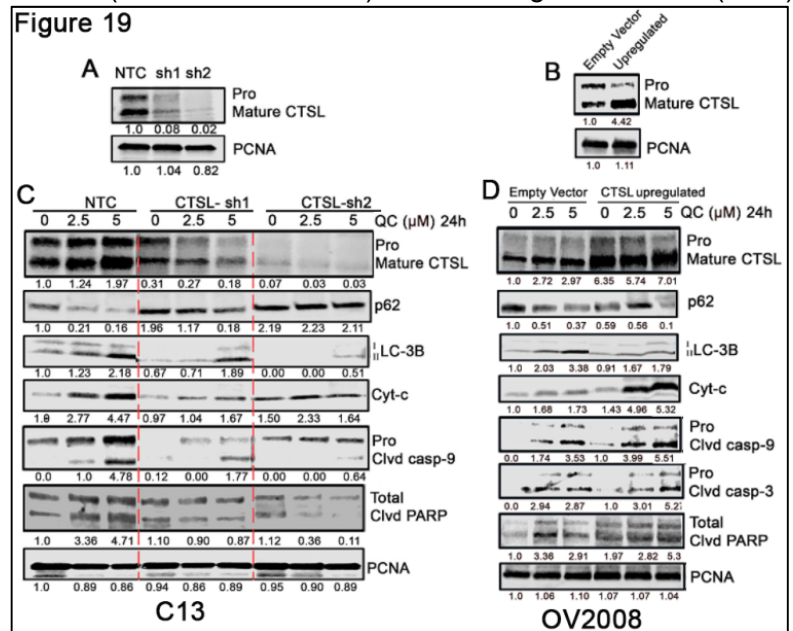
Figure 18

As shown in Figures 18 A and B there is a dose dependent increase in the activity of CTSL (Increase in red flourescence) which is completely abrogated in the presence of the CTSL inhibitor Z-FY(tBU)-DMK. Quantification of the fold increase in CTSL activity levels are indicated in the bar graph below the confocal images for both C13 and HeyA8MDR cells respectively.

To address the impact of CTSL in QC mediated apoptotic signaling cascade, we knocked down (KD) CTSL expression in C13 cells using two different CTSL shRNA (CTSL-sh1 and sh2) with nontargeted shRNA (NTC) as control. Conversely, we generated CTSL over-expressing clones in OV2008 cells with low endogenous CTSL expression with empty vector (EV) transfected control. The CTSL expression plasmid was obtained from Addgene and the shRNA clones (Sigma shRNA mission library) from the Mayo Clinic RISR core facility. Efficient downregulation and /or upregulation of CTSL at the protein level in C13 and OV2008 cells were verified by western blot respectively (Figures 19A and B). C13 cells (NTC, sh1 and sh2) were treated with 0, 2.5 and 5 µM of QC for 24h and the levels of pro and mature forms of CTSL, LC3BII, p62 and apoptotic markers cleaved caspases 3, 9 and PARP were assessed by immunoblot analysis. QC induced the expression of active CTSL in NTC cells but not in CTSL KD sh1 and sh2 cells that was reflected in reduced levels of p62 degradation

Figure 19

and LC3B expression. Also, CTSL knockdown cells showed reduction in apoptotic markers Cyt c, caspase-9 and cleaved PARP compared NTC cells (Fig.19C). In contrast, QC treatment of OV2008 with upregulated CTSL levels (CTSL upregulated) showed that induced higher levels of the mature form of CTSL both in the vector and CTSL transfected cells, albeit, the CTSL levels were significantly higher in the CTSL over-

expressing clone compared to the vector transfected cells (Fig 19D, top panel). Consistent with the increase in CTSL levels, there was a gradual decrease in P62 levels with a concomitant increase in the LC3BII, Cyt c, cleaved caspases 3, 9 and PARP expression compared to vector transfected cells (Fig.19D). Taken together, these results suggest that QC by inducing CTSL activity promotes both LMP and an increase in apoptotic signaling.

Data presented in figures 17A and B clearly indicates that QC induces LMP. Additional data suggests that QC-induced upregulation of CTSL may [play a role in QC-induced LMP. To validate the role of QC-induced CTSL in
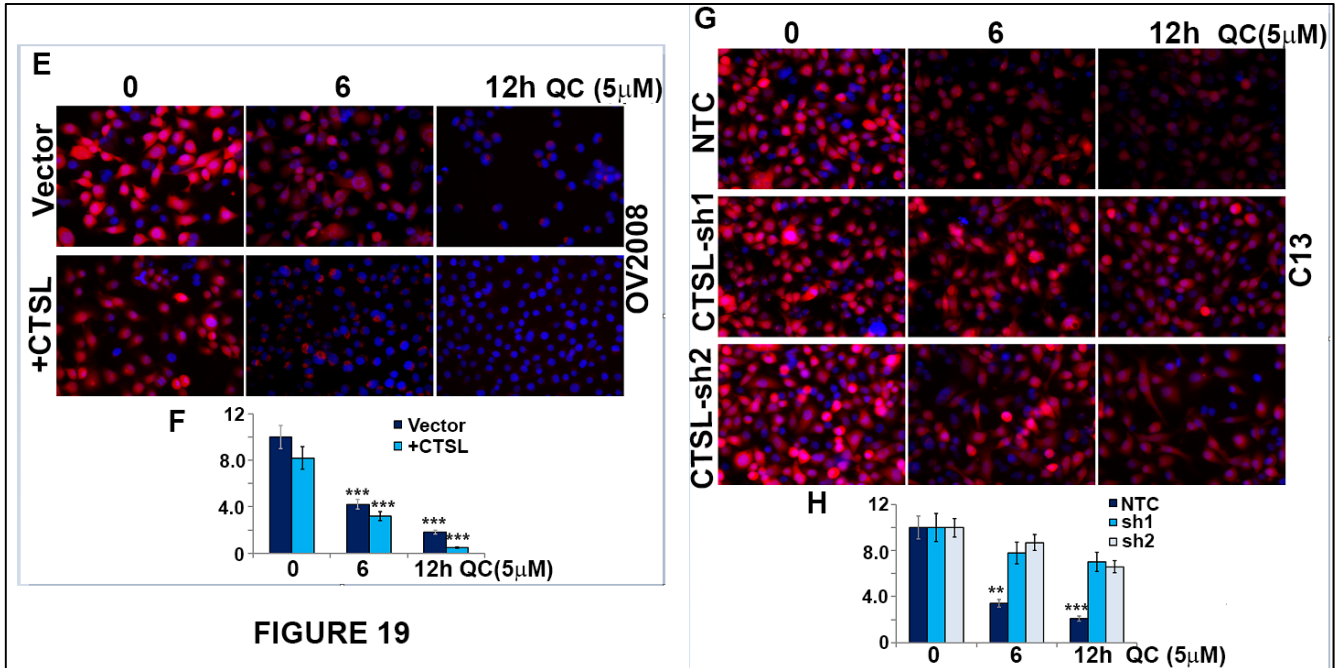
FIGURE 19

inducing LMP, we treated CTSL overexpressing 2008 cells and CTSL knock down C13 cells to varying concentrations of QC for 24 hrs and determined the extent of LMP using lysotracker red asa readout. Results shown in figures 19E shows that QC-induced LMP in OV2008 cells with ectopic expression of CTSL (Figures 19E and F) but not in CTSL downregulated C13 cells (Figures 19G and H). Collectively, these results suggest that QC-induced CTSL may have a critical role in QC-induced LMP to induce cell death.

Determine whether p62 degradation is directly regulated by QC induced upregulation of cathepsin L
To determine the effect of the CTSL on p62 degradation, HeyA8-MDR cells were treated with 5µM QC for 12h

Figure 20

and 24h and the level of p62 was visualized using confocal microscopy. Time dependent QC-induced CTSL expression (Fig 20A- compare 12hr to 24hr exposure, green signal) resulted in increased p62 degradation (Fig. 20A, compare 12hr to 24hr, red). Conversely, increased CTSL activity as assessed by CTSL Magic Red activity assay by transfecting CTSL expression construct in CTSL low expressing OV2008 cells (Fig.20B, red signal) led to p62 decrease (Fig.20B, green signal), which confirms p62 is degraded by QC mediated CTSL expression and activation. Further, to directly substantiate, recombinant CTSL (rCTSL from R&D Systems, Minneapolis, MN following manufacturer's instruction) was incubated with the lysate extracted from HeyA8MDR cells and degradation of p62 was monitored by western blot analysis. As shown in figure 20C, rCTSL degraded endogenous p62 in a dose and time dependent manner consistent with the confocal imaging results shown in figures 20A and B for the first time.
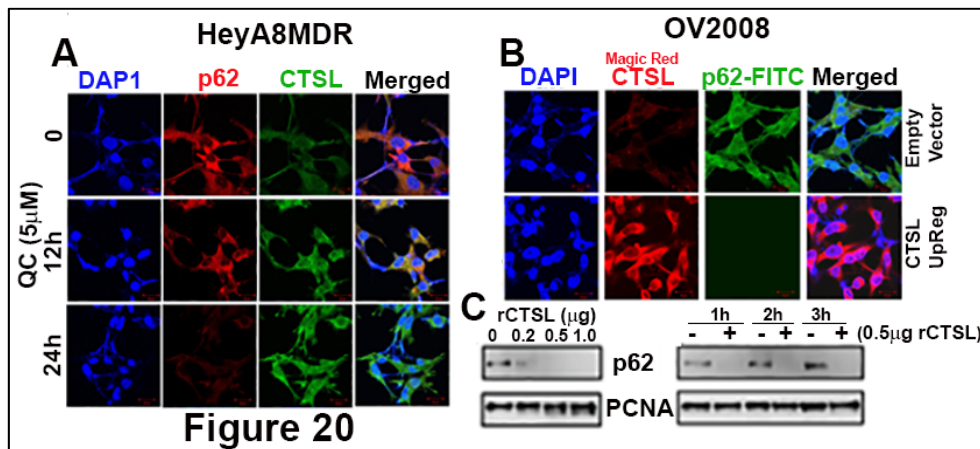
13

QC induces active CTSL *to promote* p62 degradation and caspase mediated cell death *in vivo*
We have previously reported that QC treatment of mouse-derived xenografts of HeyA8 MDR was shown to be
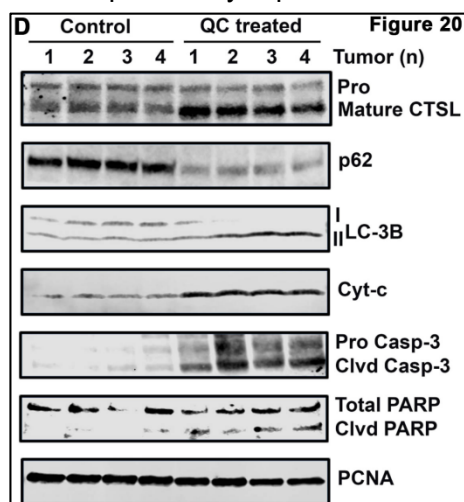
effective in reducing tumor weight, reducing cell proliferation as measured by Ki-67 staining and blocking ascitic fluid formation. Additionally, transmission electron micrographs of tumor derived QC-treated xenografts clearly showed increased formation of autophagosomes and autolysosomes. These effects were dramatic when QC was combined with carboplatin leading to complete remission of tumor growth and reduction in the proliferation index [3]. We tested 4 each of the control and QC treated xenografts to check if QC treatment induced active CTSL *in vivo*. As shown in figure 20D, there was a dramatic induction of CTSL upon QC treatment *in vivo*. This correlated with degradation of p62, upregulation of LC3BII and increase in Cyt-c, cleaved caspase 3 and cleaved PARP compared to untreated cells. Taken together these data provide strong evidence that p62 is a substrate of CTSL and gets degraded during QC-induced autophagic and caspase mediated cell death.

In Aim 2 we had proposed to *identify novel or known markers that may contribute towards QC-induced synergy* by RNA sequencing (in Collaboration with Dr. Chen Wang, Co-I)
Introduction: Based on our preliminary results, in Aim 1, we focused on increased autophagic flux in resistant cells as a contributing factor conferring sensitivity to carboplatin. However, biomarkers associated with drug sensitivity could potentially involve several other genes that may offer biological clues as to the mechanisms involved. In this Aim, we had proposed to identify additional novel or known markers that may contribute towards QC-induced synergy in resistant cells by performing RNA sequencing of all three sensitive and resistant isogenic cell lines with and without QC treatment to mechanistically define the differential transcriptional response which may ultimately shed light on the molecular players responsible for this differential drug sensitivity.

Rationale: Transcriptional response induced by chemotherapeutic agents can be used to assess the potential mechanisms of actions associated with the agents. For example, results from the Connectivity Map studies indicate that similar transcriptional response (perturbed gene expression) is induced by drugs with similar mechanisms of actions[19]. Connectivity Map has generated thousands of transcriptional profiles perturbed by hundreds of known and novel drugs [20]. This database can be queried to determine which known drugs induce transcriptional response similar to QC. Such analysis will provide us with potential mechanisms of action associated with QC. Therefore, we will characterize the perturbed gene expression induced by QC in the three sets of isogenic sensitive/resistant cell lines. To leverage the resources provided by the Connectivity Map, we will treat the cells for 6 hours with QC. The 6-hour time point was selected because it is the same time point for all the drugs tested in the Connectivity Map project[19]. The concentration of QC will be predetermined by treating the cells with various concentrations of QC and establishing the concentration at which known gene target of QC is up or downregulated by qRT-PCR.

Based on the results that p62 was downregulated as early as 6hrs treatment with 8μM QC we treated OV2008/C13*, HeyA8/HeyA8MDR and SKOV/SKOV3TR cell lines with 8μM QC or vehicle control for 6 hours collected RNA in Trizol, and prepared RNA sequencing libraries with TruSeq RNA library kit (Illumina). We performed RNA sequencing at Mayo Sequencing Core Facility. A total of at least 20 million mapped reads for each RNA library.

Primary analysis of genes that are perturbed (up- or down-regulated) by quinacrine was performed in sensitive (N=3) and resistant (N=3) cell lines. TopHat [21] was used to align reads to the Human Reference Genome (hg19), and HTSeq [22] was used to produce read counts. A heatmap was generated with Morpheus software (Broad Instituite). Gene analysis was performed with BRB Arraytools [23], DESeq2 [24], and Ballgown pairwise comparison to identify differentially expressed genes with a *p*-value of < 0.05.

The list of genes generated was evaluated by Metascape Ingenuity Pathway Analysis and Panther Analysis [25] to identify pathways and networks of genes perturbed by quinacrine in sensitive and resistant cell lines. All statistically enriched terms (GO/KEGG terms, canonical pathways, hallmark gene sets) were first

identified, and accumulative hypergeometric *p*-values and enrichment factors were calculated and used for filtering. Remaining significant terms were then hierarchically clustered into a tree based on Kappa-statistical similarities among their gene memberships. Then 0.3 kappa score was applied as the threshold to cast the tree into term clusters. The perturbed gene list was additionally queried in the Connectivity Map (CMap) [19] database to identify other drugs with similar profiles of transcriptome perturbation.

Figure 21

The initial RNA sequencing secondary analysis revealed 616 transcripts that were significantly (*p* < 0.05) differentially expressed in SKOV3-TR, C13, and HeyA8-MDR resistant cell lines when treated with quinacrine (Fig. 21A). Additional filtering analyses identified 170 differentially expressed genes in sensitive cells and 164 differentially expressed genes in resistant cells upon quinacrine treatment (Fig. 21B and Table 1). There were 31 genes differentially expressed in this analysis that were common to both sensitive and resistant cells treated with quinacrine (Fig. 21B and Table 2). Tables 1 and 2 are attached in the Appendix.
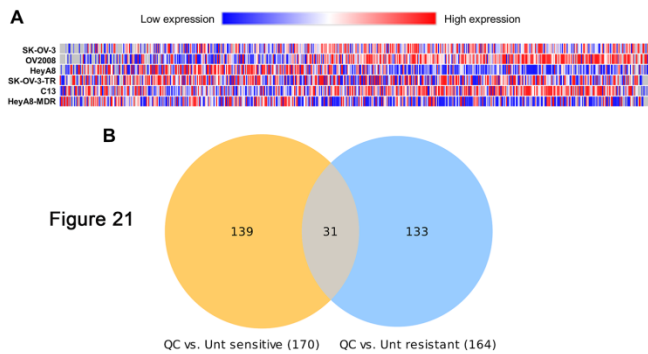
Pathway correlation analyses of RNA expression changes after quinacrine treatment The RNA sequencing results of differentially expressed genes from quinacrine treatment were submitted to the Metascape database for pathway correlation analyses [25]. Gene identifiers (Gene ID, RefSeq, or Symbol) from these results were entered as input and database conversion resulted in 117 and 120 Human Entrez Gene IDs from resistant and sensitive cell lines, respectively. After filtering statistically enriched terms, the resulting enrichment analysis identified major signaling and hallmark pathways correlated to quinacrine-induced transcription profiles for resistant cells (Fig. 22A) and sensitive cells (Fig. 22B). The hallmark p53 pathway was correlated to both resistant and sensitive cell line gene sets (Figs. 22A&B), and this pathway has been previously reported to be altered by quinacrine in cancer cells [26]. Several signaling pathways of nucleotide and DNA regulation (protein-DNA complex assembly, modification, metabolic process, replication) were perturbed, mainly in resistant cells (Fig. 22A), suggesting nucleotide regulation pathways may be important for quinacrine mechanisms in drug resistant cancer cells.

Figure 22

Validation of RNA expression changes after quinacrine treatment
Candidate genes were identified for further validation based on a casual relationship to pathway correlation analysis, high-fold change, and most significant *p*-values for RNA sequencing data after quinacrine dosing. Selected transcripts included *ASNS*, *BOP1*, and *CSTM* in resistant cells (Fig. 23A). *ATF3* and *PHDGDH* were validated for changes in both sensitive and resistant cells (Fig. 23B).

Transcription of *ASNS*, the gene for asparagine synthetase, was downregulated in C13 and SKOV3-TR cells after quinacrine treatment (Fig. 23A, Panel 1). Increased *ASNS* expression and protein levels were previously shown to have a negative correlation with L-asparaginase (L-ASP) chemotherapeutic activity in OVCAR8 and isogenic multidrug-resistant derivative ovarian cancer cells and clinical tumor microarrays [27]. By knocking down asparagine synthetase, Krall *et al.*, recently reported that asparagine regulates serine uptake influences that affect serine metabolism and nucleotide synthesis [28]. These data suggest that asparagine, by coordinating protein and nucleotide synthesis, is important in amino acid homeostasis and proliferation.
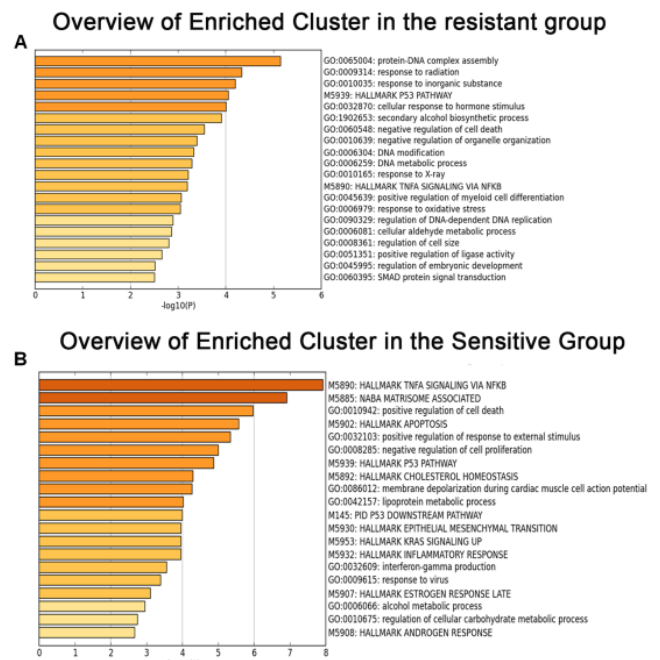
The second gene that was validated was *BOP1* (block of proliferation), which encodes the ribosome biogenesis protein BOP1. Changes in BOP1 activity are associated with ribosomal biogenesis impairment [29]. This was the most highly upregulated gene (fold change >200 fold; Table S1) in the resistant cells of the RNA sequencing data and showed significant quinacrine-induced upregulation by qPCR in HeyA8-MDR and SKOV3-TR cells to a lesser extent (Fig. 23A, Panel 2). It maps in the 8q amplicon and ~37% of primary tumors show amplification/overexpression in the ovarian TCGA database at the mRNA level. While there is very little information on BOP1 in ovarian cancer, BOP1 has been reported to promote epithelial mesenchymal transition in hepatocellular cancer [30].

A

Figure 23

The third gene validated was *CST6* (*CSTM*), a lysosomal cysteine protease inhibitor, considered to be a metastatic tumor suppressor of breast cancer [31]. There are very few reports on the function of *CSTM* in ovarian cancer. RNA sequence analysis revealed that the *CSTM* expression was induced by quinacrine in the resistant cells by 5.4 fold compared to the sensitive cells. Analysis by qPCR validated that quinacrine induced *CSTM* expression in all three resistant cell lines to about the same extent (Fig. 23A, Panel 3). The expression of *CSTM* is under epigenetic control as shown in several tumors. Specifically, one study associated *DNMT3B* expression and activity as a contributing factor for *CSTM* promoter methylation [32]. Interestingly, RNA sequence analysis showed that the expression of DNMT3B was downregulated by 1.7 fold in the resistant cells. This result was validated in all three resistant cell lines (Fig. 23A, panel 4). It is also interesting to note that the upregulation of *CSTM* by quinacrine is consistent with a study by Hossain *et al.*, that DNA-intercalators (including quinacrine) causes rapid re-expression of methylated and silenced genes in cancer cells [33]. Based on the report that
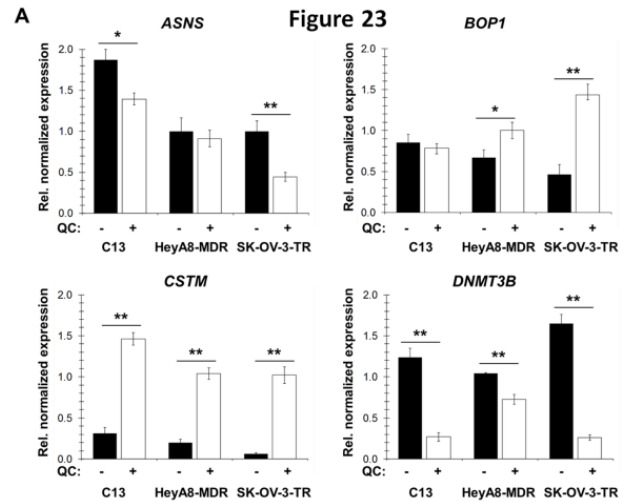
Rank	CMap name	Mean	n	Enrichment	p value	Specificity	Percent non-null
1	wortmannin	0.282	18	0.702	< 10^-5	0.0065	94
2	sirolimus	0.264	44	0.590	< 10^-5	0.0121	84
3	trichostatin A	0.265	182	0.553	< 10^-5	0.2038	85
4	LY-294002	0.265	61	0.551	< 10^-5	0.0201	80
5	tanespimycin	0.247	62	0.508	< 10^-5	0.0725	85
6	vorinostat	0.253	12	0.659	0.00004	0.2362	83
7	trifluoperazine	0.263	16	0.566	0.00004	0.1250	87
8	thioridazine	0.246	20	0.507	0.00008	0.2374	75
9	phenoxybenzamine	0.316	4	0.856	0.00056	0.2327	100
10	fluspirilene	0.296	4	0.829	0.00131	0.0050	100
11	5230742	-0.635	2	-0.974	0.00139	0	100
12	astemizole	0.279	5	0.769	0.00148	0.0853	100
13	fulvestrant	0.137	40	0.289	0.00190	0.0925	52
14	dilazep	0.283	5	0.744	0.00250	0	100
15	etacrynic acid	0.396	3	0.884	0.00314	0	100
16	prochlorperazine	0.208	16	0.431	0.00317	0.2427	75
17	alexidine	0.269	4	0.797	0.00328	0.0205	100
18	alprostadil	-0.341	7	-0.622	0.00403	0.0240	71
19	geldanamycin	0.229	15	0.434	0.00410	0.2880	80
20	anisomycin	0.300	4	0.782	0.00422	0.1804	100
21	amodiaquine	0.290	4	0.770	0.00539	0	100
22	0297417-0002B	0.330	3	0.858	0.00541	0.0790	100
23	tonzonium bromide	0.280	4	0.768	0.00557	0.0357	100
24	helveticoside	0.248	6	0.641	0.00630	0.2426	83
25	piperacillin	-0.353	5	-0.690	0.00655	0	80
26	minoxidil	-0.342	5	-0.677	0.00821	0.0170	80
27	lansoprazole	-0.546	4	-0.746	0.00826	0.0256	75
28	5182598	-0.606	2	-0.936	0.00861	0.0566	100
29	pyrvinium	0.260	6	0.620	0.00930	0.2558	83
30	hycanthone	0.405	4	0.737	0.00939	0.0933	100
31	irinotecan	0.275	3	0.833	0.00945	0.2364	100
32	terfenadine	0.340	3	0.830	0.00979	0.1527	100
33	valproic acid	0.130	57	0.213	0.00981	0.2566	52

Table 2 Ranked similarity of differentially expressed gene profiles of small molecule compounds to quinacrine in the CMap database. The treatment period for quinacrine and all compounds of the CMap database is 6 hours.

methylation-induced gene silencing of several genes is associated with chemoresistance [34,35], we surmise that CSTM regulation by quinacrine might be related to drug synergy with cisplatin in ovarian cancer cells [3].

Transcription of *ATF3* was upregulated by 2-fold in the RNA sequencing of sensitive cells compared to the resistant cells. While OV2008 and HeyA8 showed significant quinacrine-induced upregulation of *ATF3* with qPCR validation, it was downregulated in the sensitive SK-OV-3 cells (Fig. 23B, top panel). Prevailing literature suggests that ATF3 can act either as an anti-apoptotic or pro-apoptotic factor depending on the cell and tumor type. For example, ATF3 is oncogenic in breast cancer [36], and acts as a metastatic tumor suppressor in bladder cancer [12]. Similarly, some studies suggest that ATF3 is an apoptosis inducer in ovarian cancer [37], while

one study professes a worsened prognostic significance in ovarian cancer tumors [38]. It is yet to be determined if quinacrine-induced *ATF3* expression in these sensitive cells is pro- or anti-apoptotic.

Expression was validated for *PHGDH*, which codes for phosphoglycerate dehydrogenase, an enzyme involved in serine biosynthesis. PHGDH was downregulated in both sensitive and resistant cell RNA sequencing data by about 2-fold. In qPCR analysis, quinacrine reduced *PHGDH* in HeyA8, SKOV3, and SKOV3 TR cells, although *PHGDH* was upregulated in C13 and HeyA8-MDR cells (Fig. 23B, Lower panel). Serine is the third-most metabolite consumed by cancer cells after glucose and glutamine [39]. Serine is used as a building block for proteins and as a carbon donor for nucleotide biosynthesis. Since the discovery that *PHGDH* is amplified at the genomic level in breast cancer [40], several studies have shown that silencing PHGDH in PHGDH-dependent cancers significantly affected cell growth, thus making this enzyme an attractive target for cancer therapy. However, these results suggest that quinacrine is more likely to downregulate *PHGDH* expression in sensitive cells lines.

Quinacrine-induced RNA expression changes correlated to genetic profiles of other drugs
The changes in quinacrine-induced transcriptional expression were compiled from all the cell lines and compared to the CMap drug gene expression signature database [19]. CMap database comparison is based on similar transcriptional response (perturbed gene expression) being induced by drugs with similar mechanisms of actions [19]. CMap has generated thousands of transcriptional profiles from hundreds of known and experimental drugs. This database was queried to determine which drugs induce transcriptional response similar to quinacrine as evidence of potential mechanisms of action. Small molecule compounds with similar gene expression profile changes were ranked by *p*-value (Table 2). The top result was wortmannin, which is a PI3K inhibitor along with the fourth-ranked result of LY-294002, and has also been shown to inhibit DNA repair, receptor-mediated endocytosis, and cell proliferation [41]. The second-ranked result was sirolimus (rapamycin), an mTOR inhibitor that also can impact the PI3K pathway and autophagy regulation. The fifth-ranked result was tanespimycin, which is a derivative of geldanamycin (19th) and an inhibitor of Hsp90 that impacts multiple pathways including PI3K signaling [42]. The third- and sixth-ranked results are trichostatin A and vorinostat, respectively, which are histone deacetylase inhibitors. Interestingly, the 80S ribosome modulator anisomycin (20th) and the RNA synthesis inhibitor hycanthone (30th) also had significantly comparable genetic signatures to quinacrine. For both of these latter drugs, it is noted that the limited number of profiles (n = 4 for both) may have resulted in lower *p*-values (0.004 and 0.009, respectively).

The CMap database comparison identified some previously reported pathways modulated by quinacrine including PI3K/Akt/mTOR signaling (Table 1), and further study is needed to determine if this modulation is linked to the current observations, prior reports of autophagy regulation [3,18], or an independent mechanism of quinacrine. Several of the associated drugs listed in Table 1 are antipsychotic medications or related compounds (e.g. trifluoperazine, thioridazine, phenobenzamine, fluspirilene, and prochlorperazine). Quinacrine had been previously reported to non-selectively inhibit monoamine oxidases and N-methyltransferases [43,44], which may account for quinacrine-induced psychosis-related side effects at higher doses. It is not known if there is any relation between the quinacrine-induced inhibition of N-methyltransferases and inhibition of DNA methyltransferases.
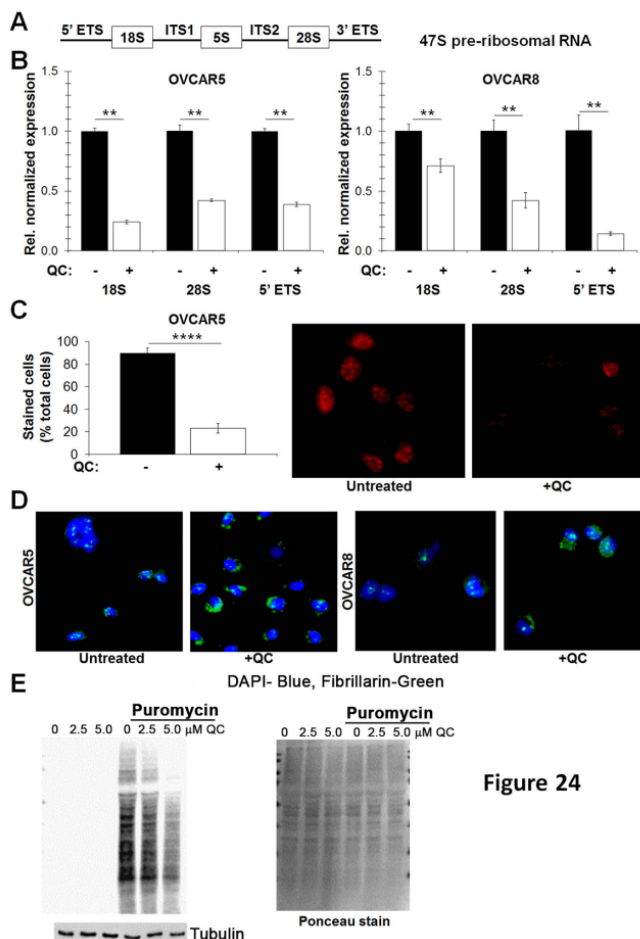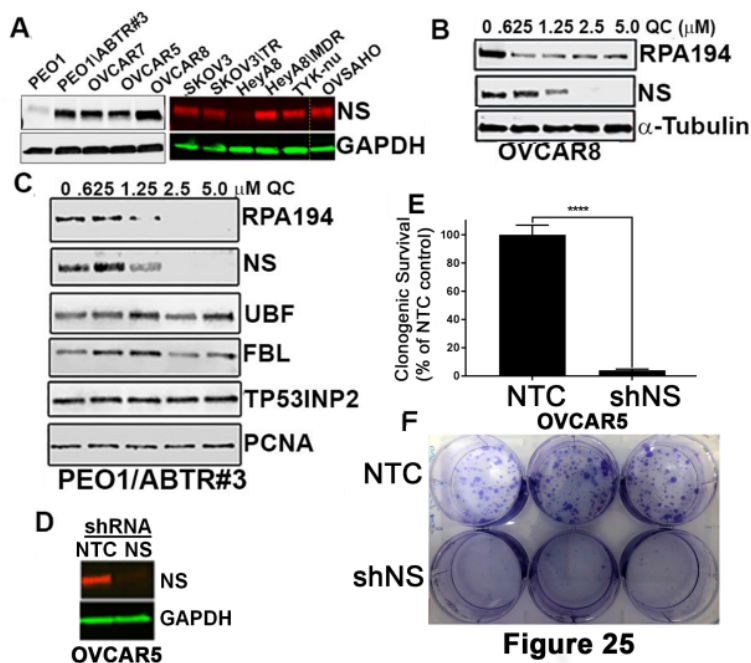
One of the things we noticed was QC treatment seemed to have upregulated some oncogenes such as HIF1a, and Bmi-1. Since the expression of Bmi-1 is associated with chemoresistance [45], we anticipated the expression of

Figure 24

17

this gene would be downregulated in resistant cells by QC. We sought to validate this RNA sequence based data using Q-PCR. In contrast to the RNA sequence data, Bmi-1 expression was downregulated in the C13 cells with no change in HeyMDR and SKOV3TR cells (Data not shown). One of the limitations of this study was that the RNA sequence was not done in replicates. This could account for the variation observed between RNA sequencing analysis and the Q-PCR based analysis for some of the genes. Keeping in mind that the expression levels for any specific gene were averaged between resistant and /or sensitive cells compared to the untreated cells to obtain statistically significant differences in gene expression in these categories compared to the untreated cells, we are cognizant of the fact that not all three resistant cells will either show up and or down regulation for any specific gene. Collectively, our data indicate that the genes we selected from the RNA sequence based identification in the different categories for the most part was validated by Q-PCR. Future studies with additional funding, we will evaluate the contribution of QC-induced alteration of couple of these genes in chemoresistance, autophagy and growth both in vitro and in vivo.

Quinacrine induces nucleolar stress.

Based on the report that QC-induced gene expression showed the highest correlation to that of ellipticine, an RNA Pol I inhibitor [46], we explored the extent to which QC inhibits RBG and produces therapeutic effects through nucleolar stress. It is well established that drugs that modulate RBG to induce nucleolar stress [47]. Based on the expression analyses, quinacrine-induced attenuation of ribosomal biogenesis was further investigated in high grade serous ovarian cancer cells. This carcinoma histotype is known for aggressiveness and lack of response to therapy. In ribosomal biogenesis, the 18S, 5.8S, and 28S rRNAs are transcribed by RNA polymerase I from a single transcription unit of 47S pre-ribosomal RNA in the nucleolus (Fig. 24A). The three rRNAs are interspersed with non-coding sequences, specified by 5'- and 3'- external transcribed spacers (5'-ETS and 3'-ETS) and internal transcribed spacers 1 and 2 (ITS1 and ITS2). To confirm that quinacrine affects ribosomal biogenesis, OVCAR5 and OVCAR8 cells were treated with 1.0 QC µM for 1 hour. qPCR analysis showed repression of 47S rRNA as assessed by the levels of short-lived 5' ETS, 18S and 28S (Fig. 24B). Immunofluorescence (IFC) analysis of ongoing rRNA synthesis monitored by FUrd nuclear run-on assays of OVCAR5 cells showed inhibition of RNA synthesis upon QC treatment (Fig 24C). IFC analysis for fibrillarin in OVCAR5 and OVCAR8 cells shows quinacrine promotes redistribution of fibrillarin in the form of extranuclear foci and nucleolar caps of this pre-ribosomal RNA methyltransferase (Fig. 24D), which is an indicator of nucleolar stress conditions [29]. Quinacrine-induced decreases in ribosomal biogenesis and maturation may also be reducing protein translation, which is suggested by reduced puromycin labeling in OVCAR5 cells (Fig. 24E). Collectively, these results suggest quinacrine attenuates the biosynthesis and processing of rRNA, which may be inducing a nucleolar stress environment.

A major consequence of nucleolar stress is inducing p53 signaling, and induced p53 has been previously described as a quinacrine target [26]. However, high grade serous ovarian cancer is well-known for *TP53* mutations [48], which suggests the importance of alternative or intermediate signaling. Nucleostemin (GNL3) is a nucleolar protein that was initially reported to regulate p53 signaling and later found to also regulate pre-ribosomal rRNA processing [49]. Nucleostemin is highly expressed in several ovarian cancer cell lines (Fig. 25A). Quinacrine downregulated RPA194, the catalytic subunit of RNAPOL1 which correlates with decreases in nucleostemin (Fig. 25B). Whilst QC treatment downregulated RPA194 and NS, other nucleolar proteins such as UBF, TP53INP2 and FBL involved in ribosomal biogenesis were not affected (Fig. 25C). Based on the report by Wang et al., [50] that NS KD inhibited growth of SKOV3 cells both *in vivo* and *in vitro*, we knocked down NS expression using shRNA. Efficient KD of NS in OVCAR5 cells is shown in figure 25D. Decreased levels of nucleostemin inhibited colony forming abilities of OVCAR5 cells

Figure 25

(Figs. 25D and E). These results suggest QC induces nucleolar stress downregulates nucleostemin, which may be related to its cytotoxic mechanism in malignant cells.

Nucleolar stress is an emerging concept where nucleolar functions may sense various cellular stresses that impair ribosomal biogenesis and activate stress-responsive signaling [29]. Ribosomal biogenesis can be suppressed at RNA polymerase I initiation, pre-ribosomal RNA processing, and ribosomal assembly stages, which can also be impacted by many other changes such as physiochemical stressors and autophagy dysregulation (e.g. key autophagic protein LC3 localizes to nucleolus). The canonical output of nucleolar stress is p53 signaling activation. Our interim hypothesis that quinacrine induces nucleolar stress was based on quinacrine modulation of ribosomal biogenesis [46], autophagy [3], and p53 activation [26]. However, *TP53* is mutated in about half of all cancer types and >95% of high grade serous ovarian cancer tumors [48]. As quinacrine is cytotoxic in *TP53*-null ovarian cancer cells [18], we identified nucleostemin as an alternative downstream target of quinacrine. Nucleostemin is nucleolar protein that regulates both p53 signaling and pre-ribosomal RNA processing [49].

It is increasingly being recognized that RNA polymerase I-induced transcription of ribosome production in the nucleolus is consistently upregulated in cancer such that it is firmly believed that cancer cells are addicted to this process to accommodate for the increasing demand for protein synthesis, growth, and proliferation. This may open a therapeutic window to specifically target cancer cells with minimal effect to normal cells. Oncogenes such as Myc and loss of tumor suppressors, for example p53 result in hyper-activation of ribosomal biogenesis. Inhibition of ribosomal biogenesis leads to nucleolar stress response to promote p53 stabilization, cell cycle arrest, and apoptosis. All of these processes, when dysregulated in cancer culminate in phenotypic hallmarks of cancer cells.

In summary, our RNA sequencing analyses followed by a further pathway investigation demonstrate that quinacrine induces nucleolar stress in our therapy-refractory ovarian cancer models. Further investigation in needed to determine if these effects of quinacrine are specific to therapy-refractory cancer cells or to ovarian cancer cells in general independent of their response to chemotherapeutic agents. Understanding the anticancer mechanisms of quinacrine will promote well-designed clinical trials for repurposing this drug.

Aim 3: Examine the role of QC in chemoresponse using *in vivo* patient-derived xenografts (PDX) models. In this aim, we had proposed to examine the role of QC in chemoresistance *in vivo* in preclinical PDX of ovarian cancer using QC alone and in combination with conventional chemotherapy (carboplatin/paclitaxel) using 5 different chemoresistant PDX models that mimic patient response. Two categories of patients were selected based on their response to carboplatin/paclitaxel regimen-PH053 and PH112 (chemoresistant) PH070 and PH095 (chemoresistant /recurrent), two models of patients with sensitive to chemotherapy (PH081 and PH095). Each model will be treated with intraperitoneal carboplatin and paclitaxel. For this study, "platinum-resistant" is defined as patients who progressed within 12 months following surgery and chemotherapy (recurrence within 6 months of the last platinum-based therapy) and "platinum sensitive" is defined as patients who progressed after 18 months after their last platinum based therapy.

Treatments were started when palpated tumors reached 0.5–1 cm^2 indicated by the dotted line in Figures 26, 29 and 30 Ai) and Bi). Growth curves above this arbitrary line is considered resistant to chemotherapy and when the growth curves fall below the dotted line – the model is considered to be responsive to chemotherapy and the tested drug- in this case QC. Chemotherapy consists of carboplatin (51 mg·kg^{-1}) and paclitaxel (15 mg·kg^{-1}) administered intraperitoneally (IP) once a week for 4 weeks. QC 100mg/kg was administered by oral gavage every other day for 4 weeks. The tumor size was assessed weekly by ultrasound; three measurements per session for each animal were made and averaged.

Initially, we tested the effect of QC alone and in combination with chemotherapeutic combination in one PDX tumor model, PH070. PH070 is a recurrent tumor model. Four different groups of mice (ten mice in each group) were assigned for our study, control, QC alone, carboplatin/paclitaxel (CP alone), and combination of QC+CP. QC (100mg/kg) treatments were done using oral gavage, whereas chemotherapeutic drugs were given intraperitoneally. The treatments were scheduled for four weeks, and the tumor volume was measured on a weekly basis using ultrasound imaging method.

Our results indicated that the tumor volume as measured by ultrasound imaging showed that QC as monotherapy was not very effective in reducing the tumor burden at days 21-28 compared to the control untreated group (Fig. 26Bi). Also, mice treated with carboplatin/paclitaxel and the combination of QC + chemo was also not very effective (Figure 26Bi) as well as CP treatment alone. It is important to understand that the

Figure 26

PH070 is not just a resistant tumor, but a recurrent tumor. Ongoing studies with this model could be extended to study if QC as a maintenance therapy may be more effective in a recurrent model. One other factor to consider is whether oral gavaging is the best route of administration of this drug since QC preferentially accumulates more in the liver.
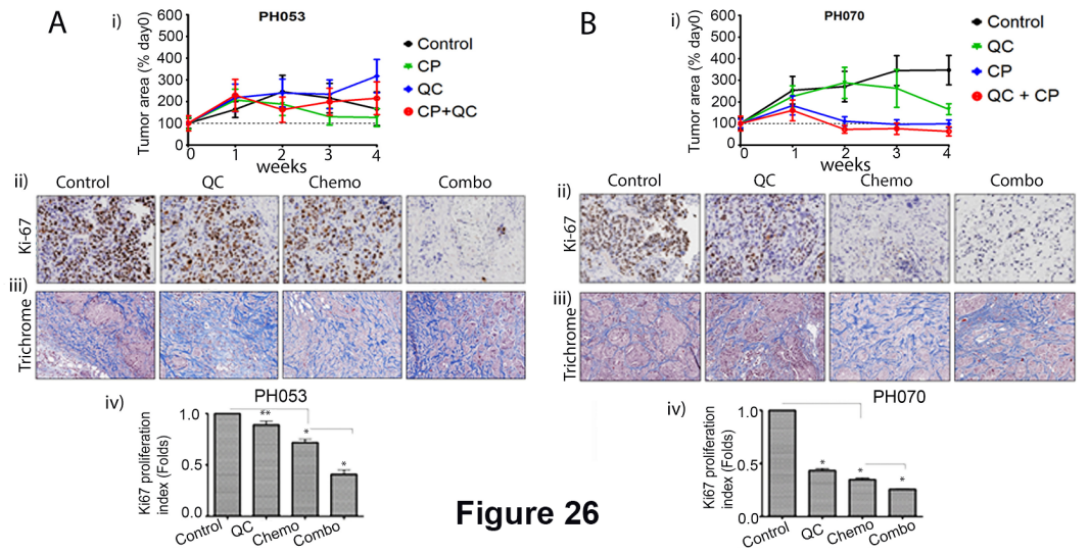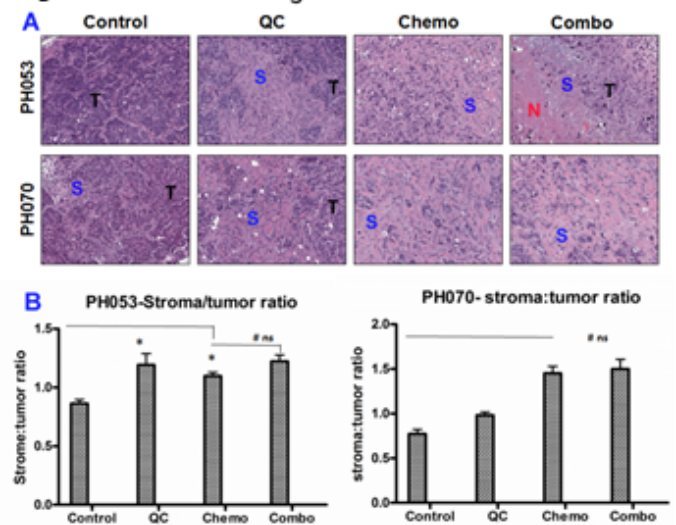
The PH070 model also produced ascites. 5 of 10 control mice had reduced volume of ascites. However, QC alone, CP alone and a combination of QC+CP was 100% effective in inhibiting ascites formation in the treatment groups.

In these ongoing studies we had proposed to test a second model, PH053 that is a resistant but not a recurrent tumor. Based on the ultrasound imaging, there is no change in tumor volume (Fig.26Ai). Based on our *in vitro* data, we had anticipated that QC as a monotherapy will be effective in the resistant models. However, in the PH053 PDX resistant model QC was not effective either as a monotherapy or in combination with CP.

Although these results were not very encouraging, we decided to analyze the tumors we derived from the 4 treatment groups for proliferative markers (Ki67 staining) to determine if the non-tumor shrinkage would be reflected in the proliferation/growth of these tumors. To our surprise, we saw a significant decrease in the proliferative index in the treated groups, specifically in the combination group compared to the control and or single agent treatment- more so in the recurrent PH070 model. Figs. 26Aii and Bii shows representative images of Ki67 staining in both the models with and without treatment in the tumorografts. The quantitation of Ki67 staining is shown below the IHC images for both the models.

Figure 27   H&E staining-PH053 and PH070

Since the Ki67 staining showed results that were not consistent with the reduction in the tumor volume as measured by ultrasound, we analyzed the H&E stained tumorografts to determine the extent of tumor vs stroma in these models. Our H&E staining of the xenografts showed extensive stromal invasion replacing the tumor cells in chemo, QC and in the QC+chemo (CP) treated groups compared to the control untreated groups. As shown in Figure 27A, there was more stromal invasion in the treated groups compared to control in both the models. The ratio between stromal and tumoral area is calculated using Image J program with fiji application (http://forum.imagej.net/) (Fig.27B) .These were statistically significant. S-Stroma, T-Tumor cells, N-Necrotic.

To clearly visualize the stromal compartment, we performed Masson's trichrome staining [51] as shown in Figure 26Aiii and 26Biii. There is clearly more stromal invasion in the treatment groups compared to the untreated control group. Recent reports analyzing the contribution of the mouse stroma to poor prognosis associated

with stem/serrated/mesenchymal (SSM) transcriptional subtype in colorectal cancers [52] and more in general to stem like poor prognosis signatures in the tumor compartment and hypoxia associated gene signature[53].

In order to understand the contribution of mouse stroma inducing resistance to QC treatment *in vivo*, we cultured PH053 and PH070 control tumors as short term primary cultures for one week and analyzed apoptotic and autophagy related markers by western blot as shown in Figure 28. Single cell suspension of PH053 and PH070 PDX tumor were grown for 48 hrs and treated with QC for 24 hrs. Human specific antibodies against LC3B, p62, Skp2 and cl-PARP were used. QC induces LC3BII and downregulates p62 and Skp2 and induces cl-PARP. In contrast to the *in vivo*

Figure28

data, QC treatment of these primary short-term cultures induced both autophagic and apoptotic cell death. These data seem to suggest that the increased stromal reaction upon QC and or Chemo treatment *in vivo* is one potential mechanism of resistance in these models. It is interesting to also note that the amount of stromal infiltration was much less in the PH070 PDX model compared to PH050. Also, the reduced Ki67 staining in the recurrent PH070 model upon QC treatment alone or in combination with chemo provides us with an opportunity to extend QC treatment as a maintenance therapy in the recurrent setting- a setting that will benefit patients with OvCa that come back with the recurrence- a patient population with limited options.
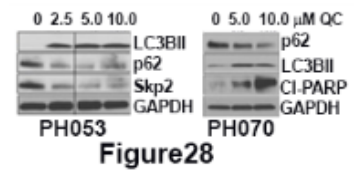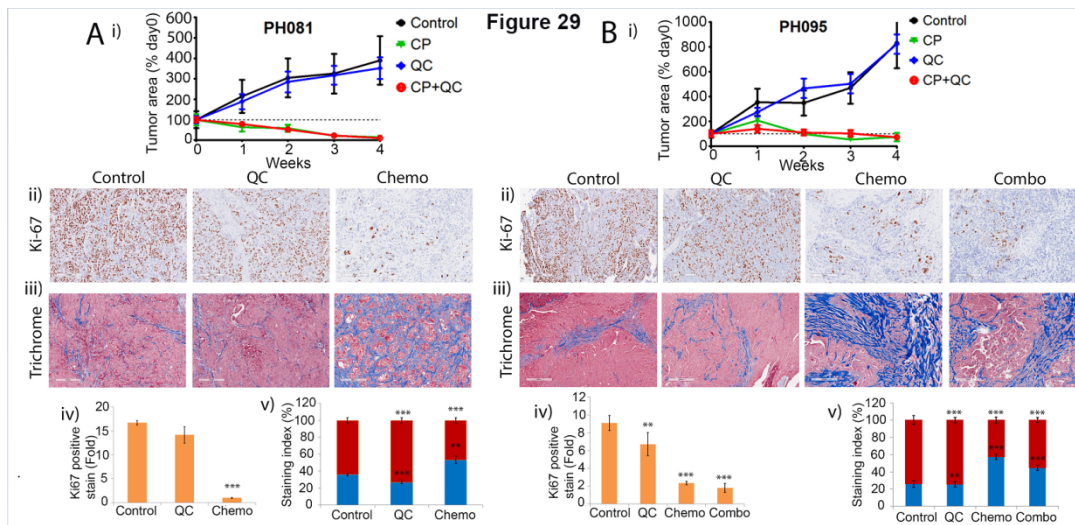
Following model PH053 and PH070 [Figs.26A & B], same mode and concentration of chemo (carboplatin/paclitaxel), QC and combo were administered in PH081, PH095 and PH112 PDX models. PH081

and PH095 (Figs. 29Ai and Bi) were both chemo sensitive group showed that chemo alone exhibited a remarkable efficacy against the tumor development when compared to QC alone but interestingly combo (chemo+QC) treatment nullified tumor proliferation which resulted in no tumor and complete tumor free animals(Figs. 29Ai and Bi). Ki-67 and Masson's trichrome stain revealed that the administration of chemo exhibited augmented tumor reticence and reduced Ki-67 proliferation marker expression when compared to control and QC treated (Fig. 29 Aii and Bii) which are statistically significant. Masson's trichrome stain revealed remarkable host stromal infiltration in Chemo and Combo treatment groups compared to control and QC treated alone mice (Figs. 29 A and B iv-v).which is similar to the results of PH053 and PH070.

Model PH112 is similar to our other models, QC alone was not effective in reducing the tumor burden compared to the untreated control group but also Chemo alone and in combination with QC was more effective in decreasing the tumor burden compared to the control and QC alone groups (Fig. 30Ai). Ki-67 and Masson's trichrome stain (Fig.30Aii-v) results were similar to other models.

With this model, we extended our study to maintain QC treatment alone for an extended length of time to determine if QC given after the termination of chemotherapy regimen may have a desirable effect in preventing the re-growth of tumors in the QC + CP arm. After the termination of chemo treatment (28 days), we randomized the mice into two groups. The control arm received no treatment while the maintenance arm continued to receive QC (100mg/kg) treatments for another 42 days. There was no change in tumor volume during 28 days between QC+CP arm and CP arm, but QC maintenance showed a slight reduction in tumor burden compared to the no treatment control group- but it was not statistically significant (Fig. 30Bi). Also, the tumor proliferation index was significantly lower when compared to that of control as assessed by Ki-67 stain (Fig.30Bii&iv). Most importantly host stromal infiltration was noticed markedly in treated group compared to control untreated mice as verified by trichrome stain (Fig.30Biii & v).

Figure 30
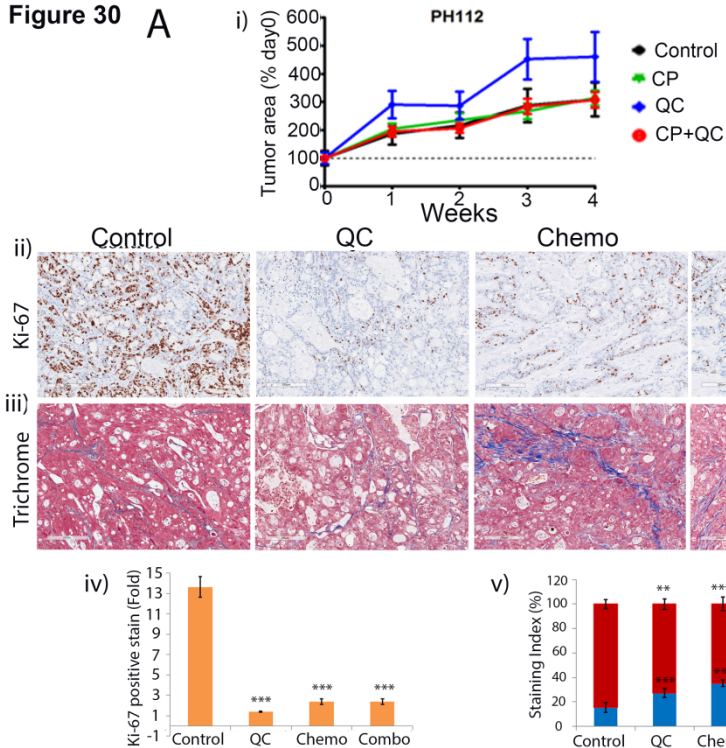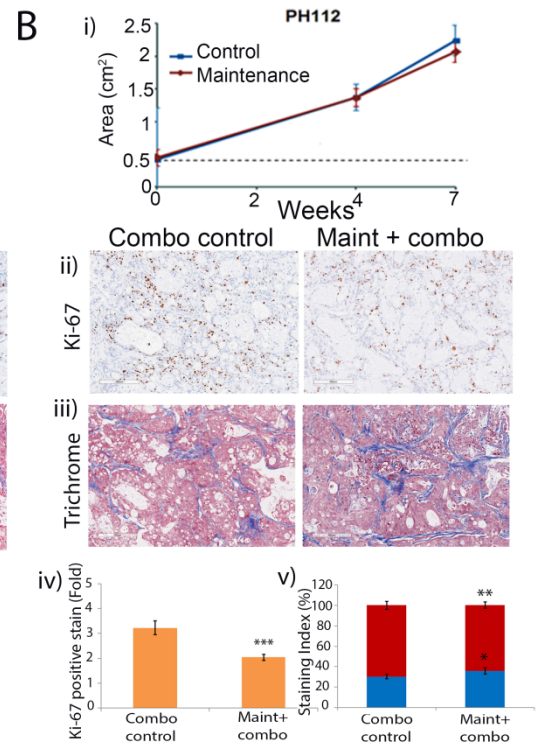
Collectively, <u>the results from the PDX models suggest</u> that irrespective of the underlying chemoresponse of the PDX tumors (sensitive, resistant or recurrent), <u>QC a monotherapy was not effective in reducing the tumor volume</u>. In the two sensitive models (PH081 and 095), as expected the chemo treatment alone was very effective and the addition of QC did not potentiate this effectiveness in terms of tumor volume. However, we noticed in all PDX models there was frequent infiltration of host stroma in treated group which may contribute to resistance to chemotherapy. It has been shown that interactions between the neoplastic cells and non-neoplastic stromal cells stimulate the extensive desmoplastic reaction and fibrosis that is responsible for the tumor recurrence and resistance to drug treatment [54,55]. Recently, the novel chemotherapeutic agent nab-paclitaxel became available for the treatment cancer [56]. Nab-paclitaxel has an additional effect on decreased collagen, CAF and tumor stroma disruption [57]. Accordingly, the combination of nab-paclitaxel with carboplatin or QC may lead to enhanced antitumor activity.

What opportunities for training and professional development has the project provided? – It has provided training to the postdoc to work with the PDX model

How were the results disseminated to communities of interest? -Nothing to Report

What do you plan to do during the next reporting period to accomplish the goals?

We will continue to complete the experiments listed in Aims 1 and 2 in year 2 and also test the effect of QC alone and in combination with chemo in two sensitive PDX models

IMPACT: What was the impact on the development of the principal discipline(s) of the project?
Based on the preliminary results from our preclinical PDX models, QC treatment alone and in combination with chemotherapy results in the increase in the infiltration of mouse stroma compared to untreated control. Future studies will concentrate on the biomarkers upregulated in the mouse stroma. The contribution of this increased stromal component to resistance to chemotherapy or targeted therapy may lead to testing QC in combination with drugs that specifically target the bioactive stroma in future studies.

What was the impact on other disciplines? *Nothing to Report.*

What was the impact on technology transfer? *Nothing to Report.*

What was the impact on society beyond science and technology? *Nothing to Report.*

CHANGES/PROBLEMS: *Nothing to Report. One of the concerns is the increase in stromal infiltration in treated groups.*

Actual or anticipated problems or delays and actions or plans to resolve them – Nothing to report

Changes that had a significant impact on expenditures – Nothing to report

Significant changes in use or care of human subjects, vertebrate animals, biohazards, and/or select agents -*Nothing to report*

Significant changes in use or care of human subjects- Not applicable

Significant changes in use or care of vertebrate animals.- Nothing to report

Significant changes in use of biohazards and/or select agents- Nothing to report

PRODUCTS: *"Nothing to Report."*

Website(s) or other Internet site(s)- Nothing to report

Technologies or techniques- Noting to report

Inventions, patent applications, and/or licenses- Nothing to report

Other Products- Nothing to report

PARTICIPANTS & OTHER COLLABORATING ORGANIZATIONS

What individuals have worked on the project?

Provide the following information for: (1) PDs/PIs- No change

Name:	Dr. Debarshi Roy*
Project Role:	*Post Doctoral Fellow*
Nearest person month worked:	*24*
Contribution to Project:	*Worked on the PDX models*
Name:	Dr. Deokbeom Jung
Project Role:	*Post Doctoral Fellow*
Nearest person month worked:	*8*
Contribution to Project:	*Worked the generation of p62 deletion constructs and INP2 related experiments*
Name:	*Dr. Prabhu Thirusangu*
Project Role:	*Post Doctoral Fellow*
Nearest person month worked:	*8*

Contribution to Project:	*Worked the role of QC-induced CTSL to degrade p62*

Dr. Roy after the first seven months is now supported on an OCRF postdoctoral award.

Dr.Jung was hired to continue the work on the project

Dr. Prabhu Thirusangu was hired after Dr. Jung left to complete the experiments related to QC-induced upregulation of cathepsin L during the no-cost extension of this grant

What other organizations were involved as partners? – *None*

Publications

Publication-Year 1
Quinacrine promotes autophagic cell death and chemosensitivity in ovarian cancer and attenuates tumor growth. Khurana A, Roy D, Kalogera E, Mondal S, Wen X, He X, Dowdy S, Shridhar V. Oncotarget. 2015 Nov 3;6(34):36354-69. doi: 10.18632/oncotarget.5632.- **Appendix attachment 1**

Publication-Year 2

Repurposing an Old Antimalarial Drug. Eleftheria Kalogera, M.D.; Debarshi Roy; Ashwani Khurana; Susmita Mondal; Amy Weaver; Xiaoping He; Sean Dowdy and **Viji Shridhar***. Quinacrine in Endometrial Cancer: Repurposing an Old Antimalarial Drug. Gynecologic Oncology 146 (2017) 187-195. **Appendix attachment 2**

Publication –Year 3
Jung Deokbeum, Ashwani Khurana, Eleftheria Kalogera, Jamie Bakkum-Gamez, Debarshi Roy, Jeremy Chien and Viji Shridhar. Quinacrine upregulates p21/p27 independent of p53 through autophagy-mediated downregulation of p62-Skp2 axis in ovarian cancer. Sci Rep. 2018 Feb 6;8(1):2487. doi: 10.1038/s41598-018-20531- **Appendix attachment 3**.

Publication –Year 4
 (Invited review article on Repurposing drugs)
Derek B. Oien*, Christopher L. Pathoulas*, Upasana Ray*, Prabhu Thirusangu, Eleftheria Kalogera, and **Viji Shridhar.** Repurposing Quinacrine for Treatment of Refractory Cancer. Seminars in Cancer Biology **Appendix attachment 4.**

Manuscripts under preparation

1. Derek B. Oien, Ling Jin, Joseph E. Kumka, Christopher L. Pathoulas, Sayantani Sarkar Bhattacharya, Debarshi Roy, Ashwani Khurana, Yinan Xiao, Jeremy Chien and **Viji Shridhar.** Quinacrine induced transcriptional changes in chemotherapy-resistant ovarian cancer.
2. Prabhu Thirusangu*, Christopher Pathoulas*, Ling Jin, Ashwani Khurana, Yinan Xiao and Viji Shridhar. Quinacrine-Induced Upregulation of CTSL Promotes Lysosomal Membrane Permeability-Mediated Cell Death in Ovarian Cancer Cells

3. **Conference presentations.**
   1. Debarshi Roy, Ashwani Khurana, Eleftheria Kalogera, Xuyang Wen, Susmita Mondal Sean Dowdy, **Viji Shridhar.** Repurposing Anti-Malarial drug Quinacrine to treat Ovarian Cancer. Advances in Ovarian Cancer Research: Exploiting Vulnerabilities special conference, being held from Saturday, October 17- 20, 2015, Orlando, FL. Abstract #B74.
   2. Debarshi Roy, Ashwani Khurana, Eleftheria Kalogera, Xuyang Wen and **Viji Shridhar**. Can we repurpose anti-malarial drug quinacrine to treat ovarian cancer? Global Cancer Summit-2015 November 18-20, Bangalore, India- **Oral Presentation.**

3. Debarshi Roy, Ashwani Khurana, Eleftheria Kalogera, Xuyang Wen, and **Viji Shridhar**. Can we repurpose anti-malarial drug quinacrine to treat ovarian cancer? Global Cancer Summit, Bengaluru, India. Nov18/2015- **Oral Presentation.**
4. Eleftheria Kalogera, Debarshi Roy, Ashwani Khurana, Susmita Mondal, Xiaoping He, Sean C. Dowdy and **Viji Shridhar.** Abstract 261: Quinacrine in endometrial cancer: repurposing an old antimalarial drug. Proceedings: AACR 107th Annual Meeting 2016; April 16-20, 2016; New Orleans, LA.

REFERENCES

1   Herzog, T. J. Recurrent ovarian cancer: how important is it to treat to disease progression? *Clinical cancer research : an official journal of the American Association for Cancer Research* **10**, 7439-7449, doi:10.1158/1078-0432.CCR-04-0683 (2004).

2   Koldsland, S., Svennevig, J. L., Lehne, G. & Johnson, E. Chemical pleurodesis in malignant pleural effusions: a randomised prospective study of mepacrine versus bleomycin. *Thorax* **48**, 790-793 (1993).

3   Khurana, A. *et al.* Quinacrine promotes autophagic cell death and chemosensitivity in ovarian cancer and attenuates tumor growth. *Oncotarget* **6**, 36354-36369, doi:10.18632/oncotarget.5632 (2015).

4   White, E. J. *et al.* Autophagy regulation in cancer development and therapy. *American journal of cancer research* **1**, 362-372 (2011).

5   Sui, X. *et al.* Autophagy and chemotherapy resistance: a promising therapeutic target for cancer treatment. *Cell death & disease* **4**, e838, doi:10.1038/cddis.2013.350 (2013).

6   Nowak, J. *et al.* The TP53INP2 protein is required for autophagy in mammalian cells. *Molecular biology of the cell* **20**, 870-881, doi:10.1091/mbc.E08-07-0671 (2009).

7   Peltonen, K. *et al.* A targeting modality for destruction of RNA polymerase I that possesses anticancer activity. *Cancer Cell* **25**, 77-90, doi:10.1016/j.ccr.2013.12.009 (2014).

8   Xu, Y. *et al.* TP53INP2/DOR, a mediator of cell autophagy, promotes rDNA transcription via facilitating the assembly of the POLR1/RNA polymerase I preinitiation complex at rDNA promoters. *Autophagy* **12**, 1118-1128, doi:10.1080/15548627.2016.1175693 (2016).

9   Huang, R. *et al.* Deacetylation of nuclear LC3 drives autophagy initiation under starvation. *Mol Cell* **57**, 456-466, doi:10.1016/j.molcel.2014.12.013 (2015).

10   Mathew, R. *et al.* Autophagy suppresses tumorigenesis through elimination of p62. *Cell* **137**, 1062-1075, doi:10.1016/j.cell.2009.03.048 (2009).

11   Nihira, K. *et al.* An activation of LC3A-mediated autophagy contributes to de novo and acquired resistance to EGFR tyrosine kinase inhibitors in lung adenocarcinoma. *The Journal of pathology*, doi:10.1002/path.4354 (2014).

12   Luo, R. Z. *et al.* Accumulation of p62 is associated with poor prognosis in patients with triple-negative breast cancer. *OncoTargets and therapy* **6**, 883-888, doi:10.2147/OTT.S46222 (2013).

13   Yu, H. *et al.* p62/SQSTM1 involved in cisplatin resistance in human ovarian cancer cells by clearing ubiquitinated proteins. *European journal of cancer* **47**, 1585-1594, doi:10.1016/j.ejca.2011.01.019 (2011).

14   Droga-Mazovec, G. *et al.* Cysteine cathepsins trigger caspase-dependent cell death through cleavage of bid and antiapoptotic Bcl-2 homologues. *The Journal of biological chemistry* **283**, 19140-19150, doi:10.1074/jbc.M802513200 (2008).

15   Turk, B. & Stoka, V. Protease signalling in cell death: caspases versus cysteine cathepsins. *FEBS letters* **581**, 2761-2767, doi:10.1016/j.febslet.2007.05.038 (2007).

16   Brunk, U. T., Neuzil, J. & Eaton, J. W. Lysosomal involvement in apoptosis. *Redox report : communications in free radical research* **6**, 91-97, doi:10.1179/135100001101536094 (2001).

17   Guicciardi, M. E. *et al.* Cathepsin B contributes to TNF-alpha-mediated hepatocyte apoptosis by promoting mitochondrial release of cytochrome c. *The Journal of clinical investigation* **106**, 1127-1137, doi:10.1172/JCI9914 (2000).

18   Jung, D. *et al.* Quinacrine upregulates p21/p27 independent of p53 through autophagy-mediated downregulation of p62-Skp2 axis in ovarian cancer. *Sci Rep* **8**, 2487, doi:10.1038/s41598-018-20531-w (2018).

19   Lamb, J. *et al.* The Connectivity Map: using gene-expression signatures to connect small molecules, genes, and disease. *Science* **313**, 1929-1935, doi:10.1126/science.1132939 (2006).

20   Lamb, J. The Connectivity Map: a new tool for biomedical research. *Nature reviews. Cancer* **7**, 54-60, doi:10.1038/nrc2044 (2007).

21   Trapnell, C. *et al.* Differential gene and transcript expression analysis of RNA-seq experiments with TopHat and Cufflinks. *Nature protocols* **7**, 562-578, doi:10.1038/nprot.2012.016 (2012).

22   Anders, S., Pyl, P. T. & Huber, W. HTSeq--a Python framework to work with high-throughput sequencing data. *Bioinformatics* **31**, 166-169, doi:10.1093/bioinformatics/btu638 (2015).

23   Simon, R. *et al.* Analysis of Gene Expression Data Using BRB-Array Tools. *Cancer Informatics* **3**, 117693510700300022, doi:10.1177/117693510700300022 (2007).

24   Love, M. I., Huber, W. & Anders, S. Moderated estimation of fold change and dispersion for RNA-seq data with DESeq2. *Genome Biol* **15**, 550, doi:10.1186/s13059-014-0550-8 (2014).

25   Zhou, Y. *et al.* Metascape provides a biologist-oriented resource for the analysis of systems-level datasets. *Nat Commun* **10**, 1523, doi:10.1038/s41467-019-09234-6 (2019).

26   Gurova, K. V. *et al.* Small molecules that reactivate p53 in renal cell carcinoma reveal a NF-kappaB-dependent mechanism of p53 suppression in tumors. *Proceedings of the National Academy of Sciences of the United States of America* **102**, 17448-17453, doi:10.1073/pnas.0508888102 (2005).

27   Lorenzi, P. L. *et al.* Asparagine synthetase is a predictive biomarker of L-asparaginase activity in ovarian cancer cell lines. *Molecular cancer therapeutics* **7**, 3123-3128, doi:10.1158/1535-7163.MCT-08-0589 (2008).

28   Krall, A. S., Xu, S., Graeber, T. G., Braas, D. & Christofk, H. R. Asparagine promotes cancer cell proliferation through use as an amino acid exchange factor. *Nat Commun* **7**, 11457, doi:10.1038/ncomms11457 (2016).

29   Yang, K., Yang, J. & Yi, J. Nucleolar Stress: hallmarks, sensing mechanism and diseases. *Cell Stress* **2**, 125-140, doi:10.15698/cst2018.06.139 (2018).

30   Chung, K. Y. *et al.* Block of proliferation 1 (BOP1) plays an oncogenic role in hepatocellular carcinoma by promoting epithelial-to-mesenchymal transition. *Hepatology* **54**, 307-318, doi:10.1002/hep.24372 (2011).

31   Song, J. *et al.* The candidate tumor suppressor CST6 alters the gene expression profile of human breast carcinoma cells: down-regulation of the potent mitogenic, motogenic, and angiogenic factor autotaxin. *Biochemical and biophysical research communications* **340**, 175-182, doi:10.1016/j.bbrc.2005.11.171 (2006).

32   Eskelinen, E. L. & Saftig, P. Autophagy: a lysosomal degradation pathway with a central role in health and disease. *Biochimica et biophysica acta* **1793**, 664-673, doi:10.1016/j.bbamcr.2008.07.014 (2009).

33   Hossain, M. Z. *et al.* DNA-intercalators causing rapid re-expression of methylated and silenced genes in cancer cells. *Oncotarget* **4**, 298-309 (2013).

34   Beleford, D., Rattan, R., Chien, J. & Shridhar, V. High temperature requirement A3 (HtrA3) promotes etoposide- and cisplatin-induced cytotoxicity in lung cancer cell lines. *The Journal of biological chemistry* **285**, 12011-12027, doi:10.1074/jbc.M109.097790 (2010).

35   Staub, J. *et al.* Epigenetic silencing of HSulf-1 in ovarian cancer:implications in chemoresistance. *Oncogene* **26**, 4969-4978, doi:10.1038/sj.onc.1210300 (2007).

36   Guo, C. *et al.* 9-Aminoacridine-based anticancer drugs target the PI3K/AKT/mTOR, NF-kappaB and p53 pathways. *Oncogene* **28**, 1151-1161, doi:10.1038/onc.2008.460 (2009).

37   Syed, V. *et al.* Identification of ATF-3, caveolin-1, DLC-1, and NM23-H2 as putative antitumorigenic, progesterone-regulated genes for ovarian cancer cells by gene profiling. *Oncogene* **24**, 1774-1787, doi:10.1038/sj.onc.1207991 (2005).

38   Murph, M. M. *et al.* Lysophosphatidic acid-induced transcriptional profile represents serous epithelial ovarian carcinoma and worsened prognosis. *PloS one* **4**, e5583, doi:10.1371/journal.pone.0005583 (2009).

39   Hosios, A. M. *et al.* Amino Acids Rather than Glucose Account for the Majority of Cell Mass in Proliferating Mammalian Cells. *Developmental cell* **36**, 540-549, doi:10.1016/j.devcel.2016.02.012 (2016).

40   Okamoto, N. *et al.* Maintenance of tumor initiating cells of defined genetic composition by nucleostemin. *Proc Natl Acad Sci U S A* **108**, 20388-20393, doi:10.1073/pnas.1015171108 (2011).

41   Ninomiya, N. *et al.* Involvement of phosphatidylinositol 3-kinase in Fc gamma receptor signaling. *J Biol Chem* **269**, 22732-22737 (1994).

42   Jeon, Y. K. *et al.* The heat-shock protein 90 inhibitor, geldanamycin, induces apoptotic cell death in Epstein-Barr virus-positive NK/T-cell lymphoma by Akt down-regulation. *J Pathol* **213**, 170-179, doi:10.1002/path.2219 (2007).

43   Maher, P. & Davis, J. B. The role of monoamine metabolism in oxidative glutamate toxicity. *J Neurosci* **16**, 6394-6401 (1996).

44   Hui, J. Y. & Taylor, S. L. Inhibition of in vivo histamine metabolism in rats by foodborne and pharmacologic inhibitors of diamine oxidase, histamine N-methyltransferase, and monoamine oxidase. *Toxicol Appl Pharmacol* **81**, 241-249 (1985).

45   Siddique, H. R. & Saleem, M. Role of BMI1, a stem cell factor, in cancer recurrence and chemoresistance: preclinical and clinical evidences. *Stem Cells* **30**, 372-378, doi:10.1002/stem.1035 (2012).

46   Eriksson, A. *et al.* Drug screen in patient cells suggests quinacrine to be repositioned for treatment of acute myeloid leukemia. *Blood Cancer J* **5**, e307, doi:10.1038/bcj.2015.31 (2015).

47   Burger, K. *et al.* Chemotherapeutic drugs inhibit ribosome biogenesis at various levels. *J Biol Chem* **285**, 12416-12425, doi:10.1074/jbc.M109.074211 (2010).

48   Oien, D. B. & Chien, J. TP53 mutations as a biomarker for high-grade serous ovarian cancer: are we there yet? *Translational Cancer Research* **5**, S264-268 (2016).

49   Romanova, L. *et al.* Critical role of nucleostemin in pre-rRNA processing. *J Biol Chem* **284**, 4968-4977, doi:10.1074/jbc.M804594200 (2009).

50   Wang, J., Wang, L., Ji, Q., Zhu, H. & Han, S. Knockdown of Nucleostemin in an ovarian cancer SKOV-3 cell line and its effects on cell malignancy. *Biochem Biophys Res Commun* **487**, 262-267, doi:10.1016/j.bbrc.2017.04.046 (2017).

51   Masson Trichrome & Verhoeff Stain. vetmed.vt.edu. URL: http://education.vetmed.vt.edu/Curriculum/VM8054/Labs/Lab2/Examples/exvrmass.htm.

52   Isella, C. *et al.* Stromal contribution to the colorectal cancer transcriptome. *Nat Genet* **47**, 312-319, doi:10.1038/ng.3224 (2015).

53   Bradford, J. R. *et al.* Whole transcriptome profiling of patient-derived xenograft models as a tool to identify both tumor and stromal specific biomarkers. *Oncotarget*, doi:10.18632/oncotarget.8014 (2016).

54   Chu, G. C., Kimmelman, A. C., Hezel, A. F. & DePinho, R. A. Stromal biology of pancreatic cancer. *J Cell Biochem* **101**, 887-907, doi:10.1002/jcb.21209 (2007).

55   Neesse, A. *et al.* Stromal biology and therapy in pancreatic cancer. *Gut* **60**, 861-868, doi:10.1136/gut.2010.226092 (2011).

56   Daniel D. Von Hoff, R. K. R., Mitesh J. Borad, Daniel A. Laheru, Lon S. Smith, Tina E. Wood,, Ronald L. Korn, N. D., Vuong Trieu, Jose L. Iglesias, Hui Zhang, Patrick Soon-Shiong, Tao Shi, & N.V. Rajeshkumar, A. M., and Manuel Hidalgo. Gemcitabine Plus nab-Paclitaxel Is an Active Regimen in Patients With Advanced Pancreatic Cancer: A PhaseI/II Trial. *Journal of Clinical oncology* **29** (2011).

57   Alvarez, R. *et al.* Stromal disrupting effects of nab-paclitaxel in pancreatic cancer. *Br J Cancer* **109**, 926-933, doi:10.1038/bjc.2013.415 (2013).

Quinacrine promotes autophagic cell death and chemosensitivity in ovarian cancer and attenuates tumor growth

Ashwani Khurana[1,*], Debarshi Roy[1,*], Eleftheria Kalogera[2,*], Susmita Mondal[1], Xuyang Wen[1], Xiaoping He[1], Sean Dowdy[2], Viji Shridhar[1]

[1]Department of Experimental Pathology, Mayo Clinic College of Medicine, Rochester, MN, USA

[2]Department of Obstetrics and Gynecology, Mayo Clinic College of Medicine, Rochester, MN, USA

[*]These authors have contributed equally to this work

Correspondence to:
Viji Shridhar, **e-mail:** shridhar.vijayalakshmi@mayo.edu

ABSTRACT

A promising new strategy for cancer therapy is to target the autophagic pathway. In the current study, we demonstrate that the antimalarial drug Quinacrine (QC) reduces cell viability and promotes chemotherapy-induced cell death in an autophagy-dependent manner more extensively in chemoresistant cells compared to their isogenic chemosensitive control cells as quantified by the Chou-Talalay methodology. Our preliminary data, *in vitro* and *in vivo*, indicate that QC induces autophagy by downregulating p62/SQSTM1 to sensitize chemoresistant cells to autophagic- and caspase-mediated cell death in a p53-independent manner. QC promotes autophagosome accumulation and enhances autophagic flux by clearance of p62 in chemoresistant ovarain cancer (OvCa) cell lines to a greater extent compared to their chemosensitive controls. Notably, p62 levels were elevated in chemoresistant OvCa cell lines and knockdown of p62 in these cells resulted in a greater response to QC treatment. Bafilomycin A, an autophagy inhibitor, restored p62 levels and reversed QC-mediated cell death and thus chemosensitization. Importantly, our *in vivo* data shows that QC alone and in combination with carboplatin suppresses tumor growth and ascites in the highly chemoresistant HeyA8MDR OvCa model compared to carboplatin treatment alone. Collectively, our preclinical data suggest that QC in combination with carboplatin can be an effective treatment for patients with chemoresistant OvCa.

INTRODUCTION

Ovarian cancer remains a leading cause of death among women with gynecological cancers despite significant advances in the systemic as well as surgical cancer treatment modalities [1]. Ovarian cancer patients with advanced or recurrent disease frequently develop chemoresistance against paclitaxel- and platinum-based therapies which further contributes to disease progression, recurrence and, ultimately, high mortality [2]. In order to overcome the shortcomings of standard chemotherapeutic modalities, several alternative strategies including targeted therapies, multi-drug combination treatments as well as drug repurposing are being investigated. Although the majority of these therapeutic compounds induce apoptosis through type I programmed cell death (PCD), compounds

inducing type II PCD have also been shown to be effective as anti-cancer agents [3]. Predominant feature of type II or autophagic cell death is the appearance of double-membrane vesicles engulfing cytoplasmic organelles which are eventually degraded by lysosomal hydrolytic enzymes. Extensive autophagic activity leads eventually to cell death which, however, differs from the homeostatic autophagy associated with normal cellular organelle turnover [4]. Under basal cellular conditions, autophagy maintains the cellular turnover of proteins and organelles via lysosomal degradation whereas, under nutrient-deprived stress conditions such as oxidative and/or endoplasmic reticulum stress [5], it promotes cellular adaptation by supplying macromolecules for survival [6]. Various strategies have been investigated to explore the potential of autophagy as a putative anticancer modality including development of

chemical inhibitors of autophagy as well as genetic silencing of key autophagy proteins [7]. Several studies have shown that inhibiting autophagy using anti-malarial compounds such as chloroquine (CQ) and hydroxychloroquine while combining these compounds with frontline therapeutic agents such as cisplatin and taxol results in significant inhibition of tumor growth [8, 9]. Furthermore, other studies have indicated that drug-induced autophagy promotes synergy with the frontline therapy [10, 11]. Similarly it has been shown that genetic silencing of key autophagic proteins such as beclin 1 (ATG6) favors survival and decreases resistance to chemotherapy [12–14]. High beclin 1 and LC3 levels in ovarian tumors have been associated with improved overall survival [15, 16].

The two most common markers and key players associated with autophagy are LC3B and p62 [17]. Events leading to the conversion of LC3BI to LC3BII and clearance of p62 are considered hallmarks of the autophagic flux [18]. The p62 protein, also called sequestosome 1 (SQSTM1), is an ubiquitin-binding scaffold protein that co-localizes with ubiquitinated protein aggregates and is required both for the formation as well as the degradation of polyubiquitin-containing bodies by autophagy. p62 binds to LC3B through the LIR (LC3 Interacting Region) domain and is then degraded during the autophagic process [19]. Other studies have shown that elimination of p62 by autophagy suppresses tumorigenesis [20] *in vivo* and cell viability of several human carcinoma cell lines *in vitro* [21]. Since p62 accumulates when autophagy is inhibited, and alternatively, p62 levels decrease when autophagy is induced, p62 surfaces as a promising marker to study autophagic flux. Selective degradation of p62 is clinically relevant since high levels of p62 found in various types of tumor have been associated with poor prognosis and survival [22]. Studies show that the cisplatin-resistant SKOV3/DDP OvCa cells express higher levels of p62 and that siRNA downregulation of p62 in these cells resensitized them to cisplatin-mediated cytotoxicity [23].

Previous investigations have provided evidence to suggest a promising role of the antimalarial drug quinacrine (QC) in cancer treatment. The acridine "backbone" of QC allows the drug to intercalate into stacked DNA base pairs [24]. QC is known to impair DNA repair activity in a mechanism similar to other topoisomerase inhibitors, [25]. In addition, QC inhibits the FACT (Facilitates Chromatin Transcription) complex that is required for NF-kB transcriptional activity and modulates the arachidonic acid (AA) pathway [26]. Interestingly, QC has been shown to bind and inhibit proteins involved in multidrug resistance [27–32]. More importantly, it targets several signaling pathways simultaneously by affecting autophagy, apoptosis, p53, NFkB, AKT and methylation-related pathways [27, 28, 32–35]. While QC has been shown to modulate autophagy in a p53-dependent manner in colon cancer cell lines,

[36] in our study QC induced autophagic cell death in a p53- independent manner in OvCa cells. Although QC has been shown to effectively block proliferation of several cancer cell lines both *in vitro* and *in vivo*, to our knowledge, there are no *in vitro* or *in vivo* studies on the use of QC alone or in combination with standard therapy against OvCa.

In this study, we have shown that QC promotes autophagic flux across a variety of OvCa cell lines and induces cell death both in a caspase-dependent as well as independent manner utilizing autophagic-mediated cell death to enhance carboplatin sensitivity. This effect was more pronounced in cisplatin-resistant OvCA cells compared to their sensitive controls both *in vitro* and *in vivo* experimental setting. These preclinical data have direct clinical implications for OvCa patients with chemoresistant disease for which only limited therapeutic options exist.

In this study, we focused our investigation on the anticancer potential of the antimalarial drug QC against OvCA. Based on prior findings, we hypothesized that QC would exert its anticancer effect against OvCA by inducing an autophagic-mediated cell death and that by doing so it would result in restoring cisplatin-sensitivity.

RESULTS

Quinacrine inhibits cell growth and induces cell death in ovarian cancer cells

Isogenic pairs of OvCA cell lines [OV2008 (chemosensitive) and C13 (chemoresistant) cells derived from OV2008 [37]; HEYA8 (chemosensitive) and HEYA8MDR (chemoresistant) [38, 39] cells] were evaluated for the effect of QC on cell growth by colony formation and MTT assays. Colony formation assays (Figure 1A) were performed after treating the cells with 0, 0.125, 0.250, 0.500, 1.0, and 2.0 μM of QC for 24 hours. MTT assays (supplemental data) were performed after treating the cells with 0, 5.0, and 10.0 μM of QC for 24, 48 and 72 hours-time intervals. Increasing concentrations of QC effectively inhibited colony forming units with maximal inhibition at a QC concentration of 1.0 and 2.0 μM. Similarly, cell growth was also inhibited as early as 24 hours of QC treatment with IC_{50} determined from the MTT assays in all the cell lines tested were between 2.5 μM and 4 μM (Figure supplemental S1). To determine if QC treatment induced apoptotic cell death, we treated cells with 2.5, 5.0 and 7.5 μM QC for 24 hours and the apoptotic cell population was determined with the annexin/PI staining method using flow cytometric analysis. The apoptotic cell population upon QC treatment reflecting early and late apoptosis as shown in Figure 1B indicates that QC only treatment induces apoptosis. Similarly, western blot analyses of cell lysates of OV2008/C13 and Hey A8/HeyA8MDR cells treated with 5.0 and
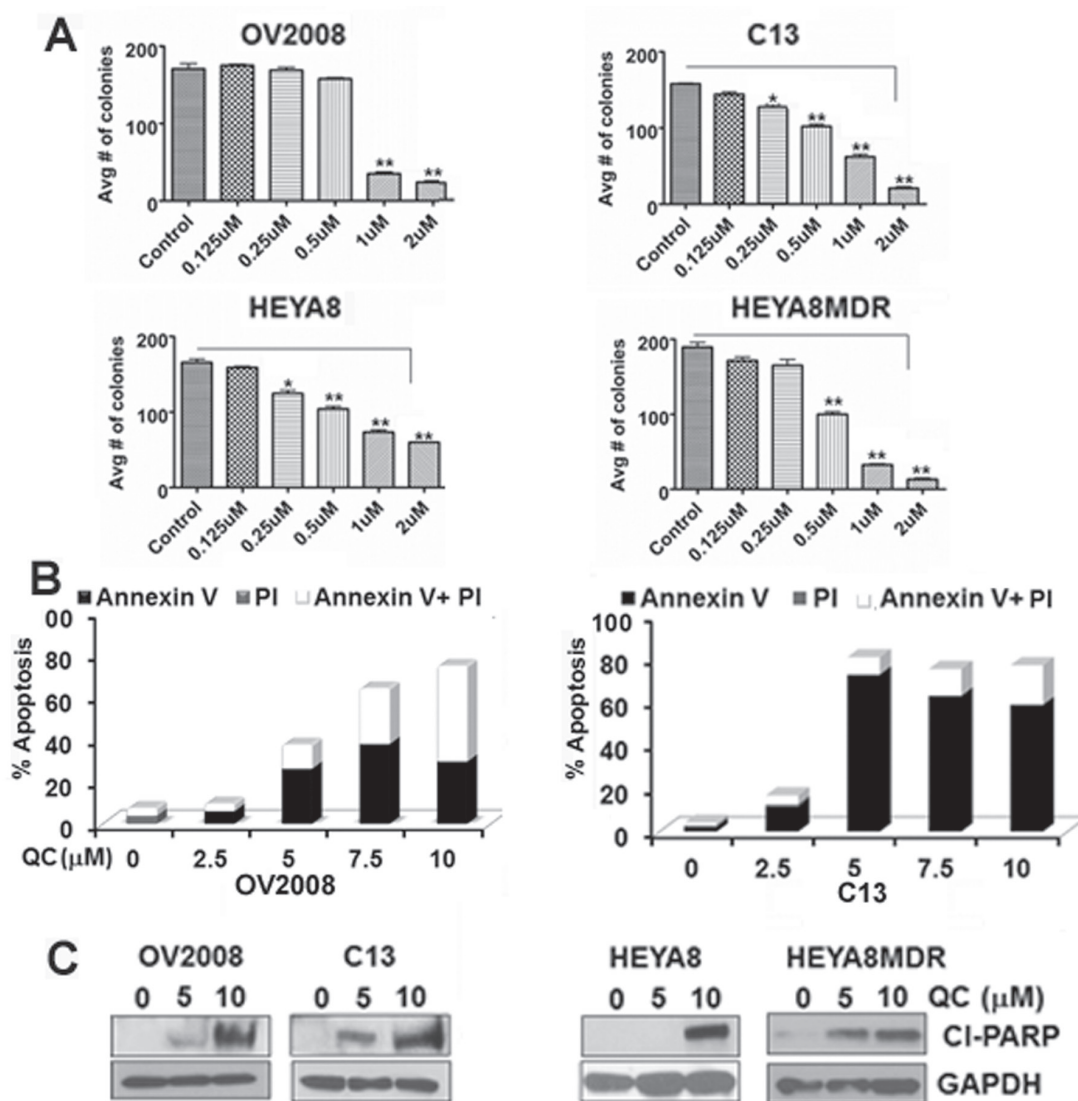
Figure 1: A. OV2008, C13, HeyA8 and HeyA8MDR cells plated in six well plates in triplicates were treated with indicated concentrations of QC for 24 hours. The resulting colonies were counted after fixing and stained with crystal violet in methanol and photographed. Data are representative of three independent experiments. *P* values were calculated using student *t* test. *p value = < 0.001, **p value = < 0.0001 **B.** AnnexinV/Propidium Iodide (PI) staining of OV2008, C13, HeyA8 and HeyA8MDR cells treated with Quinacrine for indicated concentration for 24 hours. **C.** Immunoblot analysis of cell lysates obtained from OV2008, C13, HeyA8 and HeyA8MDR cells treated with Quinacrine (0, 5.0 μM, 10.0 μM) for 24 hours with anti-cleaved PARP and anti-GAPDH antibodies. Data are representative of three independent experiments.

10 μM QC showed the presence of cleaved PARP corroborating the previous finding that QC promotes apoptosis in a caspase-dependent manner (Figure 1C).

Quinacrine induces autophagic clearance of p62/SQSTM, upregulates the autophagic marker LC3B and induces apoptosis

Since other antimalarial drugs have previously been shown to modulate autophagy [36], we tested whether QC is able to induce autophagy in addition to promoting apoptosis. Towards this end, OV2008/C13 as well as HeyA8/HeyA8MDR cells were treated with 5.0 and 10.0 μM QC for 24 hours. Western blot analysis of QC-treated cell lysates was performed using two different autophagic marker proteins, LC3B and p62. Figures 2A and 2B show induction of the lipidated form of LC3B-II in all four cell lines upon QC treatment. However, QC treatment reduced p62 levels significantly more in the chemoresistant (C13 and HEYA8MDR) cells compared to their sensitive counterparts. This induction of LC3B-II (lower band) and degradation of p62 are considered hallmarks of autophagic activation [40, 41]. QC treatment resulted in similar effects on p62 and LC3B
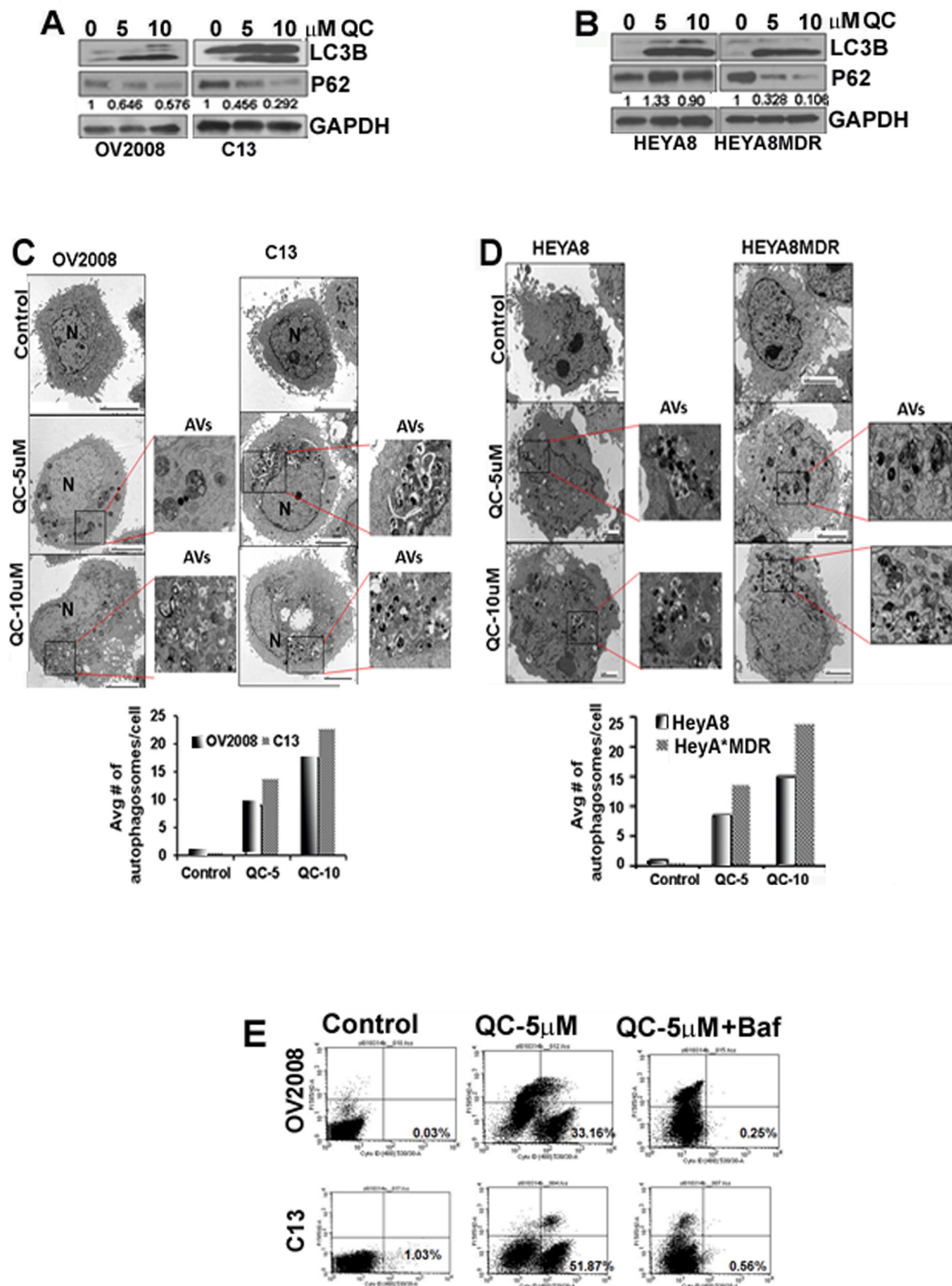
Figure 2: A. Immunoblot analysis of cell lysates obtained from OV2008, C13, **B.** HeyA8 and HeyA8MDR cells treated with Quinacrine (0, 5.0 μM, 10.0 μM) for 24 hours with anti-LC3B, p62 and anti-GAPDH antibodies. Values below the western blot panel indicate densitometry analysis of the blot. **C and D.** TEM analysis of QC treated OV2008, C13, HeyA8 and HeyA8MDR cells were performed to detect the presence of autophagic vesicles. Magnified inset shows double membrane autophagic vesicles in QC treated OV2008, C13 (C), HeyA8 and HeyA8MDR (D) cells. Quantitation of autophagy was estimated by counting the number of autophagic vesicles and results were plotted in bar graph. **E.** Autophagy was detected using cyto-ID fluorescence dye in OV2008 and C13 cells treated with QC in the presence or absence of bafilomycin A1 for 24 hours using flow cytometer. Percent of cyto-ID detection is indicated. Data are representative of three independent experiments.

independent of p53 status in high grade serous cell lines such as OVCAR3 (p53 mutant) and CAOV3 (p53 null) (Figure Supplemental S2). To further evaluate QC-induced autophagy, we utilized transmission electron microscopy (TEM). TEM analysis of QC-treated OV2008, C13, HeyA8 and HeyA8MDR cell revealed early autophagic bodies (autophagosomes) harboring intact organelles [18] (Figures 2C and 2D). Quantitation of autophagosomes is shown next to the respective figures. These data suggest that QC treatment induces autophagy.

While TEM analysis revealed qualitative and morphological features of autophagy upon QC treatment, it was unclear whether this represented increased generation of autophagosome or inhibition of autophagosomal maturation [42]. Therefore, to further clarify whether QC induces autophagic flux, OV2008 and C13 cells were treated with QC in the presence or absence of a potent late-autophagy inhibitor, bafilomycin A1, and then stained with the autophagolysosome-specific dye cyto-ID. Cyto-ID retention in the cytoplasm was detected by flow-cytometric analyses (Figure 2E). This data indicates that QC's ability to promote autophagy can be completely inhibited by co-treatment with bafilomycin A1.

QC induces autophagic flux and QC-induced autophagy precedes apoptosis

To further evaluate autophagic flux, we determined whether QC-mediated upregulation of LC3BII and downregulation of p62 was affected by co-treatment with bafilomycin A. Western blot analysis revealed that QC effectively downregulated p62 expression in C13 and HeyA8MDR and co-treatment with bafilomycin A protected autophagic p62 degradation (Figure 3A). No change in p62 mRNA levels was detected upon QC treatment (data not shown). We next tested whether QC-mediated apoptosis is dependent on autophagy. OV2008, C13, HEYA8 and HEYA8MDR cells were treated with QC with or without bafilomycin A1 followed by annexin/PI staining and flow cytometric detection of apoptotic cells. QC treatment in OV2008, C13, HeyA8 and HeyA8MDR cells resulted in varying but significant increase in annexin V positive cells. Co-treatment with bafilomycin A completely abolished QC-mediated annexin V positivity in these cells as shown in Figure 3B. Consistent with the flow cytometric data, immunoflourescence analysis also confirmed that the downregulated p62 by QC were rescued by bafilomycin treatment in C13 cells (Figure supplemental S3). This data indicates that QC-promoted cell death is completely reversed by autophagic inhibitors in all the four cell lines tested. Taken together, this data suggests that QC induces apoptosis in an autophagic-dependent manner.

Our data indicates that QC-induces apoptosis and autophagic inhibition by bafilomycin A. Therefore, we next sought to determine whether autophagy preceded the QC-induced apoptotic response. To this end, we determined the temporal regulation of autophagic proteins LC3B, p62 and apoptotic proteins such as cleaved PARP upon QC treatment at set time points in C13 and HeyA8MDR OvCa cells by western blot analysis. Data in Figure 3C indicate that QC treatment induced p62 downregulation and LC3B upregulation as early as 4 hours post treatment and these levels were sustained up to 24 hours following treatment. Detection of cleaved PARP was minimal at 4 hours of treatment; however its expression increased significantly at 16 hours post QC treatment. This data suggests that QC treatment triggered an autophagic response at the earlier time points while this autophagic response coincided with an apoptosis rate at later time points it.

QC synergizes with carboplatin in ovarian cancer cell lines

After observing increased degree of apoptosis upon QC treatment in chemoresistant OvCa cells, we then sought to investigate whether QC can synergize with carboplatin treatment. In order to determine whether QC synergizes with cisplatin and carboplatin, constant ratio synergy studies were performed in isogenic cisplatin-sensitive OV2008 and cisplatin-resistant C13 cells by treating them with $1 \times IC_{50}$ of cisplatin in combination with $1 \times IC_{50}$ of QC. We observed that QC had a more potent synergistic anti-proliferative effect *in vitro* when combined with either cisplatin in C13 compared to OV2008 cells (Figures 4A and 4B). The combination indices (CI) for the corresponding fractions affected (FA) are shown in the tables below the figures. CI values between 0.1–0.3 indicate extremely strong synergism, 0.3–0.7 strong synergism, 0.7–0.85 moderate synergism, 0.85–0.9 slight synergism and 0.9–1.0 a nearly additive effect. Of note, synergy was demonstrated across nearly the entire range of the drug concentrations. Similar studies with isogenic taxol-sensitive SKOV3 and taxol-resistant SKOV3TR cells [39] indicate that QC has a more synergistic antiproliferative effect *in vitro* when combined with either cisplatin or carboplatin in SKOV3TR (Figures 4C and 4D) compared to SKOV3 cells. Consistent with this finding, chemoresistant HeyA8MDR cells showed stronger synergy when carboplatin was combined with QC compared to the parent chemosensitive HeyA8 cells (Figures 4E and 4F). Similar results were obtained with the combination of carboplatin and QC. Comparison of CI values for cisplatin and carboplatin are shown Figure Supplemental figure S4 in a tabular form for OV2002, C13, SKOV3 and SKOV3TR. The IC_{50} values for QC, cisplatin and carboplatin in all six cell lines used in synergy studies are shown in Fig S4. It is important to note that although the cell lines used in these studies are no longer considered representative of high grade serous cancers, they were initially chosen due to the availability of isogenic chemosensitive and chemoresistant pairs of OvCA cells.
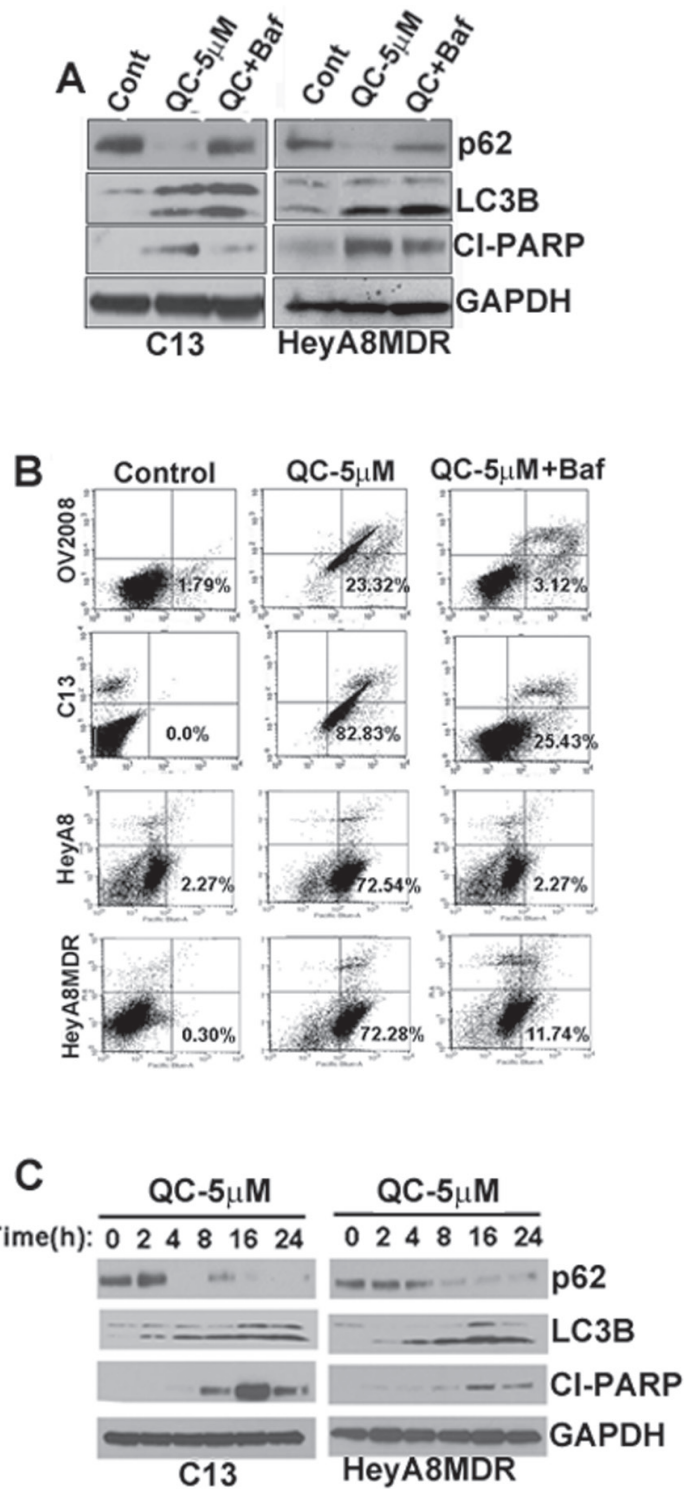
Figure 3: A. Autophagic flux was determined in C13 and HeyA8MDR cells. Cells were either treated with QC and/or co-treated with bafilomycin A1 for 12 hours. Cell lysates were subjected to Immunoblot analysis using anti-p62, anti-LC3B, anti-cleaved PARP and anti-GAPDH antibodies. **B.** AnnexinV/Propidium Iodide (PI) staining of OV2008, C13, HeyA8 and HeyA8MDR cells treated with QC and/or co-treated with Bafilomycin A (100 nM) for 24 hours. Data are representative of three independent experiments. **C.** Immunoblot analyses were performed to detect the protein expression of p62, LC3B, cleaved PARP and GAPDH in C13 and HeyA8MDR cells after treating the cells for different time points (2, 4, 8,c16 and 24 hrs) with QC.

	FA	CI	s.d.	FA	CI	s.d.	FA	CI	s.d.	FA	CI	s.d.
OV2008	0.25	1.253	0.3449	0.5	1.264	0.2717	0.75	1.281	0.2446	0.9	1.305	0.2792
C13*	0.25	0.693	0.1735	0.5	0.683	0.1197	0.75	0.676	0.1117	0.9	0.671	0.1526

	FA	CI	s.d.	FA	CI	s.d.	FA	CI	s.d.	FA	CI	s.d.
SKOV3	0.25	1.466	0.4045	0.5	1.039	0.2356	0.75	0.758	0.1823	0.9	0.568	0.178
SKOV3TR	0.25	0.265	0.0864	0.5	0.356	0.0876	0.75	0.482	0.1101	0.9	0.662	0.397

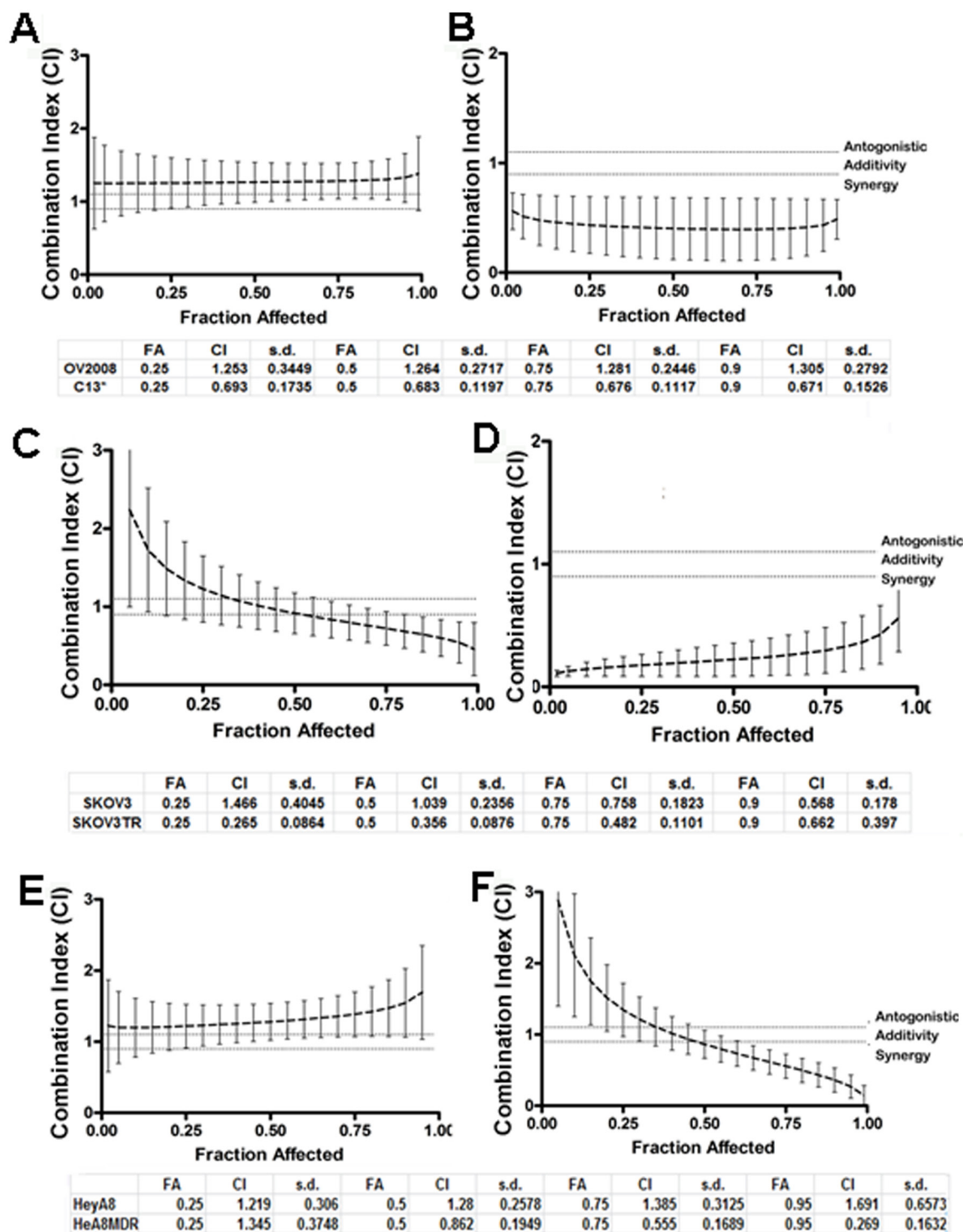|	FA	CI	s.d.	FA	CI	s.d.	FA	CI	s.d.	FA	CI	s.d.
HeyA8	0.25	1.219	0.306	0.5	1.28	0.2578	0.75	1.385	0.3125	0.95	1.691	0.6573
HeA8MDR	0.25	1.345	0.3748	0.5	0.862	0.1949	0.75	0.555	0.1689	0.95	0.269	0.1632

Figure 4: Quinacrine sensitizes ovarian cell lines to cisplatin-induced cytotoxicity. Combination of quinacrine with cisplatin in equipotent combinations (IC_{50} over IC_{50} ratio) was assessed for synergy using the Chou-Talalay method. The cells were exposed to each drug alone and in combination per protocol for 48 hours. The combination indices (CI), fraction affected (Fa) in OV2008 and C13 **A** and **B.** in SKOV3 and SKOVTR **C** and **D.** and in Hey A8 and HeyA8MDR **E** and **F.** were generated by the Calcusyn software and plotted with the use of GraphPad. Combination index (CI) values at 25, 50, 75 and 90% fraction affected (FA) are presented in the tables below the graphs. CI between 0.3–0.7 indicates strong synergism, 0.7–0.85 moderate synergism, 0.85–0.9 slight synergism, 0.9–1.10 nearly additive effect and greater than 1.10 antagonism.

QC-induced autophagy is required for sensitization to cisplatin-mediated cell death in OvCa cells

In order to test whether QC-induced autophagy is essential in order to sensitize OvCa cells to cisplatin-induced cytotoxicity, we assessed the effects of the combination of increasing concentrations of cisplatin with QC ($1 \times$ IC50) with and without bafilomycin A pretreatment in OV2008 and C13 cells. We hypothesized that by inhibiting autophagy, bafilomycin A will inhibit the ability of QC to synergize with cisplatin in inducing autophagic cell death. The cells were pretreated with 50 nM of bafilomycin for 2 hours followed by treatment with cisplatin and QC. Cell viability was assessed by MTT assays 48 hours later. As shown in figures 5A and 5B, pretreatment with bafilomycin A (green dotted line) inhibited the combined QC- and cisplatin-induced cytotoxicity (blue dotted line). This is also demonstrated by the change in the CI values from values indicating strong synergy in C13 (CI = 0.690) and nearly additive effect in OV2008 (CI = 1.054) without bafilomycin to indicating antagonism in both C13 (CI = 1.242) and OV2008 (CI = 1.396) after bafilomycin pretreatment (Figure 5C).

Collectively, these data suggest that QC-induced autophagy is necessary for resensitization to cisplatin-induced cell death in OvCa cells.

p62 knockdown enhances sensitivity to carboplatin treatment in HeyA8MDR and C13 ovarian cancer cells

Elevated levels of p62 have been previously shown to be critical in imparting chemoresistance in OvCA cells [43]. Our data indicate that QC treatment downregulated p62 levels preferentially in the chemoresistant C13 and HeyA8MDR cells (Figure 2A). Previous studies have shown that p62 downregulation sensitizes cells to cisplatin-mediated cytotoxicity [23]. To determine whether p62 plays role in QC- and carboplatin-mediated apoptosis, we generated two different p62 knockdown shRNA clones in HeyA8MDR and C13 cells as described in Materials and methods section with non-targeted control transduced cells (NTC) as controls. Efficient knockdown of p62 was confirmed in C13 and HeyA8MDR cells by western blot analysis using anti-p62 antibody (Figures 6A and 6B). To further evaluate the effect of QC in inducing apoptosis in NTC
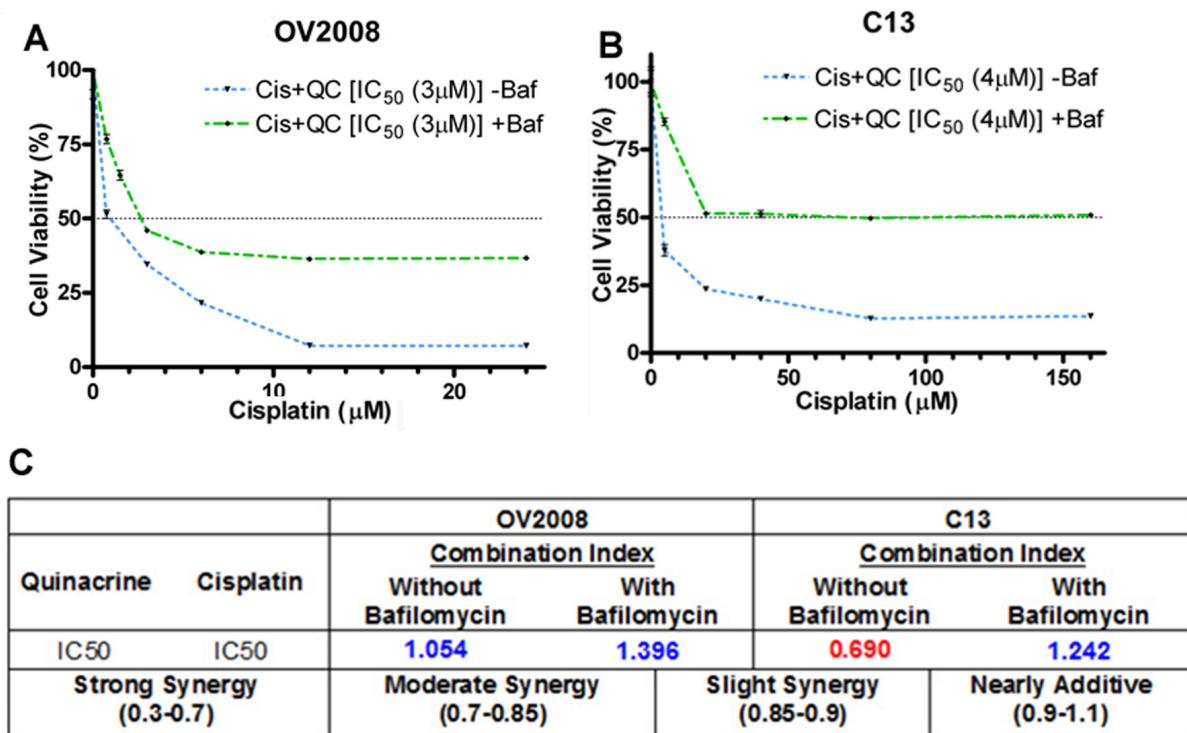

Quinacrine	Cisplatin	OV2008		C13	
		Combination Index		Combination Index	
		Without Bafilomycin	With Bafilomycin	Without Bafilomycin	With Bafilomycin
IC50	IC50	1.054	1.396	0.690	1.242
Strong Synergy (0.3-0.7)		Moderate Synergy (0.7-0.85)		Slight Synergy (0.85-0.9)	Nearly Additive (0.9-1.1)

Figure 5: A & B. Quinacrine-induced autophagy is required for sensitizing cisplatin-mediated cell death of ovarian cancer cells. Cell viability assays were performed with a combination of increasing concentrations of cisplatin with QC ($1 \times$ IC$_{50}$) with and without bafilomycin pretreatment in OV2008 and C13 cells. Cells were pretreated with 50 nM bafilomycin for 2 hours followed by drug treatment. Cell viability was assessed by MTT assays 48 hours later. Pretreatment with bafilomycin (green dotted line) inhibited the combined QC plus cisplatin-induced cytotoxicity (blue dotted line) more effectively in C13 cells compared to OV2008. **C.** CI values of combination treatment without bafilomycin indicated strong synergy in C13 (CI = 0.690) and nearly additive effect in OV2008 (CI = 1.054), whereas, after bafilomycin pretreatment, CI values indicated antagonism in both C13 (CI = 1.242) and OV2008 (CI = 1.396).
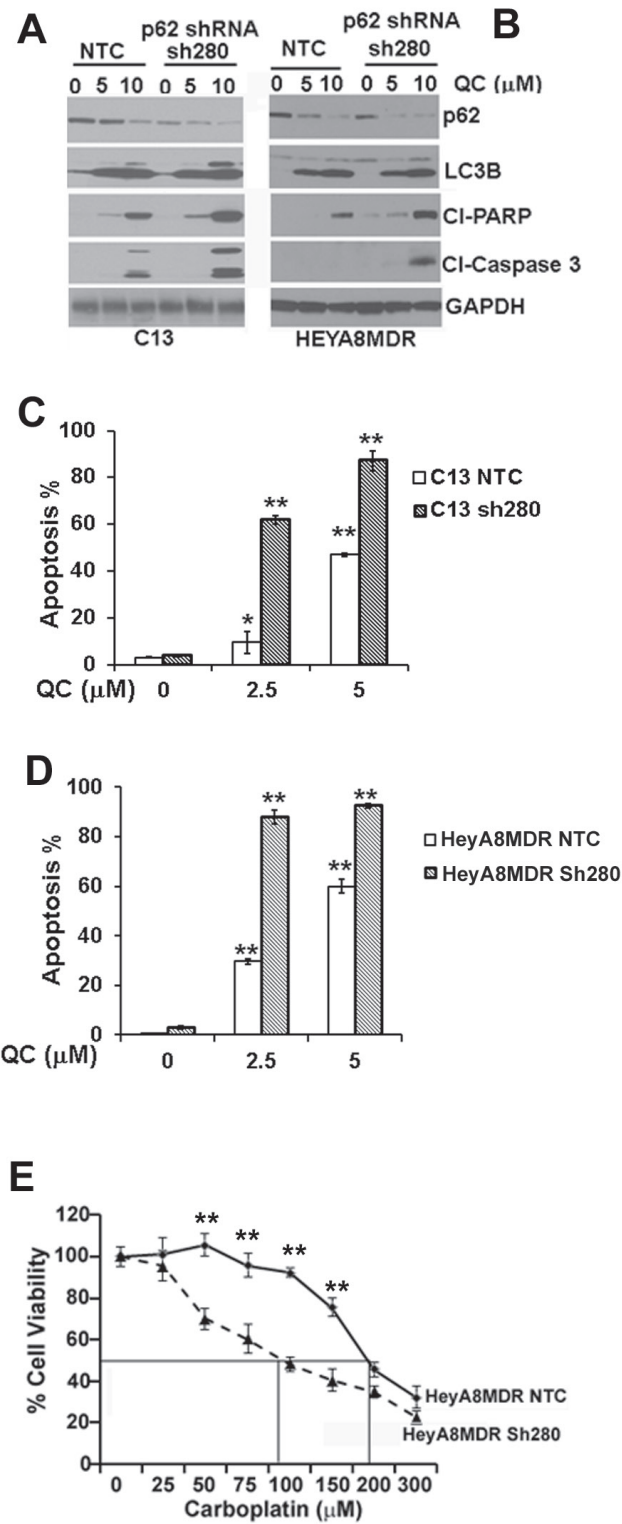
Figure 6: Immunoblot analysis of Non-targeted control shRNA (NTC) or p62 shRNA stable clones sh280 in A. C13 and B. HeyA8MDR were treated with QC (0, 5.0 μM, 10.0 μM) for 24 hours with anti-cleaved PARP, cleaved caspase 3, p62, LC3BII and anti-GAPDH antibodies. **C & D.** AnnexinV/Propidium Iodide (PI) staining of OV2008, C13, HeyA8 and HeyA8MDR cells treated with Quinacrine for indicated concentration for 24 hours. Data are representative of two independent experiments. (*P = < 0.001, **P = < 0.0001). **E.** HEYA8MDR NTC and sh280 cells were treated with different concentrations of carboplatin and cell viability was measured by MTT assay. sh280 cells showed more sensitivity towards carboplatin treatment compared to the NTC group (**P < 0.0001, Figure 6E) indicating the critical role of p62 as a determinant of chemoresistance in HeyA8MDR cells.

and p62-depleted cells, we treated C13 NTC and p62 shRNA clones with 0, 5.0, 10.0 µM of QC for 24 hours. Evaluation of apoptotic marker proteins by western blot analysis revealed that p62 knockdown cells exhibited higher degree of cleaved PARP and caspase 3 whereas no significant change was observed in LC3B II induction upon QC treatment in C13 NTC as well as p62shRNA cells (Figure 6A). Consistent with this data, QC treatment in HeyA8MDR p62shRNA cells showed increased degree of caspase 3 and PARP cleavage while no change was detected in LC3B II induction (Figure 6B). This data suggests that p62 downregulation in C13 and HeyA8MDR sensitizes the cells to QC treatment. Similarly, annexin/PI staining of these cells after treatment with QC revealed that C13 and HeyA8MDR p62 knockdown cells were more sensitive to QC-induced cell death when compared to NTC cells (Figures. 6C and 6D). More importantly, genetic downregulation of p62 in HeyA8MDR cells enhanced carboplatin sensitivity (please note the reduction in carboplatin IC50 from 176 µM in NTC cells to 110 µM in p62 knockdown cells) (Figure 6E). Collectively, these findings indicate that p62 downregulation sensitizes cells to QC-mediated cell death.

Quinacrine synergizes with carboplatin in reducing HeyA8MDR derived mouse tumor xenografts

QC effectively blocked cell growth, induced autophagy and apoptosis in OvCa cell lines *in vitro*. We next tested whether QC in combination with carboplatin is effective in attenuating tumor growth *in vivo*. For this purpose we utilized HeyA8MDR cells that have capacity to form tumors when injected intraperitoneally in nude mice [38]. The effect on tumor growth of QC alone and in combination with carboplatin (CBP in the Figure 6) was evaluated in HeyA8MDR in female nude mouse xenografts. One week after 3×10^6 HeyA8MDR cells were injected intraperitoneally in the mice, they were randomized into four groups of 10 mice when the tumors were palpable and then treated as shown in Figure 7A. Quinacrine (150 mg/kg body weight) was given as described in the materials and methods section. Quinacrine alone effectively reduced tumor volume and ascites formation (Figures 6B, 6C and 6D). Although carboplatin treatment similarly reduced tumor volume, it was associated with accumulation of ascites to an extent even greater than untreated controls (Figure 6D). Assessment of tumor weight and ascites volume as measured at the time of necropsy across treatment groups showed that combination treatment was more effective in reducing cancer progression compared to all other treatment groups (Figures 7B, 7C and 7D). Staining of the tumors with Ki-67 showed significantly reduced proliferation in QC and QC plus carboplatin treated groups, highlighting the ability of QC to reduce tumor cell proliferation *in vivo*

(Figure 7E). There was no significant body weight loss in the QC or combination treatment groups compared to the untreated control group (Figure 7F). TEM micrographs of the xenografts showed more autophagosomes (AV in red, Figure 7G) in the QC group compared to untreated and carboplatin groups. Combination treatment resulted in significantly more autophagosomes compared to QC alone (Figure 7H). H&E staining of the livers from all four groups (Figure 7I) showed that there was no difference in histology, suggesting that neither QC monotherapy nor combination treatment was toxic to the mice. These data demonstrate that QC plus carboplatin combination treatment leads to significantly enhanced antitumor activity in an OvCa mouse model.

DISCUSSION

The lack of effective treatment modalities for patients with chemoresistant disease continues to pose a therapeutic challenge in ovarian cancer. There is a growing need to identify therapeutic compounds which could promote efficacy to frontline therapeutic agents such as cisplatin and taxol. In this study, we evaluated the anti-cancer properties of the anti-malarial drug QC and tested its effectiveness in combination with carboplatin in OvCa.

QC treatment effectively caused apoptosis and promoted an autophagic response across a variety of ovarian cancer cell lines *in vitro* as well as *in vivo* in mouse-derived HeyA8MDR xenografts. QC treatment caused robust autophagosome formation, LC3B accumulation and p62 downregulation all of which are hallmarks of autophagy. Our findings suggest that QC-mediated induction of autophagy preceded the induction of apoptosis as the effects on the autophagic proteins LC3B and p62 were observed at earlier time points. Autophagy and apoptosis have been previously shown to coincide temporarily in order to cause drug-induced cell death. In agreement with these findings, we showed that by chemically blocking autophagy using bafilomycin A, QC-mediated apoptosis was significantly attenuated. At the molecular level, QC promoted autophagic clearance of p62 in OvCa cell lines. p62 is a well-known substrate of autophagy and high levels of p62 have previously been associated with chemoresistance [23]. Genetic silencing of p62 expression by shRNA in the chemoresistant HeyA8MDR cancer cells promoted apoptosis and enhanced sensitivity to carboplatin (Figure 6E). Therefore, autophagic clearance of p62 expression by QC might be one of the underlying mechanisms responsible for enhanced synergy when QC is combined with carboplatin. Several studies have shown that p62 expression is elevated in breast, pancreatic, colon as well as ovarian cancer which is consistent with our observation of increased expression of p62 in the chemoresistant cell lines that we studied, namely the C13 and HeyA8MDR cell line compared to their chemosensitive counterparts OV2008 and HeyA8.
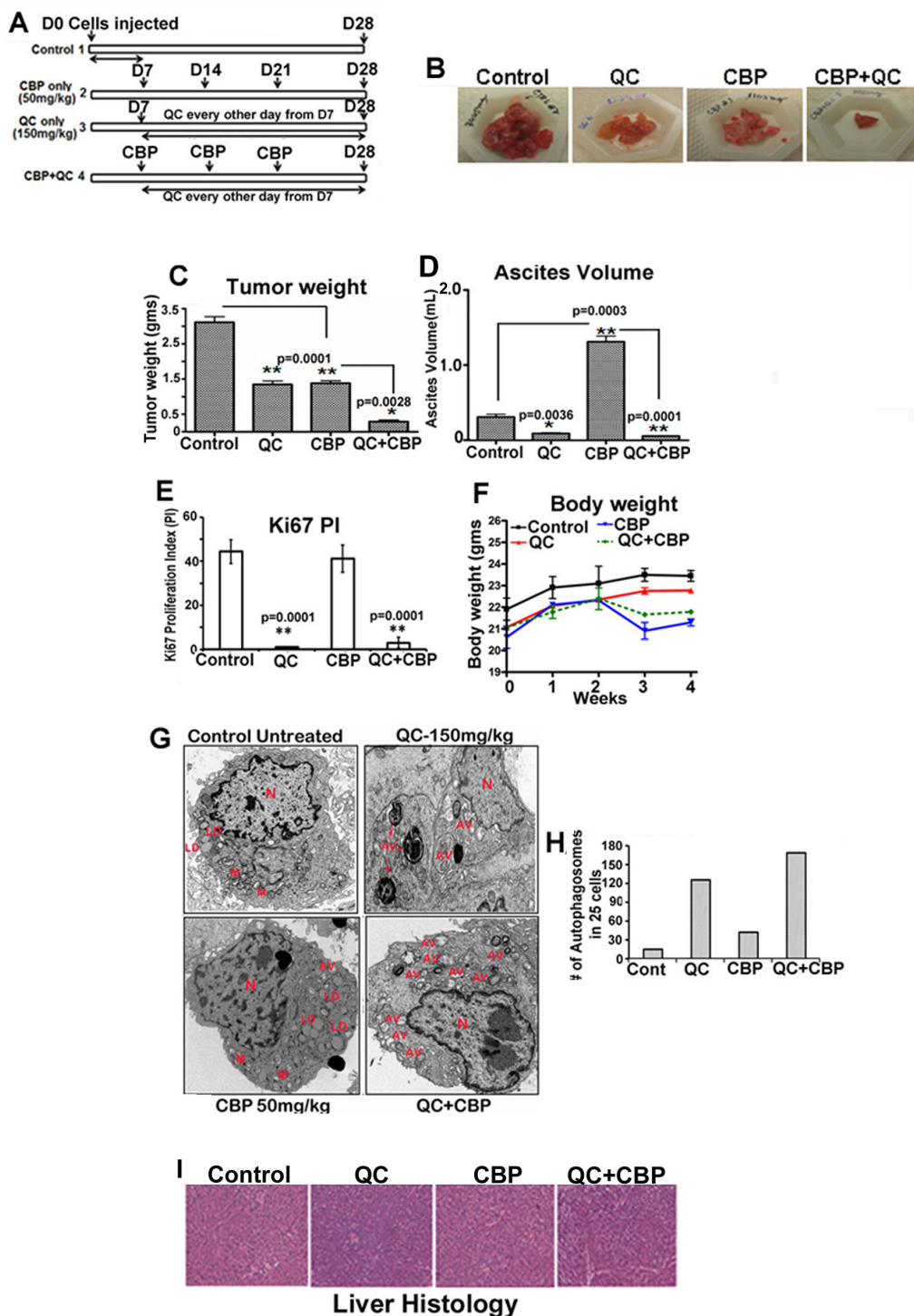
Figure 7: Quinacrine inhibits ovarian tumor growth *in vivo* A. Schematic representation of treatment plan **B.** Representative tumors obtained from vivisected mouse showing HeyA8MDR tumors from control untreated, CBP treated, QC treated and QC/CBP combination treated group. **C.** Graph indicating the excised tumor weight from each of each group (*n* = 10) with cumulative mean; untreated, CBP treated, QC treated and QC/CBP combination treated group. *P < .0028, **P < .0001, treated compared with the untreated group. **D.** Graph showing ascetic fluid volume in control untreated, CBP treated, QC treated and QC/CBP combination treated group. *P < .005 **E.** Graph showing quantitation of Ki67 staining in control untreated, CBP treated, QC treated and QC/CBP combination treated group. *P < .0001 **F.** Measurement of body weight of untreated and treated mice. **G.** TEM analysis of tumor sections obtained from control untreated, CBP treated, QC treated and QC/CBP combination treated group and quantitation *P < .005. (N-Nucleus, AV-autophagosomes and LD-lipid droplets). **H.** Quantitation of # of autophagosomes in untreated control and QC, CBP and QC+CBP treated xenografts (25 images were counted and averaged). **I.** Histology of H and E stained liver from treated and untreated mice.

QC treatment down regulated p62 expression in an autophagic-dependent manner in the C13 and HeyA8MDR OvCa cell lines. Lentiviral shRNA-mediated p62 depletion in the OV2008 and HeyA8MDR OvCa cell lines resulted in enhanced synergy between QC and carboplatin. This data suggests that combination treatment with carboplatin and QC results in an enhanced QC-mediated clearance of p62 via autophagy ultimately favoring apoptosis. This observation is further supported by our data showing that inhibition of autophagy by bafilomycin A not only effectively blocked QC-mediated p62 downregulation but also apoptosis. Being a lysosomotropic agent, it is not surprising that QC appears to be implicated in autophagy; however, our study highlights the fact that p62 downregulation plays a key role in QC-mediated apoptosis in OvCa cells and provides a description of the mechanistic interplay between autophagic and apoptotic cell death upon QC treatment.

QC treatment of mouse-derived xenografts was shown to be effective in reducing tumor weight, reducing cell proliferation as measured by Ki-67 staining and blocking ascitic fluid formation. While a similar degree of tumor reduction was achieved by carboplatin treatment alone, in contrast to QC treatment, carboplatin treatment induced ascitic fluid accumulation. TEM analysis of QC-treated xenografts clearly showed increased formation of autophagosomes and autolysosomes. These effects were dramatic when QC was combined with carboplatin leading to complete remission of tumor growth and reduction in the proliferation index. This data is in accordance with the high degree of synergy observed when chemoresistant OvCa cell lines were treated with carboplatin and QC *in vitro*. Taking into consideration the previously proven ability of carboplatin to upregulate p62 expression along with the knowledge that carboplatin-resistant OvCa cells exhibit increased levels of p62, we hypothesize that co-administration of QC with carboplatin may mitigate p62 expression *in vivo* thereby enhancing the degree of apoptosis.

QC has been shown to stabilize p53, inhibit NF-kB, and cause cell cycle arrest. However, QC-mediated p53 stabilization has been associated with its Nf-kB suppressive activities and not due to genotoxic stress [28]. Our findings revealed that QC induced robust autophagic cell death and synergized with carboplatin treatment. It is likely that multiple cellular pathways including p53 and NF-kB in addition to autophagic p62 downregulation are playing a role in QC- and carboplatin-mediated synergy. Other studies have also demonstrated the synergy between QC and other chemotherapeutic drugs such as Lycopene in breast cancer [44], cedarinib in glioma cells [45], vincristine in an MDR sub-clone of K562 cells [31] as well as other therapeutic compounds [46]. More recently, quinacrine has been shown to reverse erlotinib resistance in non-small lung cancer cells by targeting FACT complex and NF-kB activities [47]. It is important to note that

several reports have implicated autophagy as a survival mechanism in cancer cells and have demonstrated that by inhibiting autophagy with chloroquine, tumor growth can be arrested [9]. While this is true at a tumor-specific level [48], we believe that prolonged chemical inhibition of autophagy with different autophagic inhibitors might elicit differential responses than just simply inhibition of autophagy. Notably, chloroquine, in addition to inhibiting autophagy, also stabilizes p53 thereby leading to apoptosis. Similarly, another autophagy inhibitor, 3-MA, has been shown to inhibit Akt activation [49]. These observations in conjunction with our data indicate that drugs altering autophagy may also influence apoptosis. QC unlike Bafilomycin A promoted p62 degradation as a function of autophagy induction and also promoted apoptosis both *in vitro* and *in vivo*.

In summary, the present study demonstrated that QC treatment resulted in autophagic clearance of p62, promoted apoptosis and effectively synergized with carboplatin *in vivo*. QC's ability to inhibit multiple pathways simultaneously in addition to promoting autophagic cell death offers compelling evidence to support the hypothesis that it may represent an important adjunct to standard treatment against ovarian cancer especially in patients with chemoresistant disease.

MATERIALS AND METHODS

Cell lines, chemicals and antibodies

The human OvCa cell lines SKOV3, SKOV3 TR, HeyA8 and HeyA8 MDR were obtained on an MTA from MD Anderson Cancer Center, Houston, TX. C13 and OV2008, were obtained on a MTA from Dr. Barabara Vanderhyden (Ottawa Hospital Research Institute, Ottawa, Canada). OVCAR3 and CAOV3 were obtained from the American Type Culture Collection (ATCC) (Manassas, VA). All cell lines were cultured according to the providers' recommendations at 5% CO_2 and at 37°C. Quinacrine was obtained from Sigma-Aldrich. MTT dye was obtained from Promega. Carboplatin was purchased from Calbiochem (San Diego, CA). Anti-LC3B, anti-PARP, anti-p62, anti-PDI and anti GAPDH antibodies were purchased from Cell Signaling Corporation. Anti-NBR antibody was purchased from Genetex. Anti-p53 (DO-1) antibody is from Santa Cruz Biotech.

Colony formation assay

500 cells were plated in 6-well plates and treated with increasing concentrations of QC (0.12, 0.25, 0.5, 1.0 1nd 2.0, 2.0 µM) for 24 hrs. The media was replaced after day1. Colonies were fixed in methanol and stained with 0.5% crystal violet [50] on day 8 and counted using a colony counting software, Quantity One (Bio-Rad). Each treatment was carried out in triplicate and repeated twice.

Cytotoxicity assay

MTT assay was performed in order to assess the effect of QC on OvCa cell lines. Ten thousand cells from each cell line were treated with various concentrations of QC and carboplatin separately or in combination for 48 hours followed by a 4-hour period of incubation with 3-(4,5-dimethylthiazol-2-yl)-2,5-diphenyltetrazolium bromide (MTT). The violet formazan crystals were dissolved in dimethyl sulfoxide (DMSO) and the absorbance was measured at 490 nm in a microplate reader.

ShRNA transductions

The control shRNA, pTRC1-NTC (non-target shRNA vector, Sigma) contains a hairpin insert that will generate siRNAs but contains five base pair mismatches to any known human gene. shRNA for p62/SQSTM denoted as p62-sh280 was purchased from Sigma and with a sequence CGAGGAATTGACAATGGCCAT targeting cDNA region of p62. Lentivirus particles were produced by transient transfection of pTRC1-NTC and pTRC1-p62 shRNA along with packaging vectors (pVSV-G and pGag/pol) in 293T cells. The lentiviral supernatants were collected 48 hours after transduction, filtered and either used for infection or stored at -80°C. Vector titers were determined by transducing OvCa cells with serial dilutions of concentrated lentivirus, in complete growth medium containing 8 μg/ml polybrene (Invitrogen). After 7 days, the growth medium was supplemented with puromycin (2 μg/ml) for selection. The surviving colonies were counted under the microscope and the titer of lentiviral stocks was calculated using the formula: Transducing units = number of colonies × lentiviral dilution. All lentiviral stocks used in the study were selected at a multiplicity of infection of 10.

MTT assay, synergy assessment and Chou-Talalay calculations

Cell lines were treated with a wide range of concentrations of QC and cisplatin for 48 hours and the half maximal inhibitory concentration (IC_{50}) of each drug alone was derived experimentally by MTT assay as previously described [51] and calculated by Prism (GraphPad Software, La Jolla, CA). Subsequently, drug combination studies (QC with cisplatin and QC with carboplatin) were performed and their synergy was quantified using the Chou-Talalay method as previously described in the literature [52, 53]. Both constant ratio synergy (ratio of drugs 1:1) studies were carried out. Synergy was assessed by creating combination indices (CI): CI values less than 0.9 indicate synergism, CI values between 0.9 to 1.1 indicate nearly additive effect and CI values greater than 1.1 indicate antagonism [52].

Flow cytometric analysis of apoptosis and autophagy

C13 and OV2008 cells were treated with the indicated doses of QC, then harvested and resuspended in a binding buffer. Cells were then stained with Annexin V-pacific blue and Propidium iodide (BD bioscience) according to the manufacturer's instructions. Cells were analyzed in a Beckman Coulter EPICS XL/MCL flow cytometer (Beckman-Coulter Fullerton, CA, USA) and the data were analyzed with Flowjo Software (Tree Star, Ashland, OR, USA). Cyto-ID$_{TM}$ (Enzo Life Sciences) is a dye specifically labeling the autophagic vacuoles in a cell by colocalizing with LC3B. After treating the cells with various concentrations of QC, cells were collected and stained using Cyto-ID dye according to the manufacturer's instructions. Cells were analyzed as previously described in a Beckman Coulter EPICS XL/MCL flow cytometer (Beckman-Coulter Fullerton, CA, USA) and the data were analyzed with Flowjo Software (Tree Star, Ashland, OR, USA).

Western blot analysis

Western blot analysis was performed as previously described [51, 54].

Transmission electron microscopy

Cells (2×10^6) were treated with QC and then harvested and centrifuged at 1200 r.p.m. for 5 minutes. Cell samples were then pre-fixed with Trumps buffer. The images were taken using a Philips 208S electron microscope (FEI Corporation, Eindhoven, Netherlands).

Immunofluorescence

Cells were plated on coverslips and treated with QC as indicated in materials and methods. Cells were fixed with 100% methanol followed by blocking with 1% BSA in PBS. Cells were then incubated with the corresponding primary antibodies at room temperature for 1 hour followed by three washes with 1X PBS and then incubated in the dark with Alexa fluor rabbit anti-mouse (593 nm) in 1% BSA in PBS. Coverslips were washed three times before mounting with Prolong Gold Antifade reagent (Invitrogen). Stained samples were visualized using a Zeiss-LSM 510 fluorescence microscope.

Animal studies

Athymic nude mice were purchased from Harlan. 3×10^6 HEYA8MDR cells were injected intraperitoneally. Treatment was initiated after one week following the intraperitoneal inoculation of the cells. Stock solutions of QC (Sigma) were prepared in sterile

water and administered by oral gavage. Carboplatin (Hospira pharma) were injected intraperitoneally. Before initiation of treatment, animals were randomly assigned to one of four groups (10 mice per group). The control group received water by oral gavage the QC only group received 150 mg/kg body weight of QC every other day starting on day 7, the carboplatin group received carboplatin by intraperitoneal injection at a dose of 50 mg/kg body weight) on days 7, 14, 21 and 28 and the combination group received carboplatin by intraperitoneal injection at days 7, 14, 21 and 28 and QC at 150 mg/kg body weight starting on day 7, then every other day until the end of the study. All animals were sacrificed on day 28. Animal care and procedures was conducted according to institutional policies and the experimental protocol was approved by the IACUC committee of our Institution.

Statistical analysis

All results are expressed as mean ± standard deviation (S.D.). Data were obtained from three independent experiments. All statistical analyses were conducted using Graph pad Prism software (San Diego, CA). Data were analyzed using paired t test, and P values less than 0.05, unless mentioned otherwise, were considered statistically significant.

CONFLICTS OF INTEREST

There is no conflict of interest to disclose.

REFERENCES

1. Agarwal R, Kaye SB. Ovarian cancer: strategies for overcoming resistance to chemotherapy. Nat Rev Cancer. 2003; 3:502–516.

2. Klionsky DJ. Autophagy: from phenomenology to molecular understanding in less than a decade. Nat Rev Mol Cell Biol. 2007; 8:931–937.

3. Button RW, Luo S, Rubinsztein DC. Autophagic activity in neuronal cell death. Neurosci Bull. 2015.

4. Gozuacik D, Kimchi A. Autophagy as a cell death and tumor suppressor mechanism. Oncogene. 2004; 23:2891–2906.

5. Eskelinen EL, Saftig P. Autophagy: a lysosomal degradation pathway with a central role in health and disease. Biochim Biophys Acta. 2009; 1793:664–673.

6. Degenhardt K, Mathew R, Beaudoin B, Bray K, Anderson D, Chen G, Mukherjee C, Shi Y, Gelinas C, Fan Y, Nelson DA, Jin S, White E. Autophagy promotes tumor cell survival and restricts necrosis, inflammation, and tumorigenesis. Cancer Cell. 2006; 10:51–64.

7. White EJ, Martin V, Liu JL, Klein SR, Piya S, Gomez-Manzano C, Fueyo J, Jiang H. Autophagy regulation in cancer development and therapy. Am J Cancer Res. 2011; 1:362–372.

8. Fukuda T, Oda K, Wada-Hiraike O, Sone K, Inaba K, Ikeda Y, Miyasaka A, Kashiyama T, Tanikawa M, Arimoto T, Kuramoto H, Yano T, Kawana K, Osuga Y, Fujii T. The anti-malarial chloroquine suppresses proliferation and overcomes cisplatin resistance of endometrial cancer cells via autophagy inhibition. Gynecol Oncol. 2015; 137:538–545.

9. Zhao XG, Sun RJ, Yang XY, Liu DY, Lei DP, Jin T, Pan XL. Chloroquine-enhanced efficacy of cisplatin in the treatment of hypopharyngeal carcinoma in xenograft mice. PLoS One. 2015; 10:e0126147.

10. Cheng Y, Zhang Y, Zhang L, Ren X, Huber-Keener KJ, Liu X, Zhou L, Liao J, Keihack H, Yan L, Rubin E, Yang JM. MK-2206, a novel allosteric inhibitor of Akt, synergizes with gefitinib against malignant glioma via modulating both autophagy and apoptosis. Mol Cancer Ther. 2012; 11:154–164.

11. Leisching GR, Loos B, Botha MH, Engelbrecht AM. The role of mTOR during cisplatin treatment in an *in vitro* and *ex vivo* model of cervical cancer. Toxicology. 2015; 335:72–78.

12. Liang C, Feng P, Ku B, Dotan I, Canaani D, Oh BH, Jung JU. Autophagic and tumour suppressor activity of a novel Beclin1-binding protein UVRAG. Nat Cell Biol. 2006; 8:688–699.

13. Liang XH, Jackson S, Seaman M, Brown K, Kempkes B, Hibshoosh H, Levine B. Induction of autophagy and inhibition of tumorigenesis by beclin 1. Nature. 1999; 402:672–676.

14. Qu X, Yu J, Bhagat G, Furuya N, Hibshoosh H, Troxel A, Rosen J, Eskelinen EL, Mizushima N, Ohsumi Y, Cattoretti G, Levine B. Promotion of tumorigenesis by heterozygous disruption of the beclin 1 autophagy gene. J Clin Invest. 2003; 112:1809–1820.

15. Cai M, Hu Z, Liu J, Gao J, Liu C, Liu D, Tan M, Zhang D, Lin B. Beclin 1 expression in ovarian tissues and its effects on ovarian cancer prognosis. Int J Mol Sci. 2014; 15:5292–5303.

16. Valente G, Morani F, Nicotra G, Fusco N, Peracchio C, Titone R, Alabiso O, Arisio R, Katsaros D, Benedetto C, Isidoro C. Expression and clinical significance of the autophagy proteins BECLIN 1 and LC3 in ovarian cancer. Biomed Res Int. 2014; 2014:462658.

17. White E. The role for autophagy in cancer. J Clin Invest. 2015; 125:42–46.

18. Barth S, Glick D, Macleod KF. Autophagy: assays and artifacts. J Pathol. 2010; 221:117–124.

19. Pankiv S, Clausen TH, Lamark T, Brech A, Bruun JA, Outzen H, Overvatn A, Bjorkoy G, Johansen T. p62/SQSTM1 binds directly to Atg8/LC3 to facilitate degradation of ubiquitinated protein aggregates by autophagy. J Biol Chem. 2007; 282:24131–24145.

20. Mathew R, Karp CM, Beaudoin B, Vuong N, Chen G, Chen HY, Bray K, Reddy A, Bhanot G, Gelinas C, Dipaola RS, Karantza-Wadsworth V, White E. Autophagy suppresses tumorigenesis through elimination of p62. Cell. 2009; 137:1062–1075.

21. Nihira K, Miki Y, Ono K, Suzuki T, Sasano H. An inhibition of p62/SQSTM1 caused autophagic cell death of several human carcinoma cells. Cancer Sci. 2014; 105:568–575.

22. Luo RZ, Yuan ZY, Li M, Xi SY, Fu J, He J. Accumulation of p62 is associated with poor prognosis in patients with triple-negative breast cancer. Onco Targets Ther. 2013; 6:883–888.

23. Yu H, Su J, Xu Y, Kang J, Li H, Zhang L, Yi H, Xiang X, Liu F, Sun L. p62/SQSTM1 involved in cisplatin resistance in human ovarian cancer cells by clearing ubiquitinated proteins. Eur J Cancer. 2011; 47:1585–1594.

24. Gurova K. New hopes from old drugs: revisiting DNA-binding small molecules as anticancer agents. Future Oncol. 2009; 5:1685–1704.

25. Preet R, Mohapatra P, Mohanty S, Sahu SK, Choudhuri T, Wyatt MD.Kundu CN.Quinacrine has anticancer activity in breast cancer cells through inhibition of topoisomerase activity. Int J Cancer. 2012; 130:1660–1670.

26. Thommesen L, Sjursen W, Gasvik K, Hanssen W, Brekke OL, Skattebol L, Holmeide AK, Espevik T, Johansen B, Laegreid A. Selective inhibitors of cytosolic or secretory phospholipase A2 block TNF-induced activation of transcription factor nuclear factor-kappa B and expression of ICAM-1. J Immunol. 1998; 161:3421–3430.

27. Guo C, Gasparian AV, Zhuang Z, Bosykh DA, Komar AA, Gudkov AV, Gurova KV. 9-Aminoacridine-based anticancer drugs target the PI3K/AKT/mTOR, NF-kappaB and p53 pathways. Oncogene. 2009; 28:1151–1161.

28. Gurova KV, Hill JE, Guo C, Prokvolit A, Burdelya LG, Samoylova E, Khodyakova AV, Ganapathi R, Ganapathi M, Tararova ND, Bosykh D, Lvovskiy D, Webb TR, Stark GR, Gudkov AV. Small molecules that reactivate p53 in renal cell carcinoma reveal a NF-kappaB-dependent mechanism of p53 suppression in tumors. Proc Natl Acad Sci U S A. 2005; 102:17448–17453.

29. Hyafil F, Vergely C, Du Vignaud P, Gr-Perret T. In vitro and in vivo reversal of multidrug resistance by GF120918, an acridonecarboxamide derivative. Cancer Res. 1993; 53:4595–4602.

30. Inaba M, Maruyama E. Reversal of resistance to vincristine in P388 leukemia by various polycyclic clinical drugs, with a special emphasis on quinacrine. Cancer Res. 1988; 48:2064–2067.

31. Liang GW, Lu WL, Wu JW, Zhao JH, Hong HY, Long C, Li T, Zhang YT, Zhang H, Wang JC, Zhang X, Zhang Q. Enhanced therapeutic effects on the multi-drug resistant human leukemia cells in vitro and xenograft in mice using the stealthy liposomal vincristine plus quinacrine. Fundam Clin Pharmacol. 2008; 22:429–437.

32. Traunecker HC, Stevens MC, Kerr DJ, Ferry DR. The acridonecarboxamide GF120918 potently reverses P-glycoprotein-mediated resistance in human sarcoma MES-Dx5 cells. Br J Cancer. 1999; 81:942–951.

33. Dey A, Tergaonkar V, Lane DP. Double-edged swords as cancer therapeutics: simultaneously targeting p53 and NF-kappaB pathways. Nat Rev Drug Discov. 2008; 7:1031–1040.

34. Gorbachev AV, Gasparian AV, Gurova KV, Gudkov AV, Fairchild RL. Quinacrine inhibits the epidermal dendritic cell migration initiating T cell-mediated skin inflammation. Eur J Immunol. 2007; 37:2257–2267.

35. Wang W, Ho WC, Dicker DT, MacKinnon C, Winkler JD, Marmorstein R, El-Deiry WS. Acridine derivatives activate p53 and induce tumor cell death through Bax. Cancer Biol Ther. 2005; 4:893–898.

36. Mohapatra P, Preet R, Das D, Satapathy SR, Choudhuri T, Wyatt MD, Kundu CN. Quinacrine-mediated autophagy and apoptosis in colon cancer cells is through a p53- and p21-dependent mechanism. Oncol Res. 2012; 20:81–91.

37. Montopoli M, Bellanda M, Lonardoni F, Ragazzi E, Dorigo P, Froldi G, Mammi S, Caparrotta L. "Metabolic reprogramming" in ovarian cancer cells resistant to cisplatin. Curr Cancer Drug Targets. 2011; 11:226–235.

38. Apte SM, Fan D, Killion JJ, Fidler IJ. Targeting the platelet-derived growth factor receptor in antivascular therapy for human ovarian carcinoma. Clin Cancer Res. 2004; 10:897–908.

39. Halder J, Landen CN Jr., Lutgendorf SK, Li Y, Jennings NB, Fan D, Nelkin GM, Schmandt R, Schaller MD, Sood AK. Focal adhesion kinase silencing augments docetaxel-mediated apoptosis in ovarian cancer cells. Clin Cancer Res. 2005; 11:8829–8836.

40. Bjorkoy G, Lamark T, Pankiv S, Overvatn A, Brech A, Johansen T. Monitoring autophagic degradation of p62/SQSTM1. Methods Enzymol. 2009; 452:181–197.

41. Hansen TE, Johansen T. Following autophagy step by step. BMC Biol. 2011; 9:39.

42. Mizushima N, Yoshimori T, Levine B. Methods in mammalian autophagy research. Cell. 2010; 140:313–326.

43. Xia M, Yu H, Gu S, Xu Y, Su J, Li H, Kang J, Cui M. p62/SQSTM1 is involved in cisplatin resistance in human ovarian cancer cells via the Keap1-Nrf2-ARE system. Int J Oncol. 2014; 45:2341–2348.

44. Preet R, Mohapatra P, Das D, Satapathy SR, Choudhuri T, Wyatt MD, Kundu CN. Lycopene synergistically enhances quinacrine action to inhibit Wnt-TCF signaling in breast cancer cells through APC. Carcinogenesis. 2013; 34:277–286.

45. Lobo MR, Green SC, Schabel MC, Gillespie GY, Woltjer RL, Pike MM. Quinacrine synergistically enhances the antivascular and antitumor efficacy of cediranib in intracranial mouse glioma. Neuro Oncol. 2013; 15:1673–1683.

46. Wang W, Gallant JN, Katz SI, Dolloff NG, Smith CD, Abdulghani J, Allen JE, Dicker DT, Hong B, Navaraj A, El-Deiry WS. Quinacrine sensitizes hepatocellular carcinoma cells to TRAIL and chemotherapeutic agents. Cancer Biol Ther. 2011; 12:229–238.

47. Dermawan JK, Gurova K, Pink J, Dowlati A, De S, Narla G, Sharma N, Stark GR. Quinacrine overcomes resistance to erlotinib by inhibiting FACT, NF-kappaB, and cell-cycle progression in non-small cell lung cancer. Mol Cancer Ther. 2014; 13:2203–2214.

48. Geng Y, Kohli L, Klocke BJ, Roth KA. Chloroquine-induced autophagic vacuole accumulation and cell death in glioma cells is p53 independent. Neuro Oncol. 2010; 12:473–481.

49. Lin YC, Kuo HC, Wang JS, Lin WW. Regulation of inflammatory response by 3-methyladenine involves the coordinative actions on Akt and glycogen synthase kinase 3beta rather than autophagy. J Immunol. 2012; 189:4154–4164.

50. Franken NA, Rodermond HM, Stap J, Haveman J, van Bree C. Clonogenic assay of cells *in vitro*. Nat Protoc. 2006; 1:2315–2319.

51. Chien J, Aletti G, Baldi A, Catalano V, Muretto P, Keeney GL, Kalli KR, Staub J, Ehrmann M, Cliby WA, Lee YK, Bible KC, Hartmann LC, Kaufmann SH, Shridhar V. Serine protease HtrA1 modulates chemotherapy-induced cytotoxicity. J Clin Invest. 2006; 116:1994–2004.

52. Chou TC. Theoretical basis, experimental design, and computerized simulation of synergism and antagonism in drug combination studies. Pharmacol Rev. 2006; 58:621–681.

53. Chou TC. Drug combination studies and their synergy quantification using the Chou-Talalay method. Cancer Res. 2010; 70:440–446.

54. Khurana A, Liu P, Mellone P, Lorenzon L, Vincenzi B, Datta K, Yang B, Linhardt RJ, Lingle W, Chien J, Baldi A, Shridhar V. HSulf-1 modulates FGF2- and hypoxia-mediated migration and invasion of breast cancer cells. Cancer Res. 2011; 71:2152–2161.

Quinacrine in endometrial cancer: Repurposing an old antimalarial drug☆,☆☆

Eleftheria Kalogera, MD [a], Debarshi Roy, Ph.D [b], Ashwani Khurana, Ph.D [b], Susmita Mondal, Ph.D [b], Amy L. Weaver, MS [c], Xiaoping He, MD. Ph.D [b], Sean C. Dowdy, MD [a], Viji Shridhar, Ph.D [b],*

[a] Division of Gynecologic Surgery, Mayo Clinic, Rochester, USA
[b] Department of Experimental Pathology, Mayo Clinic, Rochester, USA
[c] Division of Biomedical Statistics and Informatics, Mayo Clinic, Rochester, USA

HIGHLIGHTS

- Quinacrine exhibited strong antitumor activity against endometrial cancer *in vitro*.
- Quinacrine with cisplatin or paclitaxel exhibited strong synergism *in vitro*.
- Quinacrine combined with standard chemotherapy resulted in disease stabilization.
- Combination treatment vs. standard chemotherapy resulted in longer median survival.
- Maintenance therapy vs. combination resulted in further prolongation of overall survival.

ARTICLE INFO

ABSTRACT

Objective. Generate preclinical data on the effect of quinacrine (QC) in inhibiting tumorigenesis in endometrial cancer (EC) *in vitro* and explore its role as an adjunct to standard chemotherapy in an EC mouse model.

Methods. Five different EC cell lines (Ishikawa, Hec-1B, KLE, ARK-2, and SPEC-2) representing different histologies, grades of EC, sensitivity to cisplatin and p53 status were used for the *in vitro* studies. MTT and colony formation assays were used to examine QC's ability to inhibit cell viability *in vitro*. The Chou-Talalay methodology was used to examine synergism between QC and cisplatin, carboplatin or paclitaxel. A cisplatin-resistant EC subcutaneous mouse model (Hec-1B) was used to examine QC's role as maintenance therapy.

Results. QC exhibited strong synergism *in vitro* when combined with cisplatin, carboplatin or paclitaxel with the highest level of synergism in the most chemo-resistant cell line. Neither QC monotherapy nor carboplatin/paclitaxel significantly delayed tumor growth in xenografts. Combination treatment (QC plus carboplatin/paclitaxel) significantly augmented the antiproliferative ability of these agents and was associated with a 14-week survival prolongation compared to carboplatin/paclitaxel. Maintenance with QC resulted in further delay in tumor progression and survival prolongation compared to carboplatin/paclitaxel. QC was not associated with weight loss and the yellow skin discoloration noted during treatment was reversible upon discontinuation.

Conclusions. QC exhibited significant antitumor activity against EC *in vitro* and was successful as maintenance therapy in chemo-resistant EC mouse xenografts. This preclinical data suggest that QC may be an important adjunct to standard chemotherapy for patients with chemo-resistant EC.

© 2017 Elsevier Inc. All rights reserved.

1. Introduction

Endometrial cancer (EC) is the most common gynecologic malignancy in developed countries with an estimated 167,900 new cases in 2012 and a mortality rate of 2.3 per 100,000 [1]. In the United States (US), it is estimated that 54,870 women will be diagnosed with EC and 10,170 women will die from the disease in 2015 [2]. Importantly, the incidence of EC has exhibited a slow rise in recent years in stark contrast with the downward trend in the overall cancer incidence [3]. The aging population and the increased prevalence of obesity have been stipulated as the driving forces of this alarming trend and are projected to further increase in the future. EC is thus becoming an emerging public health concern.

Although the vast majority of women with EC (68%) are diagnosed when disease is confined in the uterus and prognosis is excellent with 5-year survival of 80–90%, there is a considerable subset of patients with poor prognosis. This subset includes patients diagnosed with advanced stage disease, unfavorable histologic subtypes, and disease recurrence. While surgery is the main initial treatment for EC, chemotherapy has a critical role for these patients with poor prognosis as well as for patients with increased risk of recurrence or persistent disease after surgery. Platinum-based chemotherapy is the standard first-line chemotherapy with carboplatin (which replaced the parent compound, cisplatin, due to its improved side effect profile) plus paclitaxel being the most commonly used regimen. Nevertheless, response rates to first-line treatment are as low as 50%, with even lower responses for recurrent disease. In addition, many patients will eventually relapse with platinum-resistant disease. As the chemotherapeutic options for these patients are limited and of questionable efficacy, it is of paramount importance that novel chemotherapeutic agents are identified to increase or restore chemo-sensitization to platinum-based chemotherapy.

Quinacrine (QC) is a quinine derivative and is based on the 9-aminoacridine structure. It is an oral, inexpensive drug that was discovered in the 1920s and was initially used extensively as an antimalarial drug during World War II; extensive follow-up data on tolerance and toxicity are available [4]. The first anticancer application of the drug was in the 1970s for the treatment of malignant pleural effusions following the discovery of its *in vivo* anticancer properties two decades earlier [5,6]. The underlying anticancer mechanisms of action were only recently explored [7]. QC gradually garnered new interest as an anticancer agent in 2005 after a group discovered its ability to rescue p53 function in tumor cells with mutant p53 [8] as well as to inhibit constitutively active NF-kB [7,9].

Since that discovery, other groups have shown that QC exhibits strong cytotoxic activity against a wide range of cancer cell lines [7,9–12]. QC sensitizes colon [10,11], renal [9,12], and hepatocellular carcinoma [13] to multiple chemotherapeutic agents, exhibits anticancer activity in breast [11] and pancreatic cancer cells [14] and has the ability to restore sensitivity to cisplatin in head and neck squamous cell carcinoma [15] and to paclitaxel in prostate cancer [16]. QC is currently under investigation or scheduled to enter in clinical trials for a number of cancers such as prostate cancer, advanced colorectal cancer and advanced non-small cell lung cancer. No prior groups have studied the use of QC in EC. The purpose of this investigation was thus to examine the anti-cancer activity of QC against EC *in vitro* and *in vivo* as well as explore its role as an adjunct to standard chemotherapy in a chemo-resistant EC mouse model.

2. Materials and Methods

2.1. Chemicals and reagents

Please refer to Supplemental Materials and Methods.

2.2. Cell lines and culture conditions

Five different cell lines representing different histologies, grades of EC, sensitivity to cisplatin and p53 status were used for the *in vitro* studies. Cell lines representing type I histology included: 1) Ishikawa (well differentiated endometrioid), 2) Hec-1B (moderately differentiated endometrioid, cisplatin-resistant) and 3) KLE (poorly differentiated endometrioid). Cell lines representing type II histology included: 1) ARK-2 (advanced stage serous adenocarcinoma), and 2) SPEC-2 (papillary serous carcinoma). The p53 mutation status is as follows: Ishikawa, HEC-1b, KLE and SPEC-2: mutant p53; ARK-2: p53 status unknown.

2.3. MTT assay, synergy assessment and Chou-Talalay calculations

Please refer to Supplemental Materials and Methods.

2.4. Colony formation assay (CFA)

Please refer to Supplemental Materials and Methods.

2.5. Immunoblotting

Please refer to Supplemental Materials and Methods.

2.6. Assessment of the anti-cancer activity of Quinacrine in vivo

All experimental use of animals complied with the guidelines of the Institutional Animal Care and Use Committee (IACUC) at the Mayo Clinic Foundation.

2.7. Tumor xenograft experiments

An endometrial cancer xenograft model was established by subcutaneous implantation of HEC-1b cells (cisplatin-resistant) into the right flank of 4- to 6-week old female athymic nude mice (nu/nu strain) (NCr *nu/nu*; Animal Production Area, National Cancer Institute, Frederick Cancer Research and Development Center, Frederick, MD) (1.25–1.5 × 10⁶ cells in a total volume of 200 μL per injection of PBS). Once subcutaneous implants measured 3 mm by 3 mm, approximately day 4 after implantation based on previous studies [17], mice were randomized in 5 groups of 10 mice (total of 50 mice) and this was considered as day 0. Of note, the number of mice per group was based on an *a priori* power calculation. Treatment was initiated on day 3 (approximately 7 days post implantation). Per protocol, we followed xenograft tumor size for 30 days after which the mice continued to be followed for survival using predefined endpoint criteria for sacrifice of the xenografts (detailed below). Groups were treated as follows: Group 1. Control (no treatment); Group 2. QC only: QC alone at 100 mg/kg *via* oral gavage every 48 h for 3 weeks; Group 3. Chemotherapy only: carboplatin plus paclitaxel *via* intraperitoneal injection at 16 mg/kg and 20 mg/kg, respectively on days 3, 7, and 11 as previously described [18]; Group 4. Combination: carboplatin plus paclitaxel (as in Group 3) plus QC (dosing as in Group 2) until day 11; and Group 5. Maintenance: carboplatin plus paclitaxel (as in Group 3) plus QC (dosing as in Group 2) until the end of the study. The QC regimen was chosen based on the literature on *in vivo* study of QC use for colorectal cancer [19].

The primary endpoint was xenograft tumor size across groups on day 30. Tumor size was measured every 48 h by digital caliper measurements and tumor volume was calculated using the modified formula for ellipsoid volume (volume = π/6 × length × width²). The rate of tumor growth (TG) was calculated relative to tumor volume on day of treatment initiation within each group [(tumor volume of treatment group on day 30 − tumor volume of treatment group on day of treatment initiation)/(tumor volume of treatment group on day of treatment initiation)]. Efficacy of treatment was assessed by comparison of tumor volumes and TG between treatment and control groups. Secondary

endpoints included change in weight (measured every 48 h throughout the study), survival, as well as cell proliferation and angiogenesis using immunohistochemistry. The criteria for sacrifice of the mice for survival included: a) tumor volume greater than 1000 mm³, b) tumor diameter > 20 mm, c) weight loss > 10% loss of body weight.

Tumor volume was measured every 48 h and efficacy of treatment was assessed by comparison of tumor volume between each treatment group and the control group on day 30 of the experiment as well as with the fold-change in tumor volume [tumor growth (TG)].

2.8. Histology and immunohistochemistry

Please refer to Supplemental Materials and Methods.

2.9. Statistical analysis

Wilcoxon rank-sum test and Kruskal-Wallis test were used to compare continuous variables between independent groups. The Dunnett's test was used as a *posthoc* test for multiple comparisons which were performed as "many-to-one comparisons" (each treatment group compared against the control group). The log-rank test was used for analysis of the survival data. Survival between groups was compared similarly in a "many-to-one" fashion with the *P* value for each pairwise comparison evaluated against a Bonferroni-corrected threshold to account for multiple comparisons. For the survival as well as the Ki-67 labeling index analyses, one additional comparison was performed (standard chemotherapy against maintenance group) and this additional comparison was taken into account in the Bonferroni correction (5 comparisons in total; level of significance adjusted at 0.01). *P*-values < 0.05 were considered statistically significant unless otherwise specified. All statistical analyses were performed with JMP version 10.0.0 (SAS Institute Inc., Cary, NC).

All experiments were performed at least in triplicate and results from each experiment were analyzed and interpreted independently of the others. The most representative experiment is presented.

3. Results

3.1. Quinacrine inhibits endometrial cancer cell viability in vitro

In order to investigate QC's ability to inhibit EC cell proliferation *in vitro*, we treated EC cell lines with increasing concentrations of QC for 48 h (Supplementary Fig. S1A and B). A dose-dependent cell proliferation inhibition was noted using the MTT assay across the spectrum of type I and II EC cell lines. The experimentally derived IC$_{50}$ ranged from 4 μM to 24 μM for QC with the highest IC$_{50}$ corresponding to the HEC-1b cells mirroring the sensitivity or relative resistance of cell lines to cisplatin (Supplementary Table S1). We, thus, focused the majority of our experiments on the HEC-1b and ARK-2 cell lines representing type I and II EC, respectively, as these were known to be relatively more cisplatin-resistant within each histology subtype, which was also confirmed by our MTT assays when deriving cisplatin IC$_{50}$.

In order to confirm the MTT assay findings, we assessed the effect of increasing concentrations of QC on the ability of EC cell lines to form colonies after 24 h of drug exposure (Supplementary Fig. 1C and D). We observed that the number of colonies decreased with increasing concentration of QC confirming potent anti-tumor effect of QC against EC. Consistent with our previous findings, the IC$_{50}$ for HEC-1b was higher compared to the IC$_{50}$ for ARK-2.

3.2. Quinacrine synergizes with cisplatin, carboplatin and paclitaxel in vitro

The potential of QC to synergize with cisplatin, carboplatin, and paclitaxel was explored using the Chou Talalay methodology [20]. When QC was combined with cisplatin in an equipotent (constant) ratio, a strong synergistic effect was noted in HEC-1b with a CI value of 0.363 at 0.5 Fa;

the synergistic effect was observed for the majority of the range of Fa (Fig. 1A). The DRI for cisplatin was notably high at 12.8 at 0.5 Fa: in order to inhibit 50% of HEC-1b cell growth, 12.8 times less cisplatin would be required if cisplatin were to be combined with QC compared to using cisplatin alone. In comparison, when this combinatory regimen was tested in ARK-2, a moderate synergistic effect was observed only at higher levels of Fa with DRI in the range of 5 (Fig. 1B). Since carboplatin was the platinum-based drug that would be used *in vivo*, a similar analysis was performed combining QC with carboplatin. When tested in HEC-1b, the two-drug combination exhibited strong synergism at a clinically relevant range of Fa (>0.3) with a considerable DRI of 16.5 at 0.9 Fa (Fig. 1C). In contrast to the effect of the combination of QC with cisplatin in ARK-2, QC with carboplatin exhibited strong synergism through almost the entire range of Fa (Fig. 1D). The combined action of QC and paclitaxel was examined next (Fig. 1E and F); this combination showed strong synergism through almost the entire range of Fa in both HEC-1b and ARK-2 with CIs ranging from 0.351 to 0.635 and from 0.292 to 0.543, respectively.

To further explore the extent to which QC synergizes with cisplatin and paclitaxel, various concentrations of QC were combined with increasing concentrations of cisplatin as well as with paclitaxel in non-constant (non-equipotent) ratios. The combination of QC with cisplatin exhibited various levels of synergism with strong synergy predominantly at the higher levels of Fa in both HEC-1b and ARK-2 (Supplementary Table S2). Similar conclusions can be drawn for the combined effect of QC with paclitaxel (Supplementary Table S3).

3.3. Quinacrine sensitizes endometrial cancer cells to cisplatin and paclitaxel in vitro

In order to investigate the ability of QC to restore sensitivity to cisplatin and paclitaxel in EC, EC cells were treated with increasing concentrations of cisplatin or paclitaxel (1/8 IC$_{50}$, 1/4 IC$_{50}$, 1/2 IC$_{50}$, IC$_{50}$, IC$_{50}$ × 2, IC$_{50}$ × 4) combined with a range of fixed concentrations of QC (1/4 IC$_{50}$, 1/2 IC$_{50}$, IC$_{50}$). The underlying rationale was that in the presence of relatively low concentrations of QC, a smaller amount of cisplatin would be required for the same effect in inhibiting cell growth *in vitro*.

When we combined a fixed concentration of QC with increasing concentrations of cisplatin, we observed a shift of the cisplatin IC$_{50}$ towards lower concentrations in both HEC-1b and ARK-2 indicative of the ability of QC to sensitize EC cells to cisplatin (Fig. 2). When cisplatin or paclitaxel was combined with IC$_{50}$ of QC, each drug's IC$_{50}$ displayed a substantial reduction ranging from 10- to 21-fold. The extent to which QC was able to restore sensitivity of EC cells to cisplatin and paclitaxel is better demonstrated by the fact that even 1/4 QC IC$_{50}$ resulted in a downward shift of each drug's IC$_{50}$ from 1.5- to 16-fold (Fig. S2). The only exception to that was the combination of cisplatin with 1/4 QC IC$_{50}$ in ARK-2 (Fig. S2B). More interestingly, the magnitude of the decrease in each drug's IC$_{50}$ was greater in the more cisplatin-resistant HEC-1b compared to the more cisplatin-sensitive ARK-2 when a comparable concentration of QC was used; this held true for both cisplatin and paclitaxel (Fig. S2). This supports the hypothesis that the combination of QC with standard chemotherapy may be more effective in drug-resistant compared to drug-sensitive cancers.

3.4. Quinacrine potentiates cisplatin sensitivity by down-regulating the expression of anti-apoptotic proteins in endometrial cancer cell lines

In order to investigate the underlying mechanism involved in QC-enhanced cisplatin-induced cytotoxicity, we screened HEC-1b and ARK-2 cell lysates for important pro-apoptotic (cleaved PARP and cleaved caspase-3) and anti-apoptotic proteins (MCL-1 and XIAP). MCL-1 (myeloid leukemia cell differentiation protein-1) and XIAP (X-linked inhibitor of apoptosis protein) are antiapoptotic markers associated with chemoresistance in EC [21,22]. Cleaved PARP and cleaved caspase 3 (both pro-apoptotic markers) were slightly to moderately
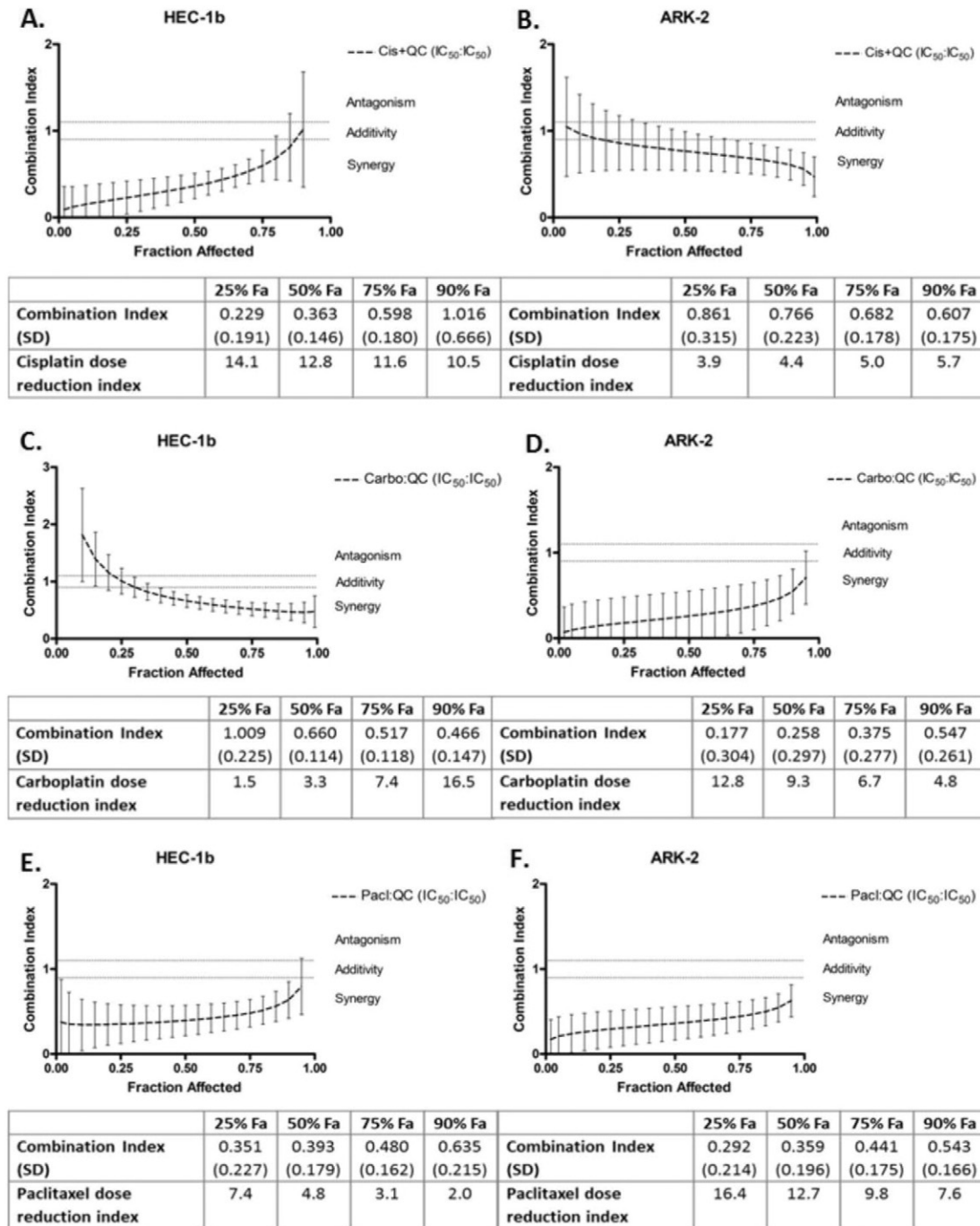
A. HEC-1b

	25% Fa	50% Fa	75% Fa	90% Fa
Combination Index	0.229	0.363	0.598	1.016
(SD)	(0.191)	(0.146)	(0.180)	(0.666)
Cisplatin dose reduction index	14.1	12.8	11.6	10.5

B. ARK-2

	25% Fa	50% Fa	75% Fa	90% Fa
Combination Index	0.861	0.766	0.682	0.607
(SD)	(0.315)	(0.223)	(0.178)	(0.175)
Cisplatin dose reduction index	3.9	4.4	5.0	5.7

C. HEC-1b

	25% Fa	50% Fa	75% Fa	90% Fa
Combination Index	1.009	0.660	0.517	0.466
(SD)	(0.225)	(0.114)	(0.118)	(0.147)
Carboplatin dose reduction index	1.5	3.3	7.4	16.5

D. ARK-2

	25% Fa	50% Fa	75% Fa	90% Fa
Combination Index	0.177	0.258	0.375	0.547
(SD)	(0.304)	(0.297)	(0.277)	(0.261)
Carboplatin dose reduction index	12.8	9.3	6.7	4.8

E. HEC-1b

	25% Fa	50% Fa	75% Fa	90% Fa
Combination Index	0.351	0.393	0.480	0.635
(SD)	(0.227)	(0.179)	(0.162)	(0.215)
Paclitaxel dose reduction index	7.4	4.8	3.1	2.0

F. ARK-2

	25% Fa	50% Fa	75% Fa	90% Fa
Combination Index	0.292	0.359	0.441	0.543
(SD)	(0.214)	(0.196)	(0.175)	(0.166)
Paclitaxel dose reduction index	16.4	12.7	9.8	7.6

Fig. 1. Combination of quinacrine with different chemotherapeutic agents in equipotent combinations (IC_{50} over IC_{50} ratio) was assessed for synergy using the Chou-Talalay method. The cells were exposed to each drug alone and in combination per protocol for 48 h. The combination indices (CI), fraction affected (Fa) and dose reduction indices (DRI) were generated by the Calcusyn software and plotted with the use of GraphPad. CI values <0.9 indicate synergism, 0.9–1.1 indicate additive effect, and >1.1 indicate antagonism. A and B: Cisplatin with quinacrine in HEC-1b (40:24 μM) and ARK-2 (14:16.5 μM). C and D: Carboplatin with quinacrine in HEC-1b (900:24 μM) and ARK-2 (480:16.5 μM). E and F: Paclitaxel with quinacrine in HEC-1b (11.8:24 μM) and ARK-2 (3.7:16.5 μM).

induced by each drug alone (Fig. 3). Increasing concentrations of QC resulted in higher levels of expression of cleaved PARP and cleaved caspase 3 in a dose-response effect. Importantly, combination treatment with cisplatin and QC strongly induced both pro-apoptotic markers greater than each drug alone. A dose-response effect was similarly observed when cells were treated with increasing concentrations of QC in the downregulation of the anti-apoptotic markers MCL-1 and XIAP. While XIAP was clearly inhibited to a greater extent when HEC-1b EC cells were treated with combination of both drugs compared to each drug alone, this effect was not observed in ARK-2.

3.5. Quinacrine in combination with carboplatin and paclitaxel inhibits endometrial cancer tumor growth in vivo

In order to assess the ability of QC to delay tumor growth *in vivo* as well as to act synergistically with standard chemotherapy, EC xenografts were treated in 5 different groups and were followed for tumor growth for 30 days as detailed in Methods (Supplementary Fig. S3). When comparing tumor volume on day 30 between treatment and control groups, neither QC monotherapy nor standard chemotherapy was effective in delaying tumor growth compared to controls ($P = 0.32$ and $P = 0.08$, respectively)
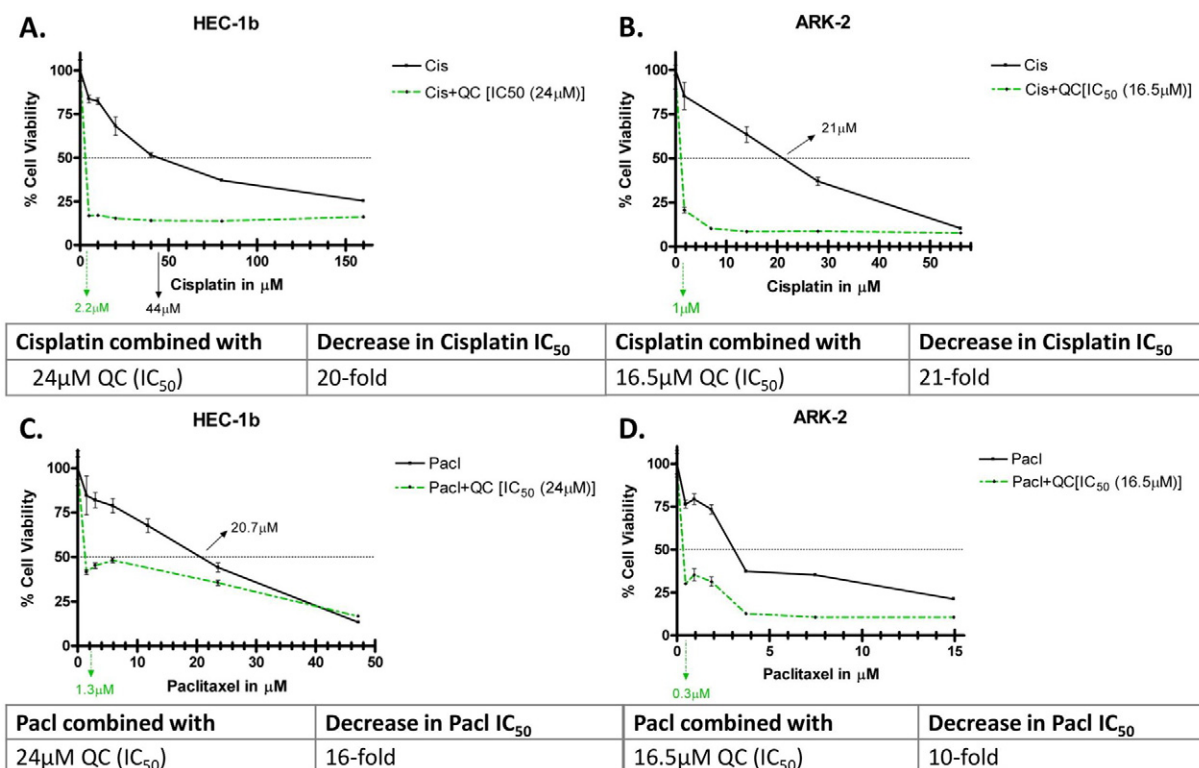
Fig. 2. Quinacrine re-sensitizes endometrial cancer cell lines to cisplatin and paclitaxel. When cells were treated with increasing concentrations of cisplatin or paclitaxel combined with QC IC$_{50}$, there was a shift of the cisplatin or paclitaxel IC$_{50}$ towards lower concentrations in both HEC-1b and ARK-2. For additional drug combinations, please refer to supplementary Fig. S2. A and B: Cisplatin with QC in HEC-1b and ARK-2, respectively. C and D: Paclitaxel with QC in HEC-1b and ARK-2, respectively.

(Fig. 4A). However, both combination and maintenance treatment groups were associated with significantly decreased tumor volumes compared to controls, indicating significant delay in tumor growth and stabilization of disease ($P = 0.002$ and $P = 0.005$, respectively) (Fig. 4A).

In order to account for the relative differences in tumor volume at initiation of treatment (day 0) between groups, we calculated the fold-change in tumor volume [tumor growth (TG)] of each xenograft between days 0 and 30 and compared the median tumor growth of each treatment group against controls (Fig. 4B.). The same conclusions on tumor growth per treatment group were reached. Xenografts treated with either QC monotherapy or standard chemotherapy did not exhibit

a significant difference in the magnitude of tumor growth compared to controls. In contrast, both combination and maintenance treatments were successful in significantly slowing tumor growth: xenografts exhibited only a 5.9-fold ($P = 0.001$) and 3.8-fold ($P = 0.008$) change in tumor volume, respectively, compared to control xenografts which had a 16.5-fold increase in their tumor volume.

3.6. Maintenance therapy with quinacrine prolongs survival of endometrial cancer mouse xenografts

In order to investigate the role of QC as maintenance therapy, xenografts were followed for survival as described in Methods. The shortest survival was observed in the controls with a median survival of 30 days, followed by the QC group with 46 days, the carboplatin plus paclitaxel group with 54 days, the combination group with 68 days, whereas median survival for the maintenance group was not reached at the end of the experiment at 72 days (Fig. 5). The survival study was terminated at day 72 as no mice were surviving in the control, QC, carboplatin plus paclitaxel, or combination groups. At the end of the experiment, 4 out of a total of 8 mice from maintenance group were alive, and 4 were previously sacrificed at low tumor volumes due to skin ulceration and thus censored. Overall survival of all treatment groups was significantly longer compared to controls. In order to assess whether maintenance conferred improved survival over standard chemotherapy, survival between these groups was compared. Importantly, maintenance exhibited a significant survival advantage compared to standard chemotherapy ($P = 0.001$).

3.7. Quinacrine treatment is well-tolerated

The safety profile of QC has been extensively studied in the past and its use has been found to be safe and tolerable. In order to assess how well QC was tolerated, the body weight of mice was measured every 48 h across all treatment groups and compared to controls.
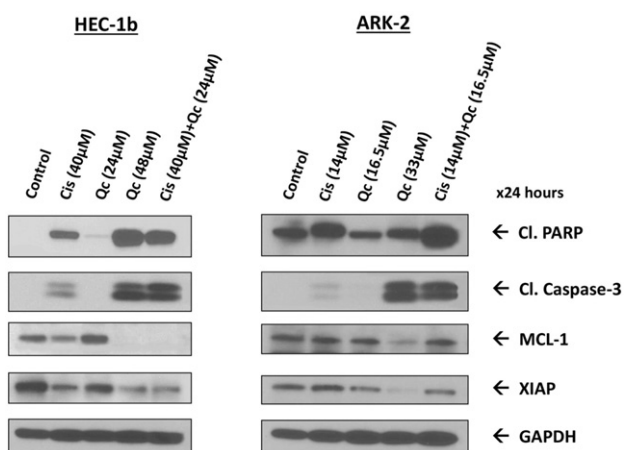

Fig. 3. Levels of pro-apoptotic and anti-apoptotic proteins after treatment with cisplatin, increasing concentrations of quinacrine and combination of cisplatin with quinacrine. Levels of important pro-apoptotic and anti-apoptotic proteins were assessed in HEC-1b and ARK-2 cancer cells after 24-hour treatment with cisplatin (IC$_{50}$), increasing concentrations of QC (IC$_{50}$ and IC$_{50}$ ×2), and combination of cisplatin (IC$_{50}$) with QC (IC$_{50}$) using whole-cell lysates immunoblotting.
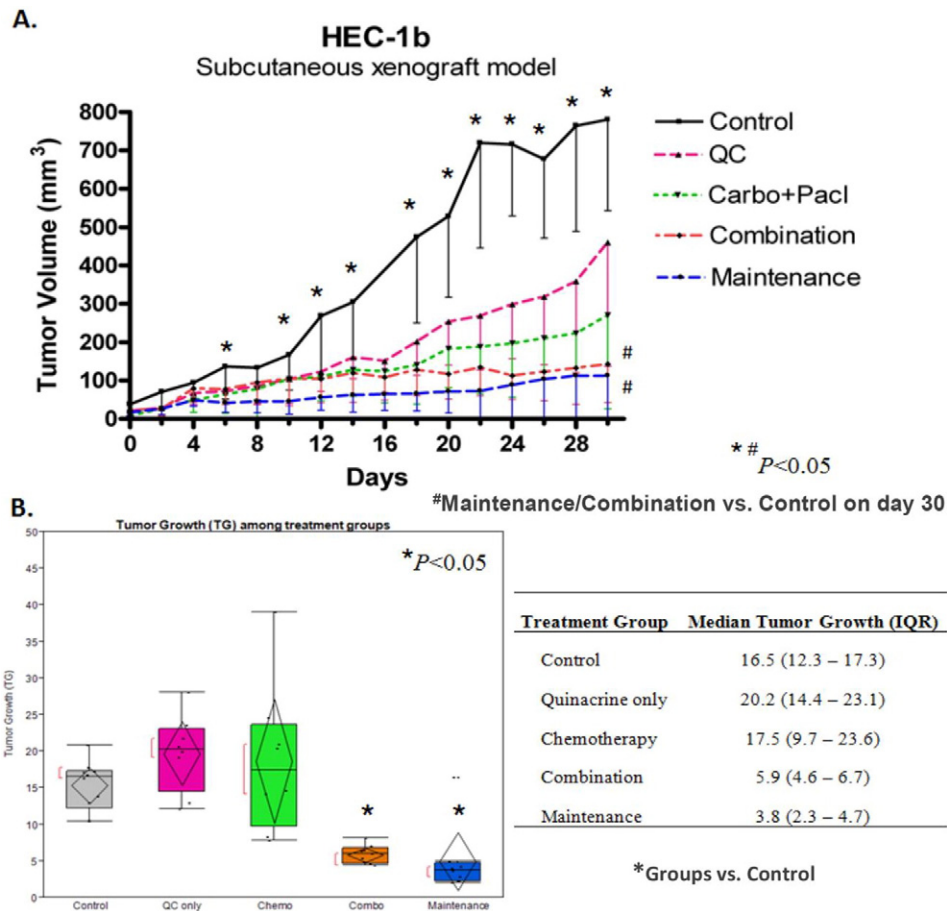
Fig. 4. Combination and maintenance treatment delay endometrial cancer tumor growth and stabilize disease *in vivo*. Treatment started at day 3 of the experiment, approximately 7 days post-implantation. Mice were treated with QC 100 mg/kg *via* oral gavage every 48 h and with carboplatin/paclitaxel *via* intraperitoneal injection at 16 mg/kg and 20 mg/kg, respectively on days 3, 7, and 11 as per Materials and Methods. (N = 8–10/group). A. Tumor volume was calculated using the modified formula for ellipsoid volume (volume = $\pi/6 \times$ length $\times$ width^2). *P < 0.05 across all groups at each time point (Kruskal-Wallis one-way analysis of variance); $^{\#}P = 0.002$ control *vs.* combination and $P = 0.005$ control *vs.* maintenance on day 30 (Dunnett's test). B. Tumor growth (TG) within each group was calculated as follows: (tumor volume on day 30 – tumor volume on day of treatment initiation)/(tumor volume on day of treatment initiation). Table with the median and IQR of TG as well as outlier box plots of TG across treatment groups; the median (IQR), mean, outliers and the "shortest half" (the more dense 50% of the observations as depicted by the red brackets) are graphed. *P < 0.05: Combination treatment *vs.* control ($P = 0.001$), maintenance *vs.* control ($P = 0.008$) (Dunnett's test).

No significant reduction in weight was observed in any of the treatment groups compared to controls (Fig. 6A). QC was thus well-tolerated as monotherapy, in combination with standard chemotherapy, and as maintenance.

One interesting adverse effect that has previously been observed with QC treatment in both animal and human studies is reversible yellow skin pigmentation. Consistent with this observation, xenografts who received QC exhibited yellow skin discoloration, primarily in the trunk, which subsided within 2 weeks following QC discontinuation (Fig. 6B). Longer duration of QC treatment did not result in more pronounced skin discoloration with maintenance group only exhibiting very subtle yellow skin changes after 72 days of QC treatment.

3.8. Quinacrine and tumor necrosis (H&E staining)

Tumor necrosis was observed both in treatment groups and controls (Supplementary Fig. S4B) suggesting that necrosis, to a certain extent, was a result of the relatively aggressive nature of the HEC-1b EC model used. Tumors from QC monotherapy demonstrated significantly increased tumor necrosis compared to controls (41.6% *vs.* 30.1%, $P = 0.01$; Supplementary Fig. S4C). However, neither standard chemotherapy nor combination treatment was associated with a significant increase in tumor necrosis compared to controls ($P = 0.64$ and $P = 0.07$, respectively). In contrast, maintenance resulted in significantly

greater tumor necrosis compared to controls (50.8% *vs.* 30.1%, $P = 0.01$) (Supplementary Fig. S4A and B).

3.9. Quinacrine and cell proliferation (Ki-67 staining)

An alternative way to assess antitumor activity *in vivo* is by correlating treatment with reduction in cell proliferation using Ki-67 immunostaining. It was noted that treatment groups that included QC had Ki-67 labeling indices numerically lower compared to controls and chemotherapy only suggesting that QC may result in enhanced antitumor activity (Supplementary Fig. S5B). QC monotherapy, combination treatment and maintenance were all associated with significantly lower Ki-67 labeling index compared to controls ($P = 0.002$ for all comparisons). However, tumor cell proliferation was significantly lower in maintenance compared to chemotherapy only ($P < 0.001$). In agreement with the tumor volume study conclusions, maintenance with QC was successful in further decreasing tumor cell proliferation and stabilizing disease compared to standard chemotherapy.

3.10. Quinacrine and angiogenesis (CD31 staining)

QC alone, in combination with standard chemotherapy, or as maintenance resulted in significantly lower iMVDs compared to controls ($P = 0.02, P = 0.005, P = 0.008$, respectively). This could mirror an overall decrease in the aggressiveness of the tumor. Specifically, this decrease
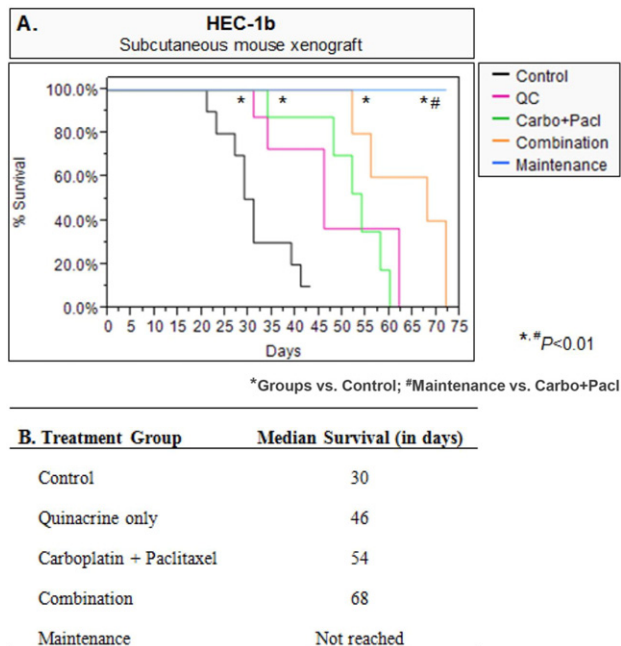
Fig. 5. Maintenance therapy with quinacrine prolongs survival of endometrial cancer mouse xenografts. Treatment began on day 3 of the experiment, approximately 7 days post-implantation. Mice were treated with QC 100 mg/kg via oral gavage every 48 h and with carboplatin/paclitaxel via intraperitoneal injection at 16 mg/kg and 20 mg/kg, respectively on days 3, 7, and 11 as per Materials and Methods. (N = 8–10/group). Mice were followed for survival and were sacrificed once tumor volume reached 1000 mm³, tumor ulcerated, became necrotic or infected or there was >10% loss of body weight. A. Kaplan-Meier survival curves reveal improved survival following maintenance treatment compared to standard chemotherapy ($P = 0.001$). *$P < 0.01$ (level of significance after Bonferroni adjustment for a total of 5 comparisons): QC monotherapy vs. control $P = 0.008$, carboplatin plus paclitaxel vs. control $P = 0.001$, combination treatment vs. control $P < 0.001$, maintenance treatment vs. control $P < 0.001$, maintenance treatment vs. carboplatin plus paclitaxel; #$P = 0.001$ (log-rank). B. Median survival in days across treatment groups.

Fig. 6. Quinacrine treatment is well-tolerated as monotherapy and in combination treatment with standard chemotherapy in endometrial cancer xenografts. A. Effect of QC on mice body weight across all treatments groups. (N = 8–10/group). B. QC treatment is associated with a temporary yellow skin discoloration during active drug administration.

in the angiogenic potential may explain why the growth of the tumors in the maintenance group appeared halted during QC maintenance, despite initially growing to a certain volume.

4. Discussion

Our study is the first to provide evidence that QC is effective against EC in vitro and in vivo. QC was successful in inhibiting EC cell viability in vitro across a range of EC cell lines representing different grades, histologic subtypes and sensitivity to standard chemotherapy. QC treatment was also associated with a dose-dependent decrease in the levels of proteins associated with chemo-resistance (MCL-1 and XIAP). Consistent with the in vitro findings, its use was associated with considerable tumor necrosis and inhibition of tumor cell proliferation in vivo. QC monotherapy delayed tumor growth in the mouse xenografts albeit not to the extent seen with standard chemotherapy. The EC xenograft model was developed using the most cisplatin-resistant EC cell line of those studied which could explain, at least in part, the suboptimal performance of QC monotherapy and standard chemotherapy in delaying tumor growth compared to controls. Despite this, overall survival with QC monotherapy was superior to controls and, importantly, comparable to standard chemotherapy. One could hypothesize that the significant anti-angiogenic effect observed in QC monotherapy group may have contributed to rendering the tumors less aggressive, leading to enhanced survival compared to controls despite comparable tumor volume between these groups.
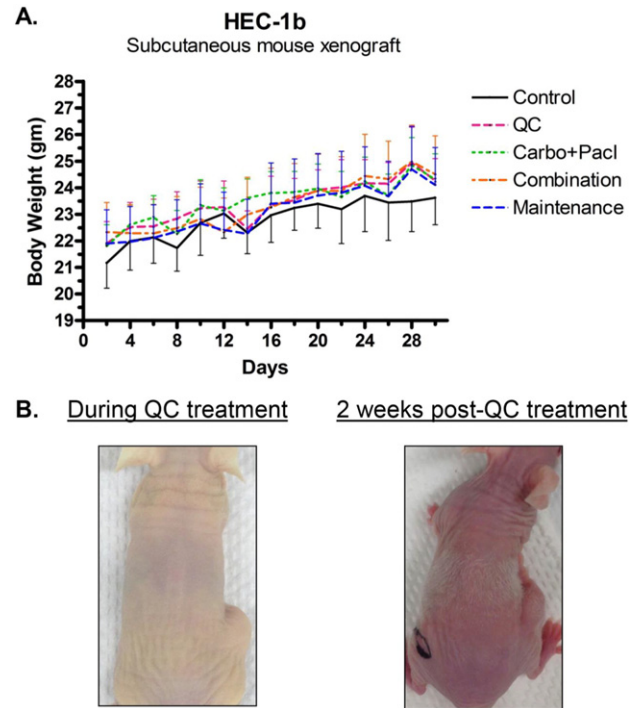
QC when co-administered with carboplatin and/or paclitaxel significantly enhanced their anticancer activity, as previously shown in other tumors [15,16]. In addition, we found evidence to suggest that the level of response to combination treatment may correlate with chemoresistance, with more chemo-resistant disease exhibiting greater response. Although strong synergy was observed between all drug combinations across both HEC-1b and ARK-2, the level of synergism was higher in the most-chemoresistant HEC-1b. Furthermore, the ability of QC to re-sensitize cells to cisplatin or paclitaxel was greater in the more chemo-resistant HEC-1b. Taken together, these data suggest that QC combined with standard chemotherapy may have greater therapeutic benefit when treating more aggressive chemo-resistant disease. Our in vivo study corroborates this finding. Finally, QC combined with paclitaxel exhibited the highest level of synergism among all drug combinations which could be proven beneficial in the treatment of Taxol-resistant disease, commonly encountered in recurrent EC.

Our in vivo study using a chemo-resistant EC mouse model corroborated our vitro results. QC augmented the antiproliferative effect of standard chemotherapy as evidenced by the significant decrease in tumor volume. What is even more interesting is the difference in the rate of tumor growth across treatment groups. Controls exhibited a relatively constant rate of tumor growth throughout the observation period. In contrast, during the active treatment period (up to day 11) as well as the immediate post-treatment period (up to approximately day 16), xenografts from all three treatment groups of interest (standard chemotherapy, combination and maintenance) were relatively stable in size. Following that period (after day 16), tumors from the standard chemotherapy group started to grow, while from the other two groups they remained relatively stable. This suggests that, in addition to potentiating its antitumor activity, QC combined with standard chemotherapy stabilizes disease. Importantly, this delay in tumor progression was associated with improved survival. Combination treatment was associated with a 14-week prolongation of median survival (26% increase) compared to

standard chemotherapy. Finally, maintenance further prolonged survival compared to standard chemotherapy with median survival not being reached during the duration of our study. These suggest that QC could be used initially as adjunct to standard chemotherapy for disease stabilization and then as maintenance for long-term disease suppression and prolongation of survival.

Use of angiogenic growth factors inhibitors or endothelial cell-specific cytotoxic agents to target tumor's blood supply has been recognized as an important adjunct to the traditional approach of inhibiting directly tumor cell proliferation [23,24]. Although we did not study directly QC's ability to target endothelial cells or decrease levels of angiogenic growth factors, we evaluated its ability to alter tumor's angiogenic potential by assessing the intratumor microvessel density by immunohistochemistry. Standard chemotherapy did not result in any significant change in the tumor's angiogenic environment, whereas QC as monotherapy, combination or maintenance resulted in a significant decrease in microvessel density. Importantly, the greatest benefit was noted with maintenance. Further studies are required to identify the exact mechanism of action by which QC alters the angiogenic make-up of the tumor (*i.e.* direct cytotoxic effect of endothelial cells *vs.* angiogenic growth factors inhibition). Albeit not a distant metastasis model, this finding offers evidence to suggest that QC may lead to a decrease in the metastatic potential of the tumor in addition to decreasing the rate of tumor growth. Of note, HEC-1b was originally characterized as an endometrioid grade 2 EC; however, upon review by a Mayo expert EC pathologist, it is now thought to be more consistent with serous EC which could also explain the more aggressive and chemo-resistant behavior observed both *in vitro* and *in vivo*. Serous EC tends to be more aggressive and is associated with distant disease at time of diagnosis. Taken together, our preclinical data suggest that QC combined with standard chemotherapy may decrease tumor's potential for distant metastasis in patients with histologies associated with poorer prognosis.

In a previous study of QC in colorectal cancer, the investigators found that mice tolerated doses up to 150 mg/kg every other day [19]. We elected in our study not to use the maximum tolerated dose as previously described but rather test a dose that would fall within already established dosing schemas in humans. Based on a previously validated formula for translation of drug doses from animal to human studies [25], a dose of 100 mg/kg in mice would translate into 8.1 mg/kg in humans: this mounts to 568 mg per day for an average person of 70 kg with 800 mg per day being the maximum previously used dose. It is thus possible that the regimen for EC treatment may fall within already safe and tolerable protocols. Finally, from a cost-effectiveness standpoint, in an era of rapidly expanding healthcare costs, QC could represent a more affordable treatment adjunct, even when used as maintenance for disease suppression, compared to the very expensive new drugs such as the anti-VEGF agents.

An inherent limitation of *in vitro* studies is that cells are being studied outside their "normal" environment and host organisms, which means that cell-to-cell and cell-to-stromal interactions, known important regulators of biological behavior, cannot be readily replicated in the *in vitro* setting. In order to address this limitation, we tested QC's ability to exert anticancer effects *in vivo* in an EC xenograft model using mice as host organism. An additional limitation is that we used a subcutaneous EC model instead of an orthotopic model. Orthotopic tumor xenografts are traditionally thought to mirror tumor-host interactions, tumor-specific metastatic patterns, and drug-tumor-host interplay more accurately than heterotopic xenografts. The decision to use a subcutaneous model was based on the prior experience of our laboratory with the use of subcutaneous xenografts and, conversely, lack of experience in implantation of EC cells in murine uteri as well as technical difficulties with following intrauterine tumor growth. Nonetheless, subcutaneous tumor xenografts are considered important in drug development research due to recognized merits such as reproducibility, reliable assessment of tumor establishment, growth, and response to treatment.

5. Conclusion

In summary, QC exhibited strong synergism *in vitro* when combined with cisplatin, carboplatin or paclitaxel with the highest level of synergism observed in the most chemo-resistant EC cell line. Combination treatment (QC plus standard chemotherapy) significantly augmented the antiproliferative ability of these chemotherapeutic agents as evidenced by the significant decrease in tumor burden, and, importantly, significantly prolonged median survival compared to standard chemotherapy alone. Maintenance therapy with QC was proven superior to combination treatment as it resulted in long-term stabilization of disease and further prolongation of overall survival compared to combination. This is the first study to provide preclinical data to support QC's efficacy as an adjunct to standard chemotherapy in the treatment of EC. These findings support the introduction of QC in a phase I/II clinical trial investigating the role of QC in combination with platinum-based chemotherapy for patients with chemo-resistant EC.

Disclosure of Potential Conflicts of Interest

There are no conflicts of interest for this manuscript.

Appendix A. Supplementary data

Supplementary data to this article can be found online at http://dx.doi.org/10.1016/j.ygyno.2017.04.022.

References

[1] L.A. Torre, F. Bray, R.L. Siegel, J. Ferlay, J. Lortet-Tieulent, A. Jemal, Global cancer statistics, 2012, CA Cancer J. Clin. 65 (2015) 87–108.

[2] R.L. Siegel, K.D. Miller, A. Jemal, Cancer statistics, 2015, CA Cancer J. Clin. 65 (2015) 5–29.

[3] R. Siegel, D. Naishadham, A. Jemal, Cancer statistics, 2013, CA Cancer J. Clin. 63 (2013) 11–30.

[4] C.W. Hays, The United States Army and malaria control in World War II, Parassitologia 42 (2000) 47–52.

[5] J.W. Vassey, J. Edmonds, J.L. Irvin, J.A. Green, E.M. Irvin, Studies on the administration of quinacrine to tumor-bearing mice, Cancer Res. 15 (1955) 573–578.

[6] E.R. Borja, R.P. Pugh, Single-dose quinacrine (atabrine) and thoracostomy in the control of pleural effusions in patients with neoplastic diseases, Cancer 31 (1973) 899–902.

[7] C. Guo, A.V. Gasparian, Z. Zhuang, D.A. Bosykh, A.A. Komar, A.V. Gudkov, et al., 9-Aminoacridine-based anticancer drugs target the PI3K/AKT/mTOR, NF-kappaB and p53 pathways, Oncogene 28 (2009) 1151–1161.

[8] W. Wang, W.C. Ho, D.T. Dicker, C. MacKinnon, J.D. Winkler, R. Marmorstein, et al., Acridine derivatives activate p53 and induce tumor cell death through Bax, Cancer Biol. Ther. 4 (2005) 893–898.

[9] K.V. Gurova, J.E. Hill, C. Guo, A. Prokvolit, L.G. Burdelya, E. Samoylova, et al., Small molecules that reactivate p53 in renal cell carcinoma reveal a NF-kappaB-dependent mechanism of p53 suppression in tumors, Proc. Natl. Acad. Sci. U. S. A. 102 (2005) 17448–17453.

[10] T.S. Jani, J. DeVecchio, T. Mazumdar, A. Agyeman, J.A. Houghton, Inhibition of NF-kappaB signaling by quinacrine is cytotoxic to human colon carcinoma cell lines and is synergistic in combination with tumor necrosis factor-related apoptosis-inducing ligand (TRAIL) or oxaliplatin, J. Biol. Chem. 285 (2010) 19162–19172.

[11] R. Preet, P. Mohapatra, S. Mohanty, S.K. Sahu, T. Choudhuri, M.D. Wyatt, et al., Quinacrine has anticancer activity in breast cancer cells through inhibition of topoisomerase activity, Int. J. Cancer 130 (2012) 1660–1670.

[12] K. Sasaki, N.H. Tsuno, E. Sunami, G. Tsurita, K. Kawai, Y. Okaji, et al., Chloroquine potentiates the anti-cancer effect of 5-fluorouracil on colon cancer cells, BMC Cancer 10 (2010) 370.

[13] W. Wang, J.N. Gallant, S.I. Katz, N.G. Dolloff, C.D. Smith, J. Abdulghani, et al., Quinacrine sensitizes hepatocellular carcinoma cells to TRAIL and chemotherapeutic agents, Cancer Biol. Ther. 12 (2011) 229–238.

[14] L.M. Oppegard, A.V. Ougolkov, D.N. Luchini, R.A. Schoon, J.R. Goodell, H. Kaur, et al., Novel acridine-based compounds that exhibit an anti-pancreatic cancer activity are catalytic inhibitors of human topoisomerase II, Eur. J. Pharmacol. 602 (2009) 223–229.

[15] J. Friedman, L. Nottingham, P. Duggal, F.G. Pernas, B. Yan, X.P. Yang, et al., Deficient TP53 expression, function, and cisplatin sensitivity are restored by quinacrine in head and neck cancer, Clin. Cancer Res. 13 (2007) 6568–6578.

[16] P.L. de Souza, M. Castillo, C.E. Myers, Enhancement of paclitaxel activity against hormone-refractory prostate cancer cells in vitro and in vivo by quinacrine, Br. J. Cancer 75 (1997) 1593–1600.

[17] K. Narita, J. Staub, J. Chien, K. Meyer, M. Bauer, A. Friedl, et al., HSulf-1 inhibits angiogenesis and tumorigenesis in vivo, Cancer Res. 66 (2006) 6025–6032.

[18] R. Rattan, R.P. Graham, J.L. Maguire, S. Giri, V. Shridhar, Metformin suppresses ovarian cancer growth and metastasis with enhancement of cisplatin cytotoxicity in vivo, Neoplasia 13 (2011) 483–491.

[19] J.N. Gallant, J.E. Allen, C.D. Smith, D.T. Dicker, W. Wang, N.G. Dolloff, et al., Quinacrine synergizes with 5-fluorouracil and other therapies in colorectal cancer, Cancer Biol. Ther. 12 (2011) 239–251.

[20] T.C. Chou, Theoretical basis, experimental design, and computerized simulation of synergism and antagonism in drug combination studies, Pharmacol. Rev. 58 (2006) 621–681.

[21] V. Gagnon, C. Van Themsche, S. Turner, V. Leblanc, E. Asselin, Akt and XIAP regulate the sensitivity of human uterine cancer cells to cisplatin, doxorubicin and taxol, Apoptosis 13 (2008) 259–271.

[22] Y. Konno, P. Dong, Y. Xiong, F. Suzuki, J. Lu, M. Cai, et al., MicroRNA-101 targets EZH2, MCL-1 and FOS to suppress proliferation, invasion and stem cell-like phenotype of aggressive endometrial cancer cells, Oncotarget 5 (2014) 6049–6062.

[23] J. Folkman, What is the evidence that tumors are angiogenesis dependent? J. Natl. Cancer Inst. 82 (1990) 4–6.

[24] G. Gasparini, A.L. Harris, Clinical importance of the determination of tumor angiogenesis in breast carcinoma: much more than a new prognostic tool, J. Clin. Oncol. 13 (1995) 765–782.

[25] S. Reagan-Shaw, M. Nihal, N. Ahmad, Dose translation from animal to human studies revisited, FASEB J. 22 (2008) 659–661.

SCIENTIFIC REPORTS

OPEN

Quinacrine upregulates p21/p27 independent of p53 through autophagy-mediated downregulation of p62-Skp2 axis in ovarian cancer

DeokBeom Jung[1], Ashwani Khurana[1], Debarshi Roy[1], Eleftheria Kalogera[2], Jamie Bakkum-Gamez[2], Jeremy Chien[3] & Viji Shridhar[1]

We have previously shown that the anti-malarial compound Quinacrine (QC) inhibits ovarian cancer (OC) growth by modulating autophagy. In the present study we extended these studies to identify the molecular pathways regulated by QC to promote apoptosis independent of p53 status in OC. QC exhibited strong anti-cancer properties in OC cell lines in contrast to other anti-malarial autophagy inhibiting drugs. QC treatment selectively upregulated cell cycle inhibitor p21, and downregulated F box protein Skp2 and p62/SQSTM1 expression independent of p53 status. Genetic downregulation of key autophagy protein ATG5 abolished QC-mediated effects on both cell cycle protein p21/Skp2 as well as autophagic cargo protein p62. Furthermore, genetic silencing of p62/SQSTM1 resulted in increased sensitivity to QC-mediated apoptosis, downregulated Skp2 mRNA and increased accumulation of p21 expression. Likewise, genetic knockdown of Skp2 resulted in the upregulation of p21 and p27 and increased sensitivity of OC cells to QC treatment. In contrast, transient overexpression of exogenous p62-HA plasmid rescued the QC-mediated Skp2 downregulation indicating the positive regulation of Skp2 by p62. Collectively, these data indicate that QC-mediated effects on cell cycle proteins p21/Skp2is autophagy-dependent and p53-independent in high grade serious OC cells.

The Majority of high grade serous Ovarian Cancers (OC) that harbor p53 mutations and deletions are often associated with high mortality[1]. So far, limited therapeutic options are available to treat these cancers that are associated with high recurrence rates. There are currently in development various therapeutic agents that are being considered for their ability to promote tumor regression. Preclinical tumor models have confirmed tumor regression via drug-induced apoptotic and autophagic pro-death signaling mechanisms in several cancers[2,3]. Both pro-survival as well as pro-apoptotic roles have been associated with autophagy. Autophagy is a catabolic process where portions of the cytoplasm and defective organelles are engulfed in autophagosomes for delivery to the lysosomes for bulk degradation. Autophagy is induced by various cellular events such as nutrient deprivation in the form of glucose or amino acid starvation. Under nutrient deprived conditions, autophagy provides amino acids and other macromolecules following degradation of cellular organelles and membranes leading to cancer cell survival[4]. However, drug-induced autophagy, also known as type II programmed cell death, has been shown to promote apoptosis and cell death[5]. Therefore, agents regulating autophagy by either promoting or inhibiting it might have differential impact on tumor growth. Autophagy involves at least 40 known autophagy-related proteins including ATG5[6]. Both chemical inhibitors (such as Bafilomycin A and 3-MA) and genetic silencing of ATG5 and ATG7 have been shown to inhibit autophagy and promote or augment apoptosis in response to treatment with combination of therapeutic agents in cancer cells[7–9].

[1]Department of Experimental Pathology, Mayo Clinic, Rochester, MN, USA. [2]Division of Gynecologic Surgery, Department of Obstetrics and Gynecology, Mayo Clinic, Rochester, MN, USA. [3]Division of Molecular Medicine, University of New Mexico School of Medicine, Albuquerque, NM, USA. Correspondence and requests for materials should be addressed to V.S. (email: shridhar.vijayalakshmi@mayo.edu)
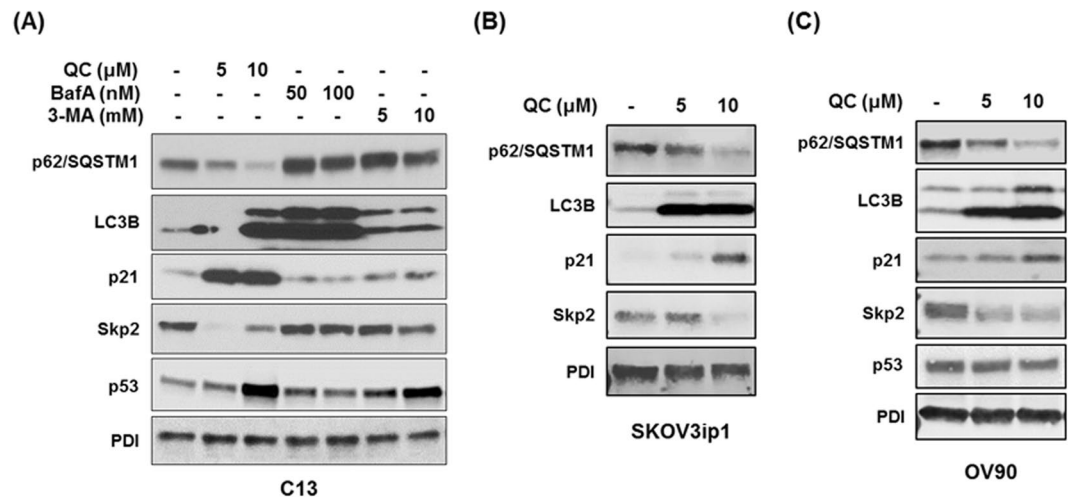
Figure 1. Autophagy modulators have differential effects on p62, p21 and Skp2 expression. C13 cells were treated with increasing concentrations of QC (5 and 10 μM), Bafilomycin A (50 and 100 nM) and 3-MA (5 and 10 mM) for 24 hours. (**A**) Western blot analysis in QC, Bafilomycin A, 3-MA treated C13 cells using anti-p62/SQSTM1, anti-LC3B, anti-p21, anti-Skp2, anti-p53 and anti-PDI antibodies. (**B**) SKOV3ip1 cells (p53 null), (**C**) OV90 cells (p53 mutated) were treated with QC (5 and 10 μM) for 24 hours. The protein expression levels were assayed by western blot analysis.

Both pro-apoptotic and autophagy modulators are in clinical trials to treat several types of cancers including OC[10]. Specifically anti-malarial agents have been shown to be effective in attenuating cancer growth both *in vitro* and *in vivo* in mouse models. The anti-malarial drug Quinacrine (QC) alters a range of cellular activities including stabilization of p53, inhibition of NFkB and in modulating heat shock response in cancer cells[11,12]. We previously showed that QC induces autophagic mediated cell death to promote chemosensitivity of OC cells *in vitro* and attenuated tumor growth in HeyA8MDR mouse xenografts *in vivo*[13]. QC selectively degraded p62 and promoted autophagic flux more in the chemo-resistant cells compared to their isogenic sensitive counterparts. However, underpinning QC mediated mechanisms have remained elusive.

Among other anti-cancer properties of anti-malarial agents, these agents have also been found to be effective inhibitors of cell cycle and cell proliferation[11,14]. Majority of autophagy modulators promote apoptosis by targeting distinct and essential pathways in addition to causing cell cycle arrest. However, it is not known if there is an association between cell cycle and autophagic cell death[15,16]. Specifically, the molecular mechanism linking autophagy induction and cell cycle arrest is not well documented. Among the cell cycle inhibitors, p21 and p27, two tumor suppressor proteins targeted for degradation by S-phase kinase–associated protein 2 (Skp2)[17–21], play a significant role in inhibition of cellular growth[22]. Studies have shown SKp2 is overexpressed in several cancers[23–25]. Specifically high Skp2 expression was reported in 61% of ovarian tumors. In another study, elevated levels of Skp2 and downregulation of p27 was associated with late stage disease[26] as well as with lower p21 levels[27]. The relationship between Skp2 and p53 is controversial with studies supporting both p53- dependent and -independent regulation of Skp2's activity[28,29]. In this context, it is important to note that the majority of high grade serous OC have mutated p53. Therefore, identifying chemical entities that regulate cell cycle and cell proliferation independent of p53 status might be a useful strategy to target cancers such as OC.

In the present study we examined anti-tumor activities of QC in several OC cell lines with different p53 status. Mechanistically, we have characterized the effects of QC on two critical molecular signaling pathways, namely, the attenuation of p62 to promote autophagic flux leading to SKp2 downregulation to restrain cell cycle progression resulting in the inhibition of cancer growth and proliferation.

Results

Autophagy modulators affect cell cycle differentially.
Our previous finding showed that QC induces autophagy in OC cells. To determine if other autophagy modulators have similar effects, we first analyzed autophagy and cell cycle related proteins by Western blot analysis (Fig. 1A). We observed that when C13 cells are treated with QC, Bafilomycin A (BafA) and 3-methyladenine (3-MA) at indicated doses, QC treatment resulted in degradation or downregulation of p62 expression in C13 cells whereas BafA and 3-MA in stabilization of p62 expression (Fig. 1A). LC3B was also stabilized by treatment with both QC and BafA. Importantly, QC but not BafA or 3-MA treatment stabilized the cell cycle inhibitor p21 expression in these cells. Furthermore, QC treatment downregulated Skp2, an F-box protein known to target p21/p27 for degradation, while BafA and 3-MA showed no effect on Skp2/p21 expression. These data indicate that while autophagy inhibitors BafA and 3MA stabilized p62 expression, QC treatment downregulated p62 expression, which is an indication of autophagy induction[9]. Since p21 is a direct target of p53 and QC has been reported previously to stabilize p53[11], we next examined whether QC is able to promote these observed changes in a p53-dependent manner. QC treatment of p53 null SKOV3ip1 and p53 mutant OV90 (S215R) cell lines resulted in the downregulation of p62, Skp2 and
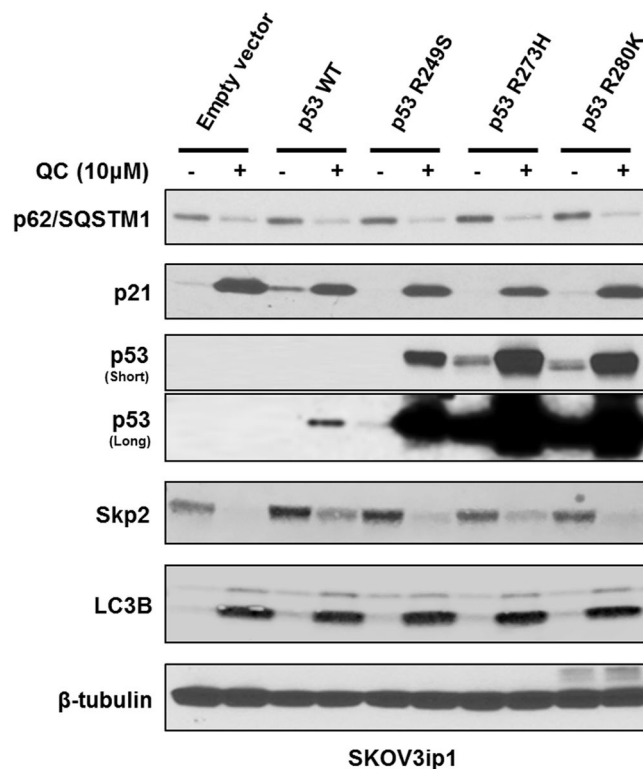
54

Figure 2. Empty vector clones and p53 mutant clones generated in SKOV3ip1 cells were treated with QC for 24 hours. Western blot analysis of transfected cells using anti-p62 /SQSTM1, p21, p53, Skp2, LC3B and anti-beta tubulin antibodies.

upregulation of p21 expression (Fig. 1B and C). These data indicate that QC-mediated effects on p62, Skp2 and p21 expression are independent of p53 expression. To further verify these findings, we generated stable clones expressing wild type p53, R249S, R273H and R280H mutant forms of p53 in SKOV3ip1 cells that are void of p53 expression as described in the materials and methods. Western blot analysis showed that QC treatment downregulated p62 and Skp2 expression and upregulated p21 and LC3B expression in these cells irrespective of p53 status (Fig. 2). Of note, QC treatment also stabilized p53 expression in wild type and mutant p53 expressing SKOV3ip1 stable clones further confirming that QC-mediated effects are independent of p53 status. This is consistent with previous reports that QC stabilization of p53 results in p53-dependent and p53-independent tumor cell death[12].

QC-mediated p62 downregulation is independent of proteasomal degradation.
It has been shown that p62 is degraded via proteasomal- as well as autophagic-dependent manner[30]. Therefore, to determine whether QC-mediated p62 degradation is proteasome-dependent, we co-treated cells with QC and proteasomal inhibitors such as lactacystin and velcade for 24 hours. Western blot analysis revealed that QC-mediated p62 degradation was not altered upon inhibition of proteasomes with either 10 μM lactacystin or 2 μg/ml velcade treatment. Importantly, inhibition of proteasomal activity further stabilized p21 and p27 expression (Fig. 3A). We suspected that the induction of p21 and p27 expression in response to QC treatment might also inhibit CDK activities. Therefore, we determined the phosphorylation status of CDK substrates by Western blot analysis using anti-phospho CDK substrate antibody. Treatment with QC attenuated phosphorylation of several CDK substrates indicating that QC blocked CDK activities irrespective of proteasomal inhibition (Fig. 3A). Similarly, Western blot analysis using anti-ubiquitin antibody revealed that proteasomal inhibitors arrested proteins modified with poly-ubiquitinated chains demonstrating the efficacy of proteasomal inhibitors. These data indicate that QC-mediated p62 downregulation is independent of proteasomal degradation.

To determine whether QC-mediated p62 degradation is autophagy dependent, we utilized mouse embryonic fibroblasts (MEFs) lacking ATG5 expression. ATG5 plays a critical role in promoting autophagy and it has been shown that depletion of ATG5 inhibits autophagy[31,32]. Therefore, we next examined the effect of QC treatment on wild type and ATG5 null MEFs. Western blot analysis revealed that QC treatment promoted p62 downregulation, induced LC3B expression and increased apoptosis as indicated by increased PARP cleavage in WT MEFs but not in ATG5 null MEFs (Fig. 3B). Skp2 levels were too low to be detected in wild type MEFs whereas they were elevated in p62 null MEFs. Collectively, these data indicate that ATG5 is essential for QC-mediated effects. To further verify these effects, we next investigated the effect of QC on shRNA-mediated ATG5 depleted C13 cells. C13 cells were stably selected with shRNA against ATG5 and NTC respectively as described in materials and methods. Western blot analysis confirmed complete knockdown of ATG5 in C13HBF2 stable clone (Fig. 3C). While QC treatment downregulated p62 and Skp2 expression in NTC-C13 cells, it did not affect p62 and Skp2
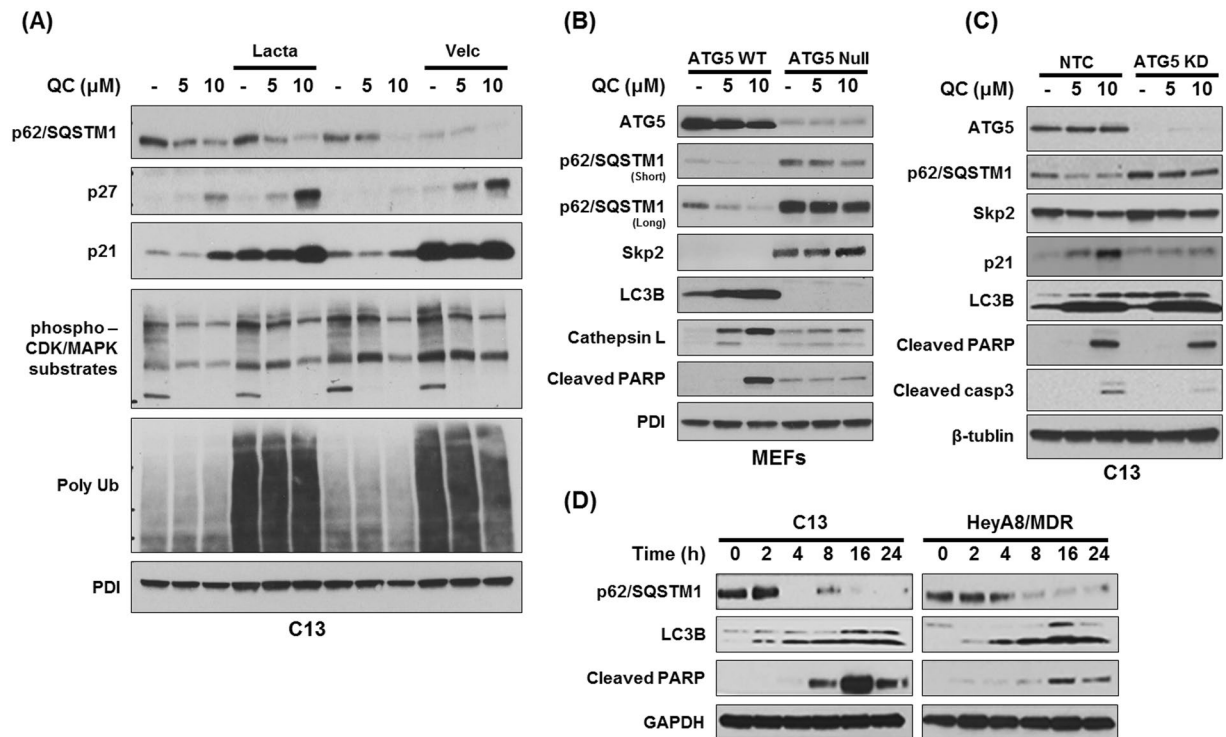
Figure 3. (**A**) Effect of co-treatment of QC and proteasome inhibitors Lactacystin (10 μM) and Velcade (2 μg/ml) for 24 hours on C13 cells. Cells were harvested and subjected to Western blot analysis using anti- p62/SQSTM1, anti-p27, anti-p21, anti-PDI, anti-Ubiquitin, anti-phospho-CDK/MAPK substrates and anti-PDI antibodies. (**B**) Effect of QC treatment on wild type and ATG5 null Mouse embryonic fibroblasts (MEFs). MEFs were treated with increasing concentrations of QC (5 and 10 μM) for 24 hours followed by Western blot analysis using anti-ATG5, anti-cleaved PARP, anti-Cathepsin L, anti-p62/SQSTM1, anti-LC3B, anti-Skp2 and anti-PDI. (**C**) Effect of QC treatment on NTC and ATG5 knockdown (HBF2) C13 cells. NTC and ATG5 knockdown C13 cells were treated with QC at 5 and 10 μM for 24 hours followed by Western blot analysis using anti-ATG5, anti-cleaved PARP, anti-cleaved caspase 3, anti-p62/SQSTM1, anti-LC3B, anti-Skp2, anti-p21 and anti-beta tubulin antibodies. (**D**) C13 and HeyA8/MDR cells were treated with QC (5 μM) for 0, 2, 4, 8, 16, 24 hours. Western blot analysis was performed using anti-cleaved PARP, anti-p62/SQSTM1, anti-LC3B and anti-GAPDH antibodies.

levels in ATG5 knockdown C13 cells. It is important to note that upon ATG5 knockdown in C13 as well as in ATG5 null MEFs cells, elevated basal level of p62 expression was also associated with elevated Skp2 expression.

Similarly, significant upregulation of p21 expression was observed in QC-treated NTC-C13 cells but not in ATG5 depleted C13 cells. Consistent with these results, QC treatment in ATG5 depleted cells resulted in diminished apoptotic response as reflected by lower level of cleaved PARP and cleaved caspase 3 expression (Fig. 3C). Importantly, no change in LC3B induction was observed in NTC and ATG5 depleted clones. Taken together, these data indicate that QC-mediated apoptosis and autophagic response is dependent on ATG5 levels.

We next wanted to examine the temporal regulation of autophagy and apoptosis upon treatment with QC. Western blot analysis of QC treated C13 and Hey8MDR cells show that p62 expression was downregulated as early as 4 hours following treatment in C13 cell and 8 hours in HeyA8MDR cells, whereas appearance of cleaved PARP was detected in a 16 to 24 hours window (Fig. 3D). These data suggest that QC treatment triggers autophagic clearance of p62 leading to apoptosis in both C13 and HeyA8MDR cancer cells.

To determine whether PARP cleavage was due to the activation of initiator caspases as well as effector caspases, we did immunoblotting in C13 and HeyA8MDR cells treated with 5.0 and 10 μM QC for 24hrs. We observed activation of Caspase 8 and Caspase 9, and increased the activity of Caspase 3, indicating that both extrinsic and intrinsic apoptotic pathways are activated by QC (Fig. S1).

p62 knockdown promotes QC-mediated p21 upregulation via Skp2. We have previously reported that QC downregulated p62 expression and that p62 expression plays a critical role in promoting cell survival[13]. Since we observed parallel changes in p62, Skp2 and p21 expression upon QC treatment, we next wanted to determine the relationship between p62 and cell cycle inhibitor p21. To further determine the role of p62 in QC-mediated cell death, we generated p62 knockdown cells via lentiviral mediated shRNA in OV2008 cells as described in materials and methods. We treated NTC and p62 knockdown OV2008 cells with QC and evaluated the effect on apoptosis and cell cycle proteins. Western blot analysis showed that treatment with QC resulted in extensive apoptosis in p62 depleted cells when compared to NTC OV2008 cells as reflected in the levels of cleaved PARP (Fig. 4A). Importantly, p62 knockdown also resulted in diminished basal levels of Skp2 which was further downregulated upon QC treatment in OV2008 cells. The decrease in Skp2 expression was also found to
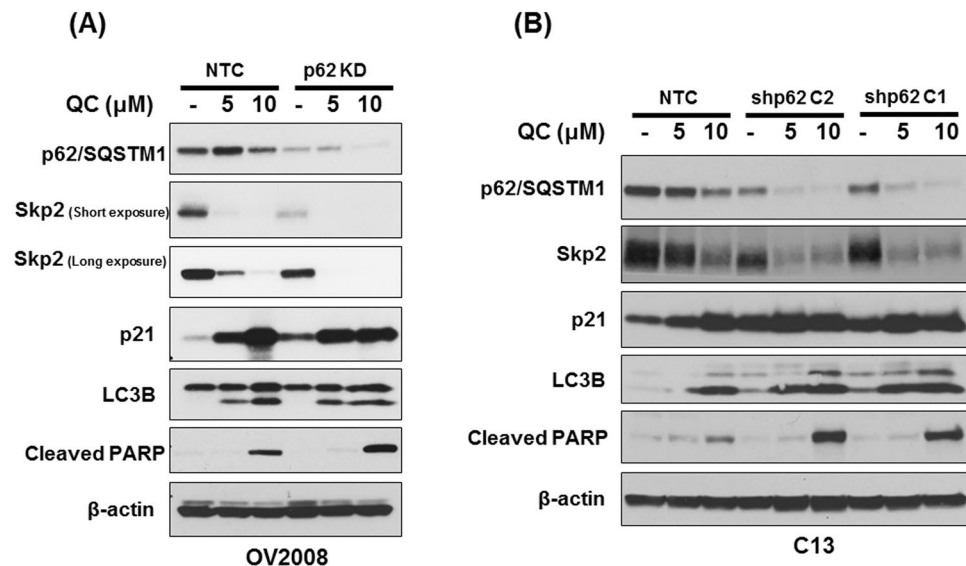
Figure 4. (**A**) Effect of QC treatment on NTC and p62 knockdown (shRNA 280) OV2008 cells for 24 hours. Cells were harvested and subjected to Western blot analysis using anti-cleaved PARP, anti-cleaved PARP, anti-p62/SQSTM1, anti-p21 and anti-beta actin antibodies. (**B**) Effect of QC treatment on NTC and p62 knockdown (shRNA clone1 and shRNA clone2) C13 cells for 24 hours. Cells were harvested and subjected to Western blot analysis using anti-cleaved PARP, anti-cleaved PARP, anti-p62/SQSTM1, anti-p21 and anti-beta actin antibodies.

be associated with an increase in p21 expression which was further increased upon QC treatment in p62 depleted OV2008 cells. In order to confirm that the effects are not specific to only OV2008 cancer cells, we generated NTC and two separate p62 shRNA expressing stable clones in C13 cells. Consistent with our previous findings, QC treatment downregulated p62 and promoted increased apoptosis in p62 knockdown clones as indicated by cleaved PARP expression without causing any significant change in autophagy in NTC and p62 shRNA clones. Interestingly, knockdown of p62 in C13 cells also resulted in p21 upregulation and Skp2 downregulation, changes that were further enhanced upon QC treatment (Fig. 4B). Together, these data indicate that p62 positively regulated Skp2 levels in these cells.

QC-mediated p21 stabilization is post-transcriptional. We next investigated whether the increase in p21 expression was due to its increased transcription or post-translational stabilization. To this end, we transiently transfected pcDNA3.1-p21 Flag expression vector in OV2008 NTC and OV2008 p62 shRNA cells followed by QC treatment. Western blot analysis showed that QC treatment, upregulated p21-Flag expression in NTC as well as p62shRNA cells (Fig. 5A). Interestingly, p21 expression was high at basal levels in p62 knockdown cells and was significantly more upregulated upon treatment with QC when compared with NTC cells. These data indicate that p21 was stabilized at the post-transcriptional level upon QC treatment.

We further tested the effect of p62 expression on p21 stability. For this purpose, we utilized two contrasting cellular models 1) ATG5 depleted C13 cells to achieve high levels of cellular p62 and 2) p62 knockdown c13 cells showing depleted cellular p62 levels. The cells were treated with 20 µg/ml cyclohexamide (CHX) for indicated time intervals. Western blot analysis showed that ATG5 knockdown C13 cells had increased levels of p62 and Skp2 expression which remained stable up to 6 hours of cyclohexamide treatment, whereas NTC cells exhibited increased degradation of p62 (Fig. 5B). Interestingly, CHX treatment had more pronounced effect on stability of p21 levels in ATG5 depleted cells harboring high levels of both p62 and Skp2. Half-life of p21 was markedly lower in ATG5 deficient cells. In contrast, p62 knockdown C13 cells showed high levels of p21 expression owing to lower levels of Skp2 thereby enhancing the half-life of p21 (Fig. 5C). These experiments further confirm the mechanistic basis of QC-mediated cellular changes involving the p62-Skp2 axis.

QC promotes Skp2 downregulation in an autophagy dependent manner. In order to determine if Skp2/p21 regulation by QC and p62 is autophagy dependent given that p62 is a bona fide autophagy cargo protein, we co-treated C13 cells with QC and autophagy inhibitor BafA and then checked Skp2 expression. Western blot analysis revealed that QC downregulated p62, Skp2 and upregulated p21 and p27 respectively (Fig. 6A). Co-treatment with BafA rescued QC mediated downregulation of p62 and Skp2 expression. Consistent with these data, BafA also blocked QC mediated upregulation of p21 and p27. To determine whether BafA also rescued Skp2 levels at transcriptional level, the above treated samples were subjected to qPCR as described in materials and methods. Real time PCR analysis revealed that co-treatment with BafA rescued QC mediated Skp2 mRNA downregulation (Fig. 6B). These data support the hypothesis that autophagy inhibition with BafA prevents the downregulation of Skp2 thereby resulting in downregulation of the cell cycle inhibitors p21 and p27. Furthermore, our data show that QC treatment downregulated Skp2 at the transcriptional level.
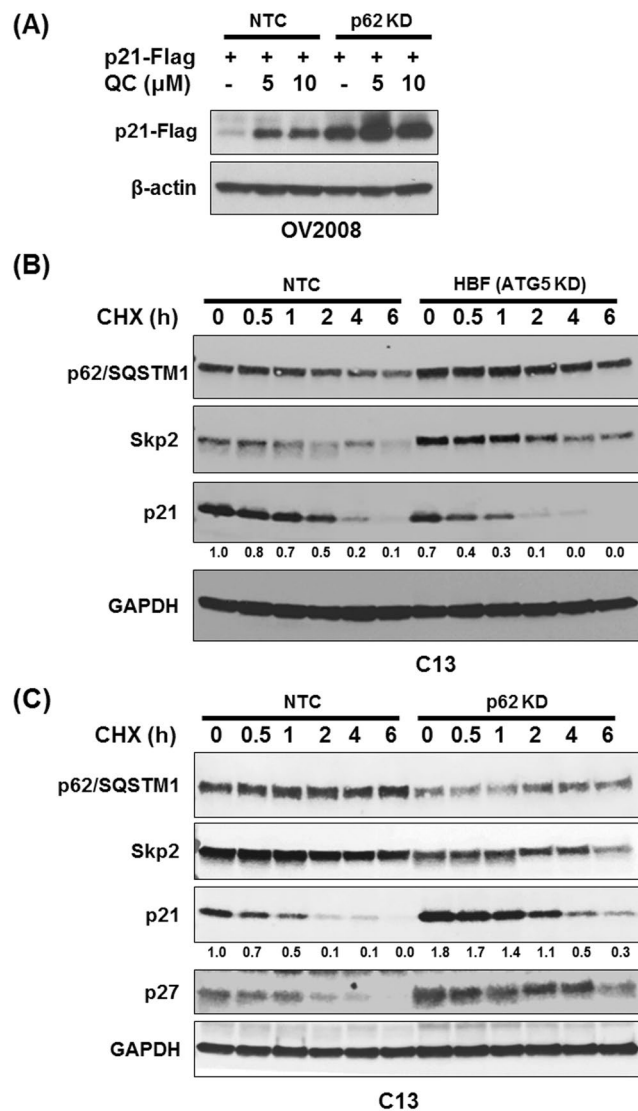
Figure 5. (**A**) Effect of QC treatment on exogenous pcDNA-p21-Flag expression. Transiently transfected NTC and p62 shRNA OV2008 cells with empty vector and pcDNA-p21-Flag vector. Cells were exposed to QC (5 and 10 μM) for 24 hours. Cells were harvested and subjected to Western blot analysis using anti-Flag and beta-actin antibodies. (**B**) C13 NTC and ATG5 knockdown (HBF2) C13 cells were treated with Cyclohexamide (20 μg/ml) for 0, 0.5, 1, 2, 4 and 6 hours. Cell lysates were subjected Western blot analysis using anti-p62/SQSTM1, Skp2, p21 and anti-GAPDH antibodies. (**C**) C13 NTC and p62 knockdown cells were treated with Cyclohexamide (20 μg/ml) for 0, 0.5, 1, 2, 4 and 6 hours. Cell lysates were subjected Western blot analysis using anti-p62/SQSTM1, Skp2, p21, p27 and anti-GAPDH antibodies.

We next determined whether p62 overexpression in p62 depleted cells will rescue its effects. For this purpose, we generated C13 cells stably expressing shRNA targeting 3′UTR region of p62 which were then transfected with pcDNA-p62-HA plasmid. Western blot analysis revealed efficient p62 knockdown in these cells (Fig. 7A). Transfection of full length p62 plasmid restored expression of Skp2 and downregulated p21 expression in p62 depleted cells. These data indicate that p62 positively regulates Skp2 expression. We further evaluated whether p62 knockdown affects Skp2 mRNA. To this end, we utilized NTC and p62 knockdown C13 cells treated with QC. Real time analysis showed that QC treatment as well as p62 knockdown downregulated Skp2 mRNA in C13 cells (Fig. 7B), whereas there was no effect of QC on p62 mRNA (Fig. 7C).

Skp2 knockdown promotes QC mediated p21 upregulation. Our data shows that p62, by positively regulating cell cycle protein Skp2 leads to the degradation of p21 and p27. To gain further insight into whether Skp2 directly regulated p21 and p27 in OC cells, we generated stable knockdown of Skp2 in C13 (p53 wild type), OV90 (p53 mutant) and SKOV3ip1 (p53 null) cells. Two separate shRNA against the coding region of Skp2 was utilized and stable knockdown was determined by western blot analysis. Knockdown of Skp2 in C13 and OV90 cells resulted in upregulation p21 expression. In contrast, Skp2 knockdown in SKOV3ip1 cells did not show any change in p21 expression (Fig. 8A).
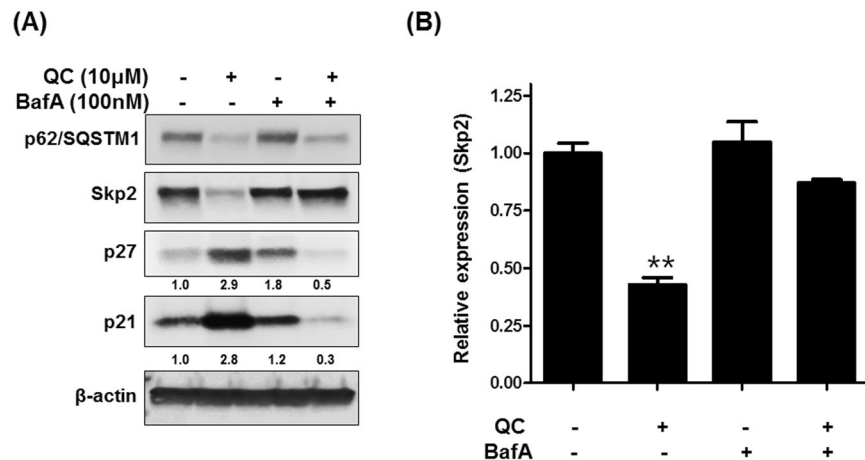
58

Figure 6. (**A**) Co-treatment of QC and autophagy inhibitor Bafilomycin A in C13 cells. C13 cells were treated with QC and Bafilomycin A as indicated. Cell lysates were subjected to Western blot analysis using anti-p62/SQSTM1, anti-Skp2, anti-p27, anti-p21 and anti-beta actin antibodies. (**B**) The mRNA expression levels of Skp2 were assayed by Real-time PCR. GAPDH was used as an internal control in the mRNA analysis experiments.
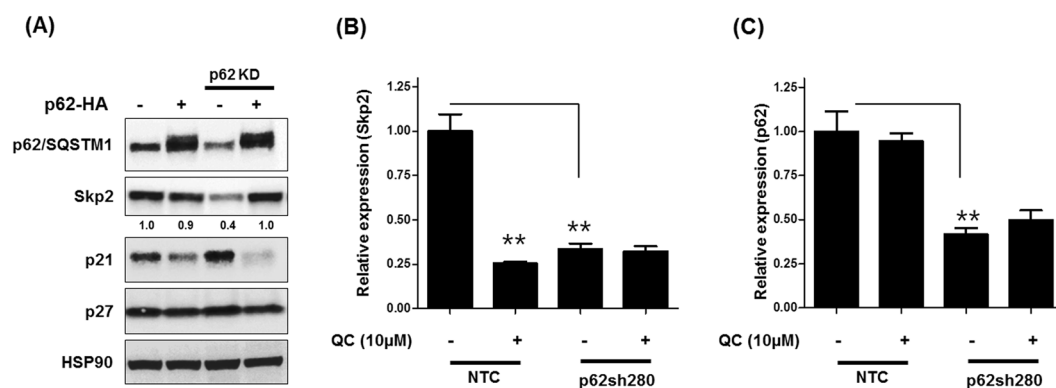

Figure 7. Effect of exogenous expression of p62-HA in p62 knockdown C13 cells. (**A**) Western blot analysis using anti-Skp2, anti-p62/SQSTM1, anti-p27, anti-p21 and anti-HSP90. (**B,C**) Real time PCR analysis of Skp2 and p62 mRNA expression in NTC and p62 (sh280) C13 cells upon QC treatment. GAPDH was used as an internal control in the mRNA analysis experiments.

To further understand the effect of QC in this context, we treated NTC and Skp2 shRNA OV90 and SKOV3ip1 cells with increasing concentrations of QC. Western blot analysis revealed that while Skp2 knockdown stabilized p21 in OV90 cells, QC treatment upregulated p21 in Skp2 knockdown cells both in OV90 (Fig. 8B) and Skov3ip1 cells (Fig. 8C). While these data demonstrate that QC mediated upregulation of p27 and p21 is Skp2-dependent, it appears that there may be additional mechanisms that could contribute towards upregulation of p21 in SKOV3ip1 cells. Equally important is the observation that there was no effect on QC mediated p62 degradation in these Skp2 deficient cells which also exhibited increased PARP cleavage indicating that Skp2 is downstream of p62. We observed activation of Caspase 8 and Caspase 9, and increased the activity of Caspase 3, indicating that both extrinsic and intrinsic apoptotic pathways are activated by QC (Fig. S1).

Discussion

Autophagy modulators have been used against several diseases including cancer. In this study, we have characterized the cellular effects mediated by anti-malarial drug Quinacrine (QC) in OC cell lines. Previously, we have shown that QC effectively attenuated growth of OC cells both *in vitro* and *in vivo* by promoting autophagic mediated cell death[13]. Although QC has been shown to modulate autophagy, the cellular mechanisms responsible for mediating its effects are not clearly defined. We have now uncovered a unique mechanism of action for QC that affects two major players of two distinct pathways (namely autophagy and cell cycle) critical for supporting proliferation and survival of cancer cells. Mechanistically, we show that QC has two important cellular targets p62/SQSTM1 and F-box protein Skp2. Although QC has been shown to exert antitumor activity in several solid tumor cell line models, this is the first paper to show that QC-induced autophagic degradation of p62 leads to cell cycle inhibition by upregulating CDK inhibitors p21 and p27 expression in OC cells. In addition, it is a common perception that autophagy and cell cycle arrest are a result of stress-induced nutrient deprivation and/or a
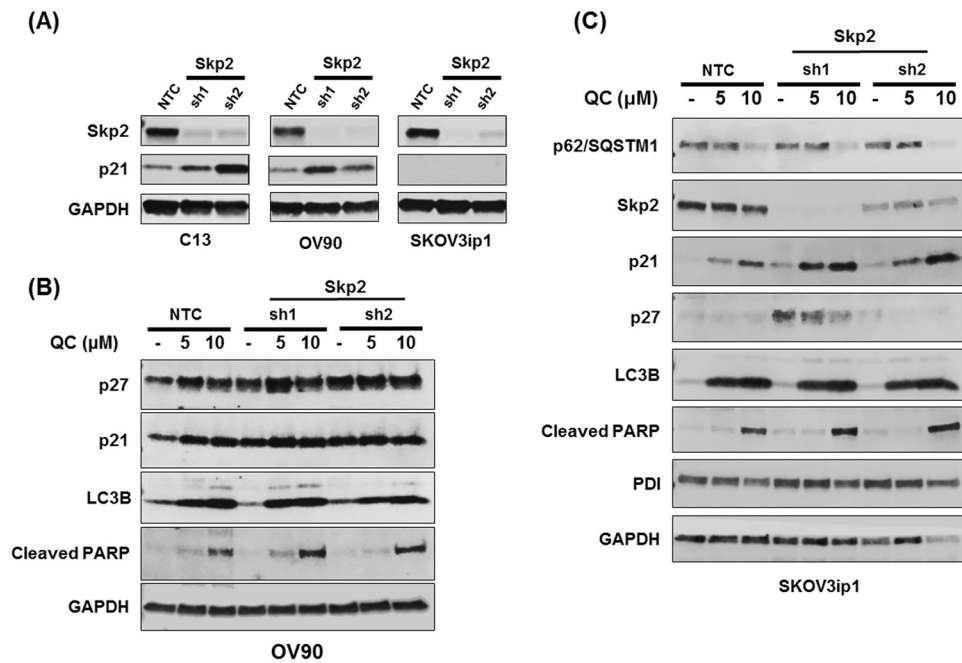
Figure 8. (**A**) Western blot analysis of Skp2, p21 protein expression in NTC and Skp2 shRNA clones in C13, OV90 and Skov3ip1. (**B**) OV90 NTC and Skp2 shRNA1 (HAX49), shRNA2 (HAX50) were exposed with QC at 5 and 10 μM for 24 hours. Cells were harvested and subjected to Western blot analysis using anti-p27, anti-p21, anti-LC3B, anti-cleaved PARP, and anti-GAPDH antibodies. (**C**) Skovip3 NTC and Skp2 shRNA1 (HAX49), shRNA2 (HAX 50) were exposed with QC at 5 and 10 μM for 24 hours. Cells were harvested and subjected to Western blot analysis using anti-p62/SQSTM1, anti-Skp2, anti-p21, anti-p27, anti-LC3B, anti-cleaved PARP, anti-PDI and anti-GAPDH antibodies.

result of small molecule inhibitor treatment[15]. Our data thus challenges the notion that autophagy is essentially a pro-survival pathway supporting cancer growth.

P62 is a known bona fide substrate for autophagy. Induction of autophagy triggers breakdown of several cellular proteins leading to either cell survival or cell death in a context dependent manner[6,10,33–35]. In this study, we show that QC-mediated downregulation of p62 and Skp2 expression promoted apoptosis. Autophagy inhibition, but not proteasomal inhibition, rescued QC-mediated p62 degradation. Similarly, ATG5-null MEFs exhibited increased levels of p62, Skp2 and no autophagic accumulation of LC3B in response to QC treatment. More importantly, we show that QC-mediated effects on p62, Skp2 and p21 are independent of p53 status. Data also indicated that QC-mediated autophagic degradation of p62 was intact in cells lacking functional p53. Although QC has been shown to stabilize p53 and promote apoptosis, our data shows that QC-mediated effects on autophagy and cell cycle inhibitors are independent of p53. More specifically, we show that QC treatment upregulated p21 (a transcriptional target of p53) at the protein level. These data emphasize that downregulation of both critical cell survival proteins p62 and Skp2 is required for QC-mediated autophagy. Additionally we also show that QC-mediated cell death involves both the intrinsic and extrinsic pathways to induce apoptosis.

Both p62 and Skp2 are well known for their proliferative and pro-tumorigenic roles in multiple cancers. It is important to note that they are both elevated in OC and have been shown to serve as poor prognostic factor in overall survival in this patient population[36,37]. Importantly, elevated levels of both p62 and Skp2 have been associated with therapeutic resistance[38–40] and as such. efforts are currently underway to identify small molecule inhibitors[37,39,41–43] to block their function and/or activity. While several reports indicate that autophagy plays a pro-survival role in a variety of cancers[44], other studies indicate that autophagy induced by anti-neoplastic agents results in cell death[44]. In our experimental conditions, QC treatment induced autophagy and resulted in cell death in multiple OC cells. By using ATG5 deficient MEFs and specific shRNA targeting ATG5 in C13 OC cells, we showed that induction of apoptosis by QC was completely blocked in MEFs and to a significant degree in C13 cells depleted of ATG5 expression. The observed modest change in C13 can be attributed to the presence of other ATG related genes that could play role in autophagy. Nevertheless, ATG5 depletion had effect on QC mediated apoptosis and on its cellular targets. Consistent with these findings, QC treatment in ATG5 deficient cells or co-treatment with autophagy blocker Bafilomycin A in C13 cells also attenuated degradation of p62 as well as downregulation of Skp2 expression.

It is not surprising that downregulation of Skp2 expression by QC was associated with upregulation of cell cycle inhibitors such as p21 and p27 given that Skp2 has been shown to promote proteasomal degradation of p21 and p27. It has been also shown that autophagy is associated with several phases of the cell cycle[45]. However, the molecular mechanism linking both of these processes is not clearly defined. Our data provided explanation of p53 independent p21 upregulation observed in p53 null/mutated OC upon QC treatment. Other investigators have also reported QC mediated cell cycle inhibition in other cancer types[46]. Our data expands this understanding and
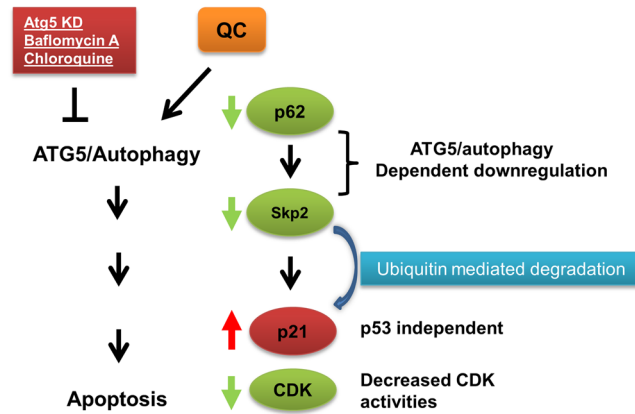
60

Figure 9. Schematic representation of effects mediated by QC.

highlights the presence of a relationship between cell cycle and autophagy. By blocking autophagy by chemical inhibitor Bafilomycin A, we demonstrate that QC's effects on p21 and Skp2 were reversed. This prompted us to ask whether p62 downregulation has any role in Skp2/p21 regulation. Genetic silencing of p62 downregulated Skp2 expression and caused upregulation of cell cycle inhibitors p21 and p27. Further treatment with QC resulted in extended half-life of p21 in p62 and Skp2 deficient cells thereby resulting in significant upregulation of these cell cycle inhibitors. Further, we confirmed that p62 positively regulated Skp2 mRNA. These findings reveal the connection between autophagic substrate p62 and Skp2 and hence cell cycle inhibitor p21. Ultimately, our work indicates a link between autophagy and cell cycle. Additionally, we showed temporal regulation of apoptosis and autophagy upon QC treatment. Onset of autophagy in the form of p62 degradation was present as early as 4 hours of QC treatment in C13 cells whereas apoptotic marker appeared at later time points. These findings suggest that autophagy is an early indicator leading to apoptosis upon QC treatment.

Upon genetic silencing of either p62 and/or Skp2 expression, OC cells became sensitive to QC treatment. This was associated with pronounced upregulation of cell cycle inhibitors p21 and p27 (Model in Fig. 9) in three different OC cell lines carrying wild type p53, mutant p53 and p53 null. These findings along with other findings using SKOV3 cell lines overexpressing wild type and mutant p53 indicated that QC mediated effects on autophagy and cell cycle were largely independent of p53. However, it is plausible that presence of p53 and its resulting stabilization by QC might further promote apoptotic effects. Indeed, previous reports indicated that QC stabilized p53 without causing any genotoxicity and that it promoted apoptosis in colon, breast and cervical cancers[47–49].

In conclusion, in this study, we showed that QC is able to induce apoptosis by modulating autophagy and cell cycle independent of p53 status. This is particularly clinically relevant given that the majority of high grade serous OC harbors p53 mutations. Importantly, our work provides additional insight into the mechanisms by which QC arrests cell growth in OC. Finally, these findings suggest that Skp2, an important oncogene that is overexpressed in OC and is associated with chemo resistance, may be a novel target for QC treatment.

Conclusions

We demonstrate that QC treatment promotes anti-tumorigenic effects in OC cells by downregulating the protein expression of p62 and Skp2 and by triggering the protein expression of p21 and p27. We propose a novel molecular mechanism of action for QC in OC where the cell cycle related protein p21 and the oncogene Skp2 are both altered upon QC treatment in an autophagy dependent but p53 independent manner.

Materials and Methods

Cell culture. SKOV3, C13, OV2008, OVCAR 3 and 293 T cells were grown in recommended growth media according to American Type Culture Collection (ATCC) (VA, USA) as described previously[13]. OV90 cells were grown in OSE media consisting of 50:50 medium 199:105 (Sigma-Aldrich, St. Louis, MO) supplemented with 15% fetal bovine serum, and sodium bi-carbonate (2.2 gm/L). Antibiotic penicillin and streptomycin was added in all the growth media (Thermo Fisher Scientific, Waltham, MA, USA). All cell lines were kept in humidified incubator at 37 C with 5% CO_2. The authenticity of the cell lines used in this report was confirmed by STR genotyping at the Genome Analysis Core, Rochester, MN. ATG5 wild type and null mouse embryonic fibroblasts were gift from Dr. Dan Billadeau, Mayo Clinic, Rochester, MN.

Reagents and Antibodies. Quinacrine (Q3251), Bafilomycin A (B1793), 3-Methyladenine (3MA) (M9281) and Cyclohexamide (C7698) and were all purchased from Sigma-Aldrich (St. Louis, MO, USA). Lactacystin (426100) and Velcade (5043140001) were from Calbiochem, USA. p21-Flg Construct was purchased form Addgene (MA,USA). Primary antibodies used for western blot are shown in Table 1. Densitometry analyses were performed using ImageJ, and graphs were plotted using GraphPad Prism.

Transient Transfections. OC cells were transiently transfected with Lipofectamine 2000 (Thermo Fisher Scientific, MA, USA) according to manufacturer's protocol. Briefly, plasmids were transfected in cancer cells in serum free medium followed by addition of serum containing medium. After 48 hours of transfections, cells

Primary Antibodies	Catalog #	Company
Caspase 8	66093	Proteintech group
Cathepsin L	sc6498	Santa Cruz Biotechnology
Caspase 3	#9661S	Cell Signalling Technology
Caspase 9	9501S	Cell Signalling Technology
Cleaved PARP	#9541S	Cell Signalling Technology
GAPDH (14C10)	#2118S	Cell Signalling Technology
HSP-90	ADI-SPA-830-488	Enzo life Sciences
LC3B (D11)	#3868S	Cell Signalling Technology
p21 (F-8)	sc-271610	Santa Cruz Biotechnology
p27 Kip1 (D69C12)	#3686S	Cell Signalling Technology
p53 (D01)	sc-126	Santa Cruz Biotechnology
PDI	ADI-SPA-890	Enzo life Sciences
Phospho-MAPK/CDK Substrates	#2325S	Cell Signalling Technology
Skp2 (D3G5) XP	#2652S	Cell Signalling Technology
SQSTM1 (D3) -p62	sc-28359	Santa Cruz Biotechnology
Ubiquitin (P4D1)	#3936S	Cell Signalling Technology
β-actin	A2228	Sigma Aldrich
β-tubulin	GTX11312	Genetex Inc

Table 1. List of Antibodies.

were either left untreated or treated with indicated doses of QC. Cells were later collected for either Western blot or Real time PCR analysis. For stable transfections with p53 wild type and mutant constructs, SKOV3 cells were selected in the presence of Blasticidin 20 μg/ml (Sigma, St. Louis, MO, USA) concentrations for several weeks and single clones were picked and confirmed by Western blot analysis. p53 construct were purchased from Addgene (MA, USA).

Lentiviral mediated shRNA infection. Lentivirus particles were produced by transient transfection of pTRC2-p62, pTRC2-Skp2, pTRC2-ATG5 (Sigma, St. Louis, MO, USA), along with packaging vectors (pVSV-G and pGag/pol) in 293 T cells. The shRNA [non-target (NTC) shRNA vector, Sigma] containing a hairpin insert that generates siRNAs with five base pair mismatches to any known human gene was used as control shRNA. The lentiviral supernatant stocks were collected 48 hours after transfection. The supernatant was filtered with 0.45 μm filter and was either used for infection or stored at −80 °C. Vector titers were determined by transducing cells with serial dilutions of concentrated lentivirus supernatant in complete growth medium containing 8 μg/ml polybrene (Invitrogen, MA, USA). After 48 hours the growth medium was supplemented with puromycin 2 μg/ml. The numbers of surviving colonies were counted under the microscope and titer of lentiviral supernatant was calculated using the formula: Transducing units = number of colonies x lentiviral dilution. All lentiviral stocks used in the study were selected at a multiplicity of infection of 10. shRNA target sequence for p62/SQSTM1 GCCCTCCATTTGTAAGAACAA; shRNA target sequences for Skp2, are Sh1-AGTCGGTGCTATGATATAATA and Sh2- GCCTAAGCTAAATCGAGAGAA; shRNA target sequence for ATG5CCTTTCATTCAGAAGCTGTTT.

Western Blot analysis. Protein lysates were prepared by lysing the OC cell lines in lysis buffer (Cell Signaling Inc, MA, USA) containing 50 mM Tris–HCl (pH 7.4), 350 mM NaCl, 0.25% Nonidet P-40, 1 mM EDTA, 1 mM EGTA, 1 mM dithiothreitol, 1 mM glycerol phosphate, 1 mM sodium orthovanadate, and 30% glycerol with protease inhibitors. Protein was estimated by BCA method, separated on SDS-PAGE and transferred onto PVDF membrane using Trans-Blot Turbo (Bio-Rad, CA, USA). The membranes were blocked with 5% BSA in TBST for 1 hour (50 mM Tris-HCL, pH 8.0, 10 mM NaCl and 0.1% Tween 20) at room temperature followed by incubation with the indicated antibodies at 4 °C overnight. Membranes were washed with TBST and incubated with either mouse or rabbit-800 IR dye and finally scanned under Odyssey Fc Imaging system (Bio-Rad, CA, USA). Experiments were conducted three times.

RNA isolation and cDNA synthesis. RNA extraction was performed using Qiagen RNA isolation kits following manufacturer's instruction. 1 μg of RNA was reverse transcribed using the quantitect reverse transcription cDNA synthesis kit following manufacturer's instruction (Qiagen, MD, USA).

Quantitative real time PCR. Quantitative real-time PCR (qRT-PCR) was carried out using SYBR-Green PCR Master Mix (Applied Biosystems, Foster City, CA, USA), using the CFX96 Touch™ Real-Time PCR detection System (Bio-Rad, CA, USA). Oligonucleotides were synthesized by Integrated DNA Technologies (IDT). Primer sequences for the genes analyzed are p62FP:5′-TGAAACACCGGACATTCGG-3′, p62RP: 5′-TCAGGAAATTCACACTCCGGATC, Skp2FP:5′CTGGGTGTTCGTGATTCTCTG-3′, Skp2RP: 5′-GCTGGGTGATGGTCTCTG-3′ and GAPDH FP:5′-ACATCGCTCAGACACCATG-3′ and GAPDH RP:5′-TGTAGTTGAGGTCAATGAAGGG- After an initial step of 3 min denaturation at 95 °C, the amplification conditions were 45 cycles of 95 °C 10 sec, for denaturation and 55 °C 30 sec for annealing and elongation, with a final extension at 72 °C for 10 min. Normalization across samples was

performed using the average of the constitutive gene human GAPDH primers and calculated by $2^{-\Delta\Delta Ct}$ method as previously described[50]. Binding efficiencies of primers sets for both target and reference genes were similar. All samples were run in triplicates and repeated twice. Expression levels of the genes in the two designated groups were analyzed by an unpaired t test using GraphPad PRISM (version 6.0; GraphPad Software).

References

1. Ren, Y. A. *et al*. Mutant p53 Promotes Epithelial Ovarian Cancer by Regulating Tumor Differentiation, Metastasis, and Responsiveness to Steroid Hormones. *Cancer Res* **76**, 2206–2218, https://doi.org/10.1158/0008-5472.CAN-15-1046 (2016).
2. Ertmer, A. *et al*. The anticancer drug imatinib induces cellular autophagy. *Leukemia* **21**, 936–942, https://doi.org/10.1038/sj.leu.2404606 (2007).
3. Zhang, L. *et al*. Dual induction of apoptotic and autophagic cell death by targeting survivin in head neck squamous cell carcinoma. *Cell Death Dis* **6**, e1771, https://doi.org/10.1038/cddis.2015.139 (2015).
4. Nakatogawa, H., Suzuki, K., Kamada, Y. & Ohsumi, Y. Dynamics and diversity in autophagy mechanisms: lessons from yeast. *Nat Rev Mol Cell Biol* **10**, 458–467, https://doi.org/10.1038/nrm2708 (2009).
5. Bursch, W. *et al*. Autophagic and apoptotic types of programmed cell death exhibit different fates of cytoskeletal filaments. *J Cell Sci* **113**(Pt 7), 1189–1198 (2000).
6. Auberger, P. & Puissant, A. Autophagy, a key mechanism of oncogenesis and resistance in leukemia. *Blood* **129**, 547–552, https://doi.org/10.1182/blood-2016-07-692707 (2017).
7. O'Donovan, T. R., O'Sullivan, G. C. & McKenna, S. L. Induction of autophagy by drug-resistant esophageal cancer cells promotes their survival and recovery following treatment with chemotherapeutics. *Autophagy* **5** (2011).
8. Shi, S. *et al*. ER stress and autophagy are involved in the apoptosis induced by cisplatin in human lung cancer cells. *Oncol Rep* **35**, 2606–2614, https://doi.org/10.3892/or.2016.4680 (2016).
9. Yan, Y. *et al*. Bafilomycin A1 induces caspase-independent cell death in hepatocellular carcinoma cells via targeting of autophagy and MAPK pathways. *Sci Rep* **6**, 37052, https://doi.org/10.1038/srep37052 (2016).
10. Duffy, A., Le, J., Sausville, E. & Emadi, A. Autophagy modulation: a target for cancer treatment development. *Cancer Chemother Pharmacol* **75**, 439–447, https://doi.org/10.1007/s00280-014-2637-z (2015).
11. Dermawan, J. K. *et al*. Quinacrine overcomes resistance to erlotinib by inhibiting FACT, NF-kappaB, and cell-cycle progression in non-small cell lung cancer. *Mol Cancer Ther* **13**, 2203–2214, https://doi.org/10.1158/1535-7163.MCT-14-0013 (2014).
12. Wang, W. *et al*. Quinacrine sensitizes hepatocellular carcinoma cells to TRAIL and chemotherapeutic agents. *Cancer Biol Ther* **12**, 229–238 (2011).
13. Khurana, A. *et al*. Quinacrine promotes autophagic cell death and chemosensitivity in ovarian cancer and attenuates tumor growth. *Oncotarget* **6**, 36354–36369, https://doi.org/10.18632/oncotarget.5632 (2015).
14. Wu, X. *et al*. Quinacrine Inhibits Cell Growth and Induces Apoptosis in Human Gastric Cancer Cell Line SGC-7901. *Curr Ther Res Clin Exp* **73**, 52–64, https://doi.org/10.1016/j.curtheres.2012.02.003 (2012).
15. Mathiassen, S. G., De Zio, D. & Cecconi, F. Autophagy and the Cell Cycle: A Complex Landscape. *Front Oncol* **7**, 51, https://doi.org/10.3389/fonc.2017.00051 (2017).
16. Pathania, A. S. *et al*. Interplay between cell cycle and autophagy induced by boswellic acid analog. *Sci Rep* **6**, 33146, https://doi.org/10.1038/srep33146 (2016).
17. Lee, S. H. & McCormick, F. Downregulation of Skp2 and p27/Kip1 synergistically induces apoptosis in T98G glioblastoma cells. *J Mol Med (Berl)* **83**, 296–307, https://doi.org/10.1007/s00109-004-0611-7 (2005).
18. Yu, Z. K., Gervais, J. L. & Zhang, H. Human CUL-1 associates with the SKP1/SKP2 complex and regulatesp 21(CIP1/WAF1) and cyclin D proteins. *Proc Natl Acad Sci USA* **95**, 11324–11329 (1998).
19. Bornstein, G. *et al*. Role of the SCFSkp2 ubiquitin ligase in the degradation of p21Cip1 in S phase. *J Biol Chem* **278**, 25752–25757, https://doi.org/10.1074/jbc.M301774200 (2003).
20. Carrano, A. C., Eytan, E., Hershko, A. & Pagano, M. SKP2 is required for ubiquitin-mediated degradation of the CDK inhibitor p27. *Nat Cell Biol* **1**, 193–199 (1999).
21. Wang, S., Raven, J. F. & Koromilas, A. E. STAT1 represses Skp2 gene transcription to promote p27Kip1 stabilization in Ras-transformed cells. *Mol Cancer Res* **8**, 798–805, https://doi.org/10.1158/1541-7786.MCR-10-0027 (2010).
22. Sherr, C. J. & Roberts, J. M. CDK inhibitors: positive and negative regulators of G1-phase progression. *Genes Dev* **13**, 1501–1512 (1999).
23. Zhu, L. Skp2 knockout reduces cell proliferation and mouse body size: and prevents cancer? *Cell Res* **20**, 605–607, https://doi.org/10.1038/cr.2010.71 (2010).
24. Bretones, G. *et al*. SKP2 oncogene is a direct MYC target gene and MYC down-regulatesp27(KIP1) through SKP2 in human leukemia cells. *J Biol Chem* **286**, 9815–9825, https://doi.org/10.1074/jbc.M110.165977 (2011).
25. Chan, C. H. *et al*. The Skp2-SCF E3 ligase regulates Akt ubiquitination, glycolysis, herceptin sensitivity, and tumorigenesis. *Cell* **149**, 1098–1111, https://doi.org/10.1016/j.cell.2012.02.065 (2012).
26. Hafez, M. M. *et al*. SKP2/P27Kip1 pathway is associated with Advanced Ovarian Cancer in Saudi Patients. *Asian Pac J Cancer Prev* **16**, 5807–5815 (2015).
27. Othman Al-Shabanah, M. H. a. M. S.-A. S-phase kinase-associated protein 2 gene aberration in ovarian cancer Saudi patients. *The FASEB Journal* **28** (2014).
28. Lin, H. K. *et al*. Skp2 targeting suppresses tumorigenesis by Arf-p53-independent cellular senescence. *Nature* **464**, 374–379, https://doi.org/10.1038/nature08815 (2010).
29. Hu, R. & Aplin, A. E. Skp2 regulates G2/M progression in a p53-dependent manner. *Mol Biol Cell* **19**, 4602–4610, https://doi.org/10.1091/mbc.E07-11-1137 (2008).
30. Myeku, N. & Figueiredo-Pereira, M. E. Dynamics of the degradation of ubiquitinated proteins by proteasomes and autophagy: association with sequestosome 1/p62. *J Biol Chem* **286**, 22426–22440, https://doi.org/10.1074/jbc.M110.149252 (2011).
31. Gukovsky, I. & Gukovskaya, A. S. Impaired autophagy triggers chronic pancreatitis: lessons from pancreas-specific atg5 knockout mice. *Gastroenterology* **148**, 501–505, https://doi.org/10.1053/j.gastro.2015.01.012 (2015).
32. Takamura, A. *et al*. Autophagy-deficient mice develop multiple liver tumors. *Genes Dev* **25**, 795–800, https://doi.org/10.1101/gad.2016211 (2011).
33. Bursch, W. The autophagosomal-lysosomal compartment in programmed cell death. *Cell Death Differ* **8**, 569–581, https://doi.org/10.1038/sj.cdd.4400852 (2001).
34. Gozuacik, D. & Kimchi, A. Autophagy as a cell death and tumor suppressor mechanism. *Oncogene* **23**, 2891–2906, https://doi.org/10.1038/sj.onc.1207521 (2004).
35. Mathew, R. *et al*. Autophagy suppresses tumorigenesis through elimination of p62. *Cell* **137**, 1062–1075, https://doi.org/10.1016/j.cell.2009.03.048 (2009).
36. Iwadate, R. *et al*. High Expression of SQSTM1/p62 Protein Is Associated with Poor Prognosis in Epithelial Ovarian Cancer. *Acta Histochem Cytochem* **47**, 295–301, https://doi.org/10.1267/ahc.14048 (2014).

37. Shigemasa, K., Gu, L., O'Brien, T. J. & Ohama, K. Skp2 overexpression is a prognostic factor in patients with ovarian adenocarcinoma. *Clin Cancer Res* **9**, 1756–1763 (2003).
38. Lee, Y. & Lim, H. S. Skp2 Inhibitors: Novel Anticancer Strategies. *Curr Med Chem* **23**, 2363–2379 (2016).
39. Malek, E. *et al*. Pharmacogenomics and chemical library screens reveal a novel SCFSKP2 inhibitor that overcomes Bortezomib resistance in multiple myeloma. *Leukemia* **31**, 645–653, https://doi.org/10.1038/leu.2016.258 (2017).
40. Yang, Y. *et al*. Skp2 is associated with paclitaxel resistance in prostate cancer cells. *Oncol Rep* **36**, 559–566, https://doi.org/10.3892/or.2016.4809 (2016).
41. Luo, R. Z. *et al*. Accumulation of p62 is associated with poor prognosis in patients with triple-negative breast cancer. *Onco Targets Ther* **6**, 883–888, https://doi.org/10.2147/OTT.S46222 (2013).
42. Xia, M. *et al*. p62/SQSTM1 is involved in cisplatin resistance in human ovarian cancer cells via the Keap1-Nrf2-ARE system. *Int J Oncol* **45**, 2341–2348, https://doi.org/10.3892/ijo.2014.2669 (2014).
43. Zhang, W. *et al*. Skp2 is over-expressed in breast cancer and promotes breast cancer cell proliferation. *Cell Cycle* **15**, 1344–1351, https://doi.org/10.1080/15384101.2016.1160986 (2016).
44. Choi, K. S. Autophagy and cancer. *Exp Mol Med* **44**, 109–120, https://doi.org/10.3858/emm.2012.44.2.033 (2012).
45. Kaminskyy, V., Abdi, A. & Zhivotovsky, B. A quantitative assay for the monitoring of autophagosome accumulation in different phases of the cell cycle. *Autophagy* **7**, 83–90 (2011).
46. Preet, R. *et al*. Quinacrine has anticancer activity in breast cancer cells through inhibition of topoisomerase activity. *Int J Cancer* **130**, 1660–1670, https://doi.org/10.1002/ijc.26158 (2012).
47. Das, S. *et al*. Quinacrine induces apoptosis in cancer cells by forming a functional bridge between TRAIL-DR5 complex and modulating the mitochondrial intrinsic cascade. *Oncotarget* **8**, 248–267, https://doi.org/10.18632/oncotarget.11335 (2017).
48. Fasanmade, A. A. *et al*. Quinacrine induces cytochrome c-dependent apoptotic signaling in human cervical carcinoma cells. *Arch Pharm Res* **24**, 126–135 (2001).
49. Mohapatra, P. *et al*. Quinacrine-mediated autophagy and apoptosis in colon cancer cells is through a p53- and p21-dependent mechanism. *Oncol Res* **20**, 81–91 (2012).
50. Khurana, A. *et al*. Hypoxia negatively regulates heparan sulfatase 2 expression in renal cancer cell lines. *Mol Carcinog* **51**, 565–575, https://doi.org/10.1002/mc.20824 (2012).

Acknowledgements

Author Contributions

D.J. performed the experiments in Figures 4, 5, 6, 7, and 8 and wrote the manuscript. A.K. technically performed the experiments in Figures 1, 2 and 3 and wrote the portions of the manuscript. D.R. performed one experiment in Figure 3 and edited the manuscript. E.K., J.B.J. and J.C. edited the manuscript and provided critical comments. V.S. was involved in the design, execution and analysis and wrote the manuscript with A.K. and D.J.

Additional Information

Supplementary information accompanies this paper at https://doi.org/10.1038/s41598-018-20531-w.

Competing Interests: The authors declare that they have no competing interests.

Publisher's note: Springer Nature remains neutral with regard to jurisdictional claims in published maps and institutional affiliations.

Review

Repurposing quinacrine for treatment-refractory cancer

Derek B. Oien[a,1], Christopher L. Pathoulas[a,1], Upasana Ray[a,1], Prabhu Thirusangu[a],
Eleftheria Kalogera[b], Viji Shridhar[a,*]

[a] Division of Experimental Pathology and Laboratory Medicine, Mayo Clinic, Rochester, MN, United States
[b] Division of Gynecologic Surgery, Mayo Clinic, Rochester, MN, United States

A R T I C L E   I N F O

A B S T R A C T

Quinacrine, also known as mepacrine, has originally been used as an antimalarial drug for close to a century, but was recently rediscovered as an anticancer agent. The mechanisms of anticancer effects of quinacrine are not well understood. The anticancer potential of quinacrine was discovered in a screen for small molecule activators of p53, and was specifically shown to inhibit NFκB suppression of p53. However, quinacrine can cause cell death in cells that lack p53 or have p53 mutations, which is a common occurrence in many malignant tumors including high grade serous ovarian cancer. Recent reports suggest quinacrine may inhibit cancer cell growth through multiple mechanisms including regulating autophagy, FACT (facilitates chromatin transcription) chromatin trapping, and the DNA repair process. Additional reports also suggest quinacrine is effective against chemoresistant gynecologic cancer. In this review, we discuss anticancer effects of quinacrine and potential mechanisms of action with a specific focus on gynecologic and breast cancer where treatment-refractory tumors are associated with increased mortality rates. Repurposing quinacrine as an anticancer agent appears to be a promising strategy based on its ability to target multiple pathways, its selectivity against cancer cells, and the synergistic cytotoxicity when combined with other anticancer agents with limited side effects and good tolerability profile.

1. Introduction

Quinacrine was discovered in the 1920s and historically used as an antimalarial drug both for prophylaxis and treatment [1,2]. Quinacrine (4-N-(6-chloro-2-methoxyacridin-9-yl)-1-N,1-N-diethylpentane-1,4-diamine) is an acridine derivative available as quinacrine dihydrochloride for oral administration [3]. Quinacrine has also been used as an antimicrobial for giardiasis [4,5], an anti-inflammatory for systemic lupus erythematous and rheumatoid arthritis [6–10], and an intrapleural sclerosing agent for malignant pleural effusions and pneumothorax prophylaxis in patients with high risk of recurrence [11–16]. Furthermore, it is still used in some countries for female sterilization and is under clinical evaluation for Creutzfeldt-Jakob disease [17,18]. With regards to its use as a potential anticancer agent, quinacrine has the unique advantage of having a long history of clinical use without any significant clinical concerns for increased risk of secondary cancers [18–21], which would be of relevance if used as a cancer treatment. Importantly, quinacrine has a favorable side effect profile with mostly low grade toxicity in contrast to most anticancer therapeutics, and side effects are typically reversible upon discontinuation [1,2,10].

In this review, we discuss recent research of quinacrine with a focus on treatment-refractory female cancers. Ovarian and endometrial cancers are often treated with first line platinum-based combination treatments such as carboplatin with paclitaxel. However, significant proportions of these patients are diagnosed with advanced stage disease, unfavorable histologic subtypes, or suffer disease recurrence [22,23]. To further highlight the magnitude of the problem with available systemic treatments for gynecologic cancers, endometrial cancers have a low (~50%) response rate to platinum-based first line therapies and ovarian cancers will ultimately develop chemoresistance to platinum-based treatments [22,24,25]. We also highlight emerging quinacrine studies in breast cancer, as approximately 30% of women diagnosed with breast cancer will experience recurrence after initial treatment [26]. Breast cancer disproportionately affects women, although it is not limited by gender.

---

* Corresponding author at: Division of Experimental Pathology and Laboratory Medicine, Mayo Clinic, 200 First Street SW, St-50, Rochester, MN 55905, United States.
E-mail address: shridhar.vijayalakshmi@mayo.edu (V. Shridhar).
[1] These authors contributed equally to this article.

Please cite this article as: Derek B. Oien, et al., Seminars in Cancer Biology, https://doi.org/10.1016/j.semcancer.2019.09.021

2. Repurposing drugs as cancer therapeutics

Drug repurposing is finding new indications for approved pharmaceuticals, while drug repositioning is typically reserved for new investigations on failed drug candidates [27–29]. The traditional process of designing and discovering of new chemical entities for clinical use is often a strenuous and expensive endeavor. It has been estimated that the *de novo* development of most drugs takes 10–17 years and costs over $800 million [30]. A comprehensive and industry-wide analysis conducted by Paul et al. determined that the average drug development time is 13.5 years and an estimated $1.8 billion is required to bring new chemical entities to market [31]. A study by Prasad and Mailankody on the FDA approval of 10 cancer drugs from 2006 to 2015 reported a drug development median time of 7.3 years (range 5.8–15.2 years) and median cost of $648 million (range $157 million to $1951 million) [32]; while this suggests that there may have been some progress in cost and time development in recent cancer therapies, it remains a process lacking efficiency.

Drug repurposing and drug repositioning has the potential to reduce the time and cost required to obtain approval for new clinical indications, which can support a relatively rapid bench-to-bedside transition. Drug repurposing is believed to shorten the time of drug development from an estimated 10–17 years to 3–12 years while reducing costs by approximately 40% [27,33–35]. The main sources for cost reductions in drug repurposing are derived from the fact that the pharmacodymanic/ pharmacokinetic and toxicity profiles are well established for these previously FDA approved drugs [36,37]. Repurposing of the anti-diabetic drug metformin for the treatment of several cancers including breast, ovarian, endometrial, and uterine cancer has progressed in clinical trials.[2] Similarly, aspirin has been found to exert a small effect in reducing incidence of metastatic cancer [38,39]. Repurposed drugs, especially when generic versions are available, have the potential to greatly reduce costs incurred by cancer patients. The National Center for Health Statistics recently reported a third of uninsured patients did not take their medications as prescribed in order to reduce costs [40], which underlines the problem that the financial burden to patients has important clinical implications.

Numerous studies suggest that targeted therapies selectively blocking individual enzymes or single pathways seldom result in effective cancer treatment while FDA approved less selective systemic therapies (e.g. DNA damaging agents) often damage nonmalignant tissue leading to toxicity. Thus, there is an increase need of drugs that can bind with promiscuity and modulate multiple targets, yet have minimal effects on normal cells [41,42]. Within this context, quinacrine has captured researchers' interest for its ability to target multiple pathways with limited side effects. Reports of individuals taking quinacrine as an antimalarial agent note that patients experience only minor side effects such as headache, dizziness, or gastrointestinal symptoms (e.g. diarrhea, anorexia, nausea, abdominal cramps) [10]. As an anticancer agent, quinacrine has been reported to have cytotoxic potential in cancer cells of the colon, lung, blood, prostate, kidney, and head and neck through diverse but often overlapping mechanisms [43–47]. Quinacrine has also shown potential as an anticancer agent in gynecologic and breast cancers based on studies from our group and others, which is discussed in the next sections.

3. Mechanisms of quinacrine as an anticancer agent

Quinacrine was found to induce p53 in a small molecule screen using renal cell carcinoma cells, where the untreated cells had minimal wild-type *TP53* protein expression [44]. This finding was further

validated by showing that activation of p53 by quinacrine occurred through suppression of basal and inducible activities of NFκB. In a separate small molecule library screen, quinacrine was found to be active against leukemia patient samples spanning three subtypes with concurrent minimal toxicity in peripheral blood mononuclear cells from healthy donors [45]. In this latter study, subsequent gene expression analysis indicated that quinacrine modulates ribosomal biogenesis in leukemia cells lines. These studies along with many recent studies indicate that the cytotoxic mechanisms of quinacrine against malignant cells span across multiple pathways.

The ability of quinacrine to exhibit cancer cell cytotoxicity through different mechanisms is fundamental to its use as an anticancer agent. In general, quinacrine has been shown to intercalate into DNA, impact nuclear proteins, target multi-drug resistance and arachidonic pathways, induce p53, and inhibit NFκB signaling. In the following sections, we focus on the multiple mechanisms associated with the anticancer functions of quinacrine.

3.1. Quinacrine intercalation of DNA and interaction with nuclear proteins

It is primarily believed that the cytotoxic effect of quinacrine, and other acridine agents, is at least partially linked to DNA intercalation and regulation of nuclear proteins [1,2,48–52]. Quinacrine has been shown to intercalate into DNA through heterogeneous binding with a high affinity towards AT rich sequences [49,53,54]. In addition to its traditional intercalative abilities, quinacrine also has a diaminobutyl "tail" that is capable of inserting into the minor groove of DNA [1]. Importantly, this interaction increases the binding affinity between quinacrine and DNA [1,55,56]. Given its ability to intercalate DNA, quinacrine has been long thought of as a DNA damaging agent and its potential to induce DNA damage has been investigated. In spite of this original hypothesis, several studies suggest that quinacrine is not mutagenic and does not induce DNA damage (for review see [1]). This is further supported by the safe use of quinacrine in humans for reproductive sterilization and malaria prophylaxis [57–59]. In contrast, recent work in breast cancer cell lines does suggest that quinacrine may increase single-stranded DNA damage [60]. These results are promising for the use of quinacrine as an anticancer agent and will be discussed in more detail later in this review (Section 4.1). Although this DNA intercalation may be necessary for its antitumor properties, other mechanisms are also thought to play an important role for the ability of quinacrine to exert sufficient antitumor effects [2].

One possible mechanism of action is the targeting of nuclear proteins such as telomerases, topoisomerases, and polymerases (Table 1). Malignant cells have telomerase activity which prevents telomere degradation needed for their growth and is otherwise inactive in normal somatic cells after birth. Acridine derivatives like quinacrine stabilize the G-quadruplexes in telomeric DNA, which inhibits telomerase activity resulting in growth arrest and malignant cell death [61–64]. Quinacrine has also been shown to inhibit the re-ligation activity of topoisomerases as a result of its intercalative ability leading to death of malignant cells, which overexpress these enzymes [60,65]. However, it is noted that the quinacrine concentrations required to inhibit these nuclear enzymes are often well above the half growth inhibitory (GI_{50}) doses, suggesting that other mechanisms may be more cytotoxic [1,2]. Furthermore, quinacrine demonstrates the ability to inhibit both DNA and RNA polymerases in a variety of models including yeast, viruses, bacteria, and Novikoff hepatoma cells [56,66–69]. Quinacrine was recently detected in a cytotoxic screen against acute myeloid leukemia, and in subsequent transcriptome analysis quinacrine was found to inhibit RNA polymerase I as well as modify gene expression similar to ellipticine [45]. This finding suggests that quinacrine may target ribosomal biogenesis, which has been shown to be altered in cancer [70].

Table 1
Quinacrine targets in cancer cell signaling.

Reported target	Function/pathway of target	Quinacrine Effect	Ref(s)
RNA Polymerase I	Transcribes ribosomal RNA	Inhibitor	[45]
NFκB	Transcription factor involved in cell proliferation and inflammation	Inhibitor	[44]
PLA2	Catalyzes arachidonic acid release and provides precursors for eicosanoids	Inhibitor	[79,80,82]
P-Glycoprotein	Activator for multidrug resistance pathway	Inhibitor	[79,82]
FACT (complex of SSRP-1 and SPT16/Cdc68)	Nucleosome assembly promoting transcription, DNA replication, and repair	Inhibitor	[47,110]
Topoisomerase I & II	Regulates supercoils of double-stranded DNA	Inhibitor	[60]
p62 (SQSTM1)	Autophagosome receptor protein for selective autophagy	Inhibitor	[134,135]
CHK1 & CHK2	Cell cycle checkpoint kinases involved in ATR-CHK1 and ATM-CHK2 single-stranded break and double-stranded break repair, respectively	Inhibitor	[136,141]
p53	Tumor suppressor protein that regulates the cell cycle and apoptosis	Activator	[44]
APC	Binds DNA polymerase β and blocks strand displacement synthesis in long-patch base excision repair	Activator	[137,142]
TRAIL	Binds DR4 and DR5 to induce mitochondrial apoptotic cascade	Activator	[138,139]
INP2	Induces autophagy	Activator	[135]

3.2. Quinacrine inhibition of the arachidonic acid pathway

Interruption of the arachidonic acid pathway has shown chemoprevention potential for cancers such as prostrate, lung, gastrointestinal, and esophageal [71–75]. The arachidonic acid pathway involves the activation of phospholipase A2 (PLA2) and produces a variety of biologically active metabolites through the lipooxygenase (LOX), cyclooxygenase (COX), and cytochrome P450 (CYP450) pathways [76]. Quinacrine has been shown to have a direct inhibitory effect on the activity of the PLA2 enzyme, with a binding site close to the active site (Table 1) [77–81]. Another proposed mechanism by which quinacrine inhibits PLA2 is based on its ability to interact with membrane phospholipids. Research using erythrocyte and platelet phospholipids demonstrates that quinacrine directly interacts with membrane phospholipids, primarily phosphatidylethanolamine, leading to the formation of less polar derivatives [80]. This quinacrine-phospholipid interaction is hypothesized to impact membrane structure and function which may in turn alter the activity of phospholipases and other cellular processes [79–84].

Irrespective of the precise mechanism, inhibition of PLA2 by quinacrine treatment results in decreased arachidonic acid formation [85]. This in turn inhibits leukotrienes (LOX), prostanoids (COX), and eicosanoids (MOX/CYP450), which have been previously implicated in preventing apoptosis and promoting cancer progression [82,86–97]. Furthermore, quinacrine reduces production of prostaglandin E2, a downstream metabolite of arachidonic acid, which is known to induce pro-inflammatory responses leading to tumorigenesis in various carcinomas [98–100]. In addition, quinacrine has been suggested as a direct inhibitor of P-glycoprotein (ATP-binding cassette transporter encoded by MDR1 gene) (Table 1), which is overexpressed in multi-drug resistant cells [79,82,101,102]. This transporter, along with other transporters involved in multi-drug resistance pathways, promotes drug efflux from the cells. Quinacrine was observed to enhance vincristine anti-tumor effects in multi-drug resistant chronic myelogenous leukemia cells [101]. The effect of quinacrine in multi-drug resistance pathways has also been reported in prostate cancer and hamster ovarian cells where it has been suggested that combinatorial therapy with paclitaxel can reverse the chemoresistant phenotype [43,102]. Although there are multiple potential targets in the arachidonic acid and multi-drug resistance pathways as described above, it is thought that quinacrine-induced inhibition of PLA2 accounts for the increased sensitivity of cancer cells to standard chemotherapies like vincristine [43,103,104].

3.3. Quinacrine inhibits the NFκB pathway and induces p53 expression

As previously mentioned, quinacrine was identified to induce p53 in a small molecule screen using renal cell carcinoma cells [44]. Quinacrine was validated as a result from this screen by showing that activation of p53 occurred through suppression of basal and inducible activities of NFκB (Table 1). Interestingly, Gurova et al. found that inhibition of NFκB signaling by quinacrine involved the sequestration of p65 in the nucleus where it was trapped in an inactive state [44]. Previously, quinacrine-induced PLA2 inhibition was thought to reduce NFκB signaling by preventing tumor necrosis factor-induced translocation of p65 to the nucleus [105]. However, in light of the findings by Gurova *et al,* the inhibition of NFκB signaling appears to occur downstream of p65 nuclear translocation [44]. This finding was further supported by Harada et al. who showed that quinacrine treatment did not interfere with p65 nuclear translocation but instead interfered with p65 binding to DNA at one of its promoters [106]. Additionally, Gurova and colleagues tested a variety of PLA2 inhibitors in renal cell carcinoma and found that these were not able to induce p53 or inhibit NFκB signaling [44], suggesting that quinacrine-induced p53 expression is through a mechanism separate from quinacrine-induced PLA2 inhibition.

Work by Gurova et al. also showed that treatment with 10 μM of 9-aminoacridine (9AA), which shares a common scaffold with quinacrine, reduces phosphorylation of the p65 NFκB subunit at Ser-536 [44]. However, these results contrast those by Harada et al. who used quinacrine concentrations up to 50 μM and observed minimal serine-536 reduction [106]. The interest surrounding the reduced phosphorylation of p65 stems from the observation that reduced p65 phosphorylation could serve as a mechanism leading to the recruitment of histone deacetylases and repression of NFκB signaling [44,106]. This theory is supported by experiments showing that inhibition of histone deacetylase activity by trichostatin A results in NFκB signaling that cannot be inhibited by 9AA [44].

Although differences in p65 phosphorylation illustrate quinacrine may inhibit NFκB signaling via alternative mechanisms, recent discoveries have elucidated a mechanism that is independent of p65 phosphorylation. A possible explanation on how quinacrine inhibits NFκB signaling and induces p53 is through FACT (Facilitates Chromatin Transcription) protein complex chromatin trapping (c-trapping). FACT is a nuclear complex that is formed by a heterodimer made up of two proteins: SSRP1 (homologous to yeast Pob3) and Spt16/p140 (homologous to yeast Spt16/Cdc68) [107]. FACT plays a role in RNA polymerase II-driven transcription and serves as a histone chaperone that facilitates nucleosome reassembly [108]. FACT facilitates RNA polymerase II-driven transcription by displacing H2A/H2B dimers from the nucleosome allowing transcript elongation [107,109]. This process is carried out through interactions of Spt16 with H2A/H2B dimers and SSRP1 with H3-H4 tetramers [107]. Work in yeast demonstrates that the requirement of FACT for RNA polymerase II is gene-specific and
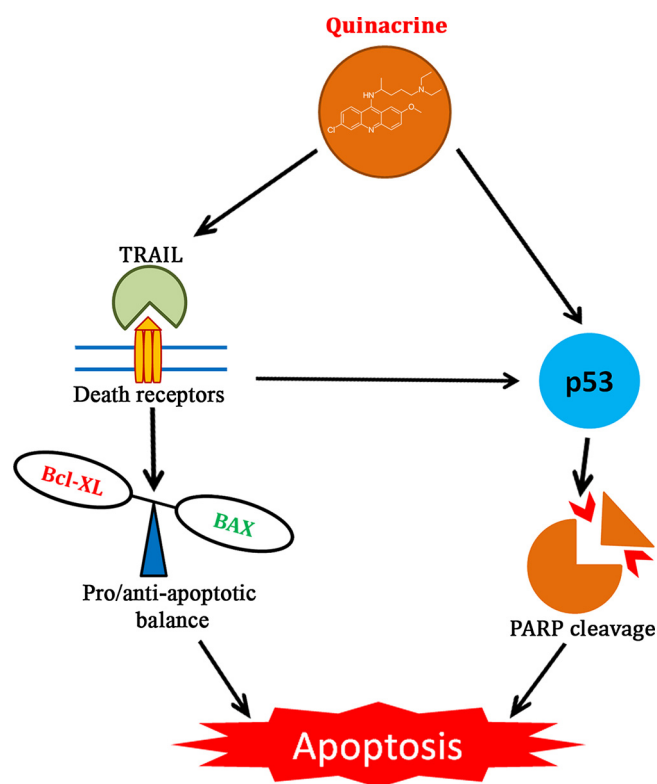
Quinacrine

Fig. 1. Quinacrine promotes TRAIL-mediated death receptor signaling. TRAIL is a homotrimeric ligand that interacts with death receptors, such as DR5 and DR4. Death receptors contain an intracellular death domain that can increase BAX and promote p53 signaling, both activating apoptotic pathways.

further work using HT1080 T fibrosarcoma cells demonstrated that FACT is enriched in areas that are highly transcribed [110,111]. In addition, FACT has also been shown to play a role in homologous recombination and DNA repair along with assisting in DNA replication-coupled nucleosome assembly [112–118].

As mentioned earlier, quinacrine has a diaminobutyl side chain that can insert into the minor groove of DNA [1]. Likewise, SSRP1 also binds to the minor groove through its HMG binding domain [119]. This HMG binding domain also allows SSRP1 to bind distorted DNA structures such as bent and cruciform DNA produced by cisplatin treatment [113,120,121]. Treatment with quinacrine, and structurally similar curaxins, alters the shape of the DNA helix and disassembles nucleosomes across the genome, thus creating multiple binding sites for FACT [122]. FACT is trapped onto the chromatin and in turn induces phosphorylation of p53 by FACT-associated CK2 [54]. This subsequently reduces NFκB signaling due to the lack of free active FACT [54].

Further research has been conducted in an effort to determine the component of chromosomes onto which FACT is specifically trapped. Work by Safina et al. offers two possibilities as they divide the phenomenon of FACT chromatin trapping into two phases. In phase one, partial nucleosome unfolding leads to the binding of the Spt16 subunit of FACT to the open nucleosome (n-trapping) [123]. In phase two, complete disassembly of the nucleosome leads to alternative DNA structures such as Z-DNA promoting the binding of the SSRP1 subunit of FACT (z-trapping) [123]. Although the precise nature of FACT chromatin trapping has not been reported for quinacrine, recent research using the structurally similar curaxin has showed that FACT becomes specifically bound to uncoiled nucleosomes upon curaxin treatment [110,123]. This suggests that curaxin promotes n-trapping of FACT, but more research is warranted to determine whether FACT specifically binds to nucleosomes or Z-DNA upon quinacrine treatment [110]. Regardless, quinacrine has been shown to reduce resistance to

the tyrosine kinase inhibitor erlotinib by inhibiting FACT, NFκB signaling, and cell cycle progression in non-small cell lung cancer [47]. Overall, these studies suggest that a possible anticancer mechanism of quinacrine is by trapping FACT on the chromosome/nucleosome.

Interestingly, FACT expression is low in most adult tissues except those that are associated with undifferentiated cells such as cells of the hematological and reproductive systems [124]. Even though gynecologic tissue was found to have high FACT expression, SSRP1 was found to be highly expressed in ovarian cancer compared to normal ovarian tissue [124,125]. Further research has demonstrated that FACT is elevated in breast cancer cell lines compared to normal breast tissue and that high FACT expression correlates with aggressive disease [126,127]. Additionally, high SSRP1 expression was found to be significantly associated with shorter disease-free survival in patients with early-stage and low-grade breast cancer [128]. Taken together, these studies suggest that the ability of quinacrine to induce FACT c-trapping would be a promising therapeutic strategy in cancer cells with high FACT expression such as those found in gynecologic and breast cancer.

4. Quinacrine studies in gynecologic and breast cancer

The high mortality associated with many cancers is often due to recurrent, metastatic disease as well as treatment-refractory tumors, which can result from acquired resistance to systemic chemotherapy [24,129–133]. Findings from recent work in gynecologic and breast cancer has expanded the knowledge of the mechanisms by which quinacrine can induce cancer cell cytotoxicity. Quinacrine was shown to resensitize chemoresistant ovarian cancer cells to carboplatin/cisplatin therapy [134] by targeting pathways of autophagy and apoptosis [134,135]. Additionally, studies in breast cancer have found that quinacrine can inhibit DNA damage repair as well as topoisomerase activity as a monotherapy and in synergistic combination with other therapies [60,136,137]. Quinacrine has also been shown to inhibit endometrial cancer cell proliferation and tumor progression both *in vitro* and *in vivo*, and, importantly, to enhance cell sensitivity to cisplatin and paclitaxel [22]. Overall, this data suggest that quinacrine treatment may be an effective treatment strategy for treatment-refractory gynecologic and breast cancer.

4.1. Quinacrine effects in breast cancer

The anticancer effects of quinacrine and associated mechanisms of action in breast cancer cell models have been extensively studied by the research program of Dr. Chanakya Kundu. This group has elucidated a variety of potential quinacrine anticancer mechanisms in breast cancer by showing that quinacrine is able to alter DNA damage repair and promote DNA damage, cause cell cycle arrest, inhibit topoisomerase, and sensitize cancer cells to tumor necrosis factor-related apoptosis-inducing ligand (TRAIL) (Fig. 1) [60,136,138,139]. They found that quinacrine is cytotoxic in MCF-7 and MDA-MB-231 breast cancer cells (clonogenic IC_{50} of 4.5 μM and 5.2 μM, respectively), while it has limited cytotoxic effects in the non-tumorigenic MCF-10A normal breast epithelial cell model [60]. The cytotoxicity of quinacrine corresponded with an S phase cell cycle arrest as well as apoptosis with increased BAX/Bcl-xL ratio, PARP cleavage, p53, and p21 levels in MCF-7 cells (Fig. 1). The investigators also reported that WT p53 MCF-7 and ZR75-1 breast cancer cells exhibited lower quinacrine IC_{50} values via MTT assay (7.0 and 8.5 μM, respectively) compared to the MDA-MB-231 and T47D cells which have mutated p53 (11 and 12 μM, respectively) [136]. The same group deleted *TP53* gene in colon cancer cells which resulted in a similar decrease in quinacrine cytotoxic sensitivity [140].

A contrasting study by a separate group recently reported that p53 knockdown in MCF-7 cells resulted in increased quinacrine cytotoxic effects at lower concentrations (shown at 2.5 μM) compared to unmodified MCF-7 cells [141]. This latter study also reported that

phosphorylated CHK1 and CHK2 were suppressed by quinacrine in these p53-null cells. This differential effect of quinacrine based on p53 status between these two studies was not addressed, but it does raise the question whether quinacrine enhanced the very low expression levels of p53 (assuming knockdown was not 100%) or whether cell death is based on alternative CHK1/2 pathways. Regardless, these studies in combination suggest that the p53 status of cancer cells impacts at least partially quinacrine cytotoxicity, and further suggest that the cell death efficacy of quinacrine cannot be solely predicted based on the p53 status of cancer cells.

The Kundu laboratory also demonstrated that quinacrine is able to induce DNA damage in a dose-dependent manner using MCF-7 breast cancer cells. Using an alkaline comet assay they found that cells treated with 0–20 μM of quinacrine showed increasing tail lengths and cells treated with 20 μM showed substantial DNA damage with a tail length increase of approximately 45% compared to 8% in the control [60]. Similarly, we have found that quinacrine can promote both single- and double-stranded DNA damage in various ovarian cancer cells lines (*unpublished data*). The Kundu group further attributed this induction of DNA damage to the ability of quinacrine to inhibit topoisomerase activity as they found quinacrine inhibits topoisomerase activity at concentrations similar to those that induce DNA damage [60]. However, more research is warranted to better understand the mechanism by which quinacrine induces DNA damage. Nonetheless, these results are novel as prior studies suggest that quinacrine does not induce DNA damage as previously mentioned. Importantly, this group also found that quinacrine showed high efficiency in killing tumor cells but had little effect on normal breast tissue [60].

Both quinacrine and etoposide (a known topoisomerase inhibitor) were found to inhibit NFκB signaling and the Wnt-TCF pathway in MCF-7 cells [142]. They further demonstrated that quinacrine increased adenomatous polyposis coli (APC) protein expression, and APC knockdown attenuated quinacrine-induced Wnt-TCF signaling changes along with lessening single-stranded DNA damage (via alkaline comet assay). Collectively, these studies in breast cancer models suggest that quinacrine can cause apoptosis by inducing DNA damage, cell cycle arrest, and inhibition of topoisomerase activity with increased cytotoxicity in p53 knockdown breast cancer cells.

Quinacrine treatment has further been shown to impact the DNA damage response in MCF-7 cells. Work by Preet et al. showed that quinacrine treatment resulted in increased Ser428 phosphorylation of ATR and decreased expression of CHK1 along with several cyclin dependent kinases (CDC2, CDC6, MDM2) suggesting that it induces stalled replication forks [136]. They further showed that quinacrine modifies base excision repair signaling with corresponding decreases in replication protein A, Pol ß, FEN1, and XRCC1. When quinacrine was combined with CHK1 inhibitor SB218078, modified base excision repair signaling was enhanced leading to further increases in DNA damage and indicative evidence of mitotic catastrophe. Siddharth et al. generated a metastatic breast cancer stem cell model by transforming MCF-10A cells via cigarette smoke extract and selectively culturing cells that had undergone epithelial-to-mesenchymal transformation. In this model, the authors demonstrated that quinacrine negatively regulated base excision repair when combined with the PARP inhibitor ABT-888 (veliparib), which correlated to increasing the APC protein expression [137]. In summary, these studies suggest that quinacrine impacts the DNA damage repair pathway, though it has not been determined whether this is by DNA intercalation.

Studies have also determined that quinacrine enhances the apoptotic activity of TRAIL, which is a natural ligand for death receptor 5 (DR5) [143,144]. Das et al. used molecular docking simulation to show that quinacrine binds at the TRAIL-DR5 interface, effectively forming a bridge between ligand and receptor. In breast cancer cell lines, they showed that the combination of quinacrine and ectopic TRAIL enhanced cellular death signaling via the intrinsic apoptotic pathway when compared to monotherapy [139]. The authors also noted that

adding quinacrine to transformed MCF-10A cells increased DR5 expression causing a mild increase in apoptosis while DR5 knockdown in these cells reduced quinacrine-induced apoptosis. TRAIL binding to DR5 promotes the recruitment of FADD, an adaptor molecule and active caspase 8 formation, thereby, inducing the mitochondrial intrinsic apoptotic cascade in select cancer cells, including the carcinogen-induced cancer cells. This group later showed that TRAIL can enhance the quinacrine induction of autophagy-induced cell death by regulating interactions between DR5 and p21, suggesting a downstream mechanism of quinacrine and TRAIL combination therapy [138]. Additionally, the ability of quinacrine to inhibit NFκB signaling may be an integral component for increasing TRAIL sensitivity considering that constitutive activation of NFκB has been implicated in TRAIL resistance [144]. In support of this hypothesis, inhibition of NFκB by quinacrine has been shown to act synergistically with TRAIL to induce cytotoxicity in colon cancer [144].

4.2. Quinacrine effects in gynecologic cancers

Work by our lab has shown quinacrine to exhibit cytotoxicity towards ovarian and endometrial cancer cells [22,134,135]. Our recent reports in ovarian cancer models highlight the ability of quinacrine to induce autophagy, which suggests autophagy as another mechanism by which quinacrine acts as an anticancer agent.

The induction of autophagic vacuoles in cancer cells upon quinacrine treatment may be a significant mechanism of cancer cell cytotoxicity. The autophagic process generally eliminates intracellular aggregates and damaged organelles, and this process can contribute to cell death when hyperactivated [145,146]. LC3B induction and degradation of p62 are the most common markers of the canonical autophagy pathway. In cancer cell biology, it still remains a matter of controversy whether autophagy is oncogenic (by promoting cell survival in the presence of nutrient stress) or tumor suppressive (through cell cycle arrest, supporting genome and organelle integrity, and inhibition of inflammation) [147,148]. Mohapatra et al. reported that quinacrine induction of autophagy was dependent on p53- and p21-associated mechanisms [140], and quinacrine also induces p21 expression in high grade serous ovarian cancer cells with loss-of-function p53 mutations [135]. In ovarian cancer, induction of autophagy is associated with increased sensitivity to platinum-based and paclitaxel chemotherapy [149–151]. The *TP53INP2* (*INP2*) gene has been reported as essential for autophagy induction [152]. The INP2 protein translocates upon induction and interacts with the transmembrane protein vacuole membrane protein-1 in the cytoplasm where it colocalizes in the autophagosomes with LC3, LC3-related proteins, and Beclin1. High expression of LC3 and Beclin1 strongly correlates with the overall survival of ovarian cancer patients [153]. Furthermore, knockdown of INP2 leads to deregulated autophagosome formation. Recent studies discovered that quinacrine treatment up-regulates the INP2 expression in ovarian cancer cells irrespective of their p53 mutational status and sensitizes tumor cells to cisplatin [134,135].

Quinacrine was also found to selectively degrade the autophagic cargo protein p62 (sequestosome 1, SQSTM1), an ubiquitin-binding scaffold protein that is required for both the formation and degradation of polyubiquitin-containing bodies by autophagy. Quinacrine-induced p62 degradation promotes the autophagic flux in chemoresistant ovarian cancer cells compared to their isogenic sensitive counterparts [134]. Quinacrine also upregulates the cell cycle inhibitor p21 and downregulates p62 in high grade serous ovarian cancer cells, suggesting that this effect is independent of p53 status [135]. In the same study, p62 knockdown increased p21 expression suggesting quinacrine-induced p21 expression is through p62 inhibition. When the key autophagy protein ATG5 was silenced, the quinacrine regulation of p21 and p62 was diminished further suggesting that these mechanisms are through autophagic pathways. In colon cancer cells, it was shown that quinacrine-induced autophagy was decreased in p53 and p21 null cells

ARTICLE IN PRESS

D.B. Oien, et al.   Seminars in Cancer Biology xxx (xxxx) xxx–xxx

compared to parental cells [140]. Quinacrine was also shown to support a p21 interaction with DR5 in breast cancer cells, which promotes autophagic and apoptotic cell death when combined with TRAIL [138]. With this observation, future mechanistic studies are needed to broaden the knowledge on how the induction of autophagy by quinacrine is essential to the sensitization of cancer cells to cisplatin/carboplatin-induced toxicity.

Quinacrine has been evaluated both *in vitro* and *in vivo* using endometrial cancer cell lines [22]. Endometrial cancer is the most common gynecologic malignancy in developed countries [154]. Many women are diagnosed at an early stage and respond well to carboplatin and paclitaxel chemotherapy. While this is the majority of patients, there is a subset with advanced-stage disease, unfavorable histology, or recurrent disease who have poor prognosis with first-line treatment response rates as low as 50%. To assess quinacrine *in vitro*, we used five different endometrial cancer cells lines (Ishikawa, Hec-1B, KLE, ARK-2, and SPEC-2) that represent different levels of platinum sensitivity, histologies, pathology grades, and p53 gene status [22]. Quinacrine inhibited endometrial cancer cell viability in all five cell lines with higher inhibitory concentrations in Hec-1B, which was the least sensitive to cisplatin among these cell lines. Quinacrine was combined separately with cisplatin, carboplatin, and paclitaxel and these drug combinations resulted in synergistic cell death in these endometrial cancer cell lines. The strongest effect was noted when quinacrine was combined with platinum-based chemotherapy in Hec-1B cells. While quinacrine treatment did not significantly delay tumor growth in a subcutaneous Hec-1B cell mouse xenograft model, it did result in prolongation of survival, an effect that was further enhanced when combined with carboplatin. Quinacrine maintenance therapy resulted in long-term stabilization of disease, which was evidenced by lack of significant tumor progression and further prolongation of overall survival. Quinacrine monotherapy, in combination with standard chemotherapy, and maintenance therapy was well-tolerated with no significant weight loss compared to control mice. A yellow skin discoloration was noted during the active treatment phase, which was entirely reversible within few days upon discontinuation of the treatment. Co-administration of quinacrine with standard chemotherapy significantly augmented the anti-proliferative effect of carboplatin as evidenced by the significant decrease in tumor burden of mice. Combination treatment was associated with a 14-week prolongation of median survival compared to standard chemotherapy alone, suggesting that quinacrine could be an important adjunct therapy to standard platinum-based chemotherapeutic regimens for patients with recurrent endometrial cancer.

5. Combining quinacrine with chemotherapy

Quinacrine has been evaluated in combination with systemic chemotherapies such as platinum agents and paclitaxel. Quinacrine was found to restore cisplatin sensitivity in head and neck cancer cells [46]. There are three other reports of quinacrine in combination with cisplatin. Quinacrine was found to enhance cisplatin cytotoxicity in multiple cell lines including HeLa cervical cancer cells [155]. We previously reported that quinacrine synergizes with cisplatin in ovarian cancer cells, particularly in chemotherapy resistant cells, and that it synergizes with carboplatin in a xenograft mouse model of drug-resistant ovarian cancer cells [134]. Recently, we reported that quinacrine synergizes with cisplatin, carboplatin, and paclitaxel in *TP53*-mutated endometrial cancer cells, and further, these combinations inhibited endometrial cancer xenograft tumor growth in mice [22]. Importantly, combinatory treatment of quinacrine with chemotherapy significantly prolonged endometrial cancer xenograft mouse median survival compared to standard chemotherapy alone. Quinacrine has also been reported to synergize with paclitaxel *in vitro* and in xenograft mouse models for prostate cancer cells [43].

In addition to being used in combination with systemic

chemotherapy, quinacrine has also been applied in combination studies with a variety of targeted therapies. It has been used in combination with vorinostat, a pan-histone deacetylase (HDAC) inhibitor, for the treatment of T-cell acute lymphoblastic leukemia cells. In these cells, quinacrine was found to increase apoptotic cell death and also induce cell death in a xenograft mouse model [156]. Interestingly, the authors of this latter study noted that both quinacrine alone and in combination with vorinostat increased p62 in the mitochondria, suggesting a mitophagy blockade in these cells. In addition, quinacrine in combination with the antiangiogenic agent cediranib reduced tumor size in a mouse model of intracranial glioma, while neither treatment alone was effective [157]. Furthermore, quinacrine has displayed cytotoxic synergy in combination with cytarabine (an antimetabolic that incorporates ribose stereoisomer into DNA), azacitidine (methyltransferase inhibitor), and geldanamycin (HSP90 inhibitor) [158]. Finally, quinacrine has also been found to synergize with PARP inhibitors, CHK1 inhibitors, and tyrosine kinase inhibitors as described above [47,136,137]. Recent approvals of PARP inhibitors for ovarian cancer have lengthened patient median progression-free survival, mainly for patients with homologous recombination repair deficiencies. We have found that adding PARP inhibitors with quinacrine has synergistic cell death effects in ovarian cancer cells (*unpublished data*), which may be related to quinacrine-induced inhibition of DNA damage repair and this remains a part of our ongoing studies.

6. Clinical trials with quinacrine for cancer indications

Quinacrine is currently in a Phase 1/2 clinical trial in combination with capecitabine in colorectal adenocarcinoma (NCT01844076) at the Fox Chase Cancer Center. Quinacrine has completed a Phase 1 trial in combination with erlotinib for recurrent/late-stage non-small cell lung cancer (NCT01839955, 2013–2016) [159] and a Phase 2 trial for androgen-independent prostate cancer as a monotherapy (NCT00417274, 2006–2008). The erlotinib and quinacrine Phase 1 trial aimed to determine the maximum tolerated doses in non-small cell lung cancer [159]. This trial evaluated nine patients and found that this drug combination was well tolerated (two patients with dose limiting toxicity), but had limited efficacy for advanced non-small cell lung cancer. The maximum tolerated dose of quinacrine was determined to be 50 mg every other day when combined with 150 mg of erlotinib. Among the 9 patients of this trial, one patient had stable disease at 8 months and one patient experienced partial response to this treatment. In the clinical trial for prostate cancer, 31 patients received 100 mg of quinacrine daily and the incidence of serious adverse events was less than 10% suggesting that treatment was well tolerated. With regards to efficacy, improvement in prostate specific antigen response has not yet been reported. Another trial in advanced renal cell carcinoma using quinacrine treatment at 100 mg daily (NCT00574483) was withdrawn in 2015 for reevaluation of compound development by the same group sponsoring the prostate cancer trial. This sponsor, Cleveland BioLabs, does not report quinacrine (CBL0102) as part of their current drug development pipeline. Currently, while the structurally similar curaxin compounds are surfacing as be more attractive for clinical trial development based on higher potency data [159], curaxins lack established safety data as compared to quinacrine, which is a long-established therapeutic. Collectively, these trials offer a guarded enthusiasm for the use of quinacrine as an anticancer agent and highlight the necessity for more precisely defined treatment indications that may need to be derived from additional mechanistic and drug combination studies.

7. Conclusion

Repurposing quinacrine as an anticancer agent has shown promising results in cell and mouse models, and may be valuable adjunct to current chemotherapy. Importantly, quinacrine has consistently been shown to have little activity on non-malignant cells, which though not

Fig. 2. Proposed quinacrine-associated mechanisms of cancer cell toxicity. *Clockwise:* Quinacrine abrogates the arachidonic acid pathway, which is essential for eicosanoids production. Quinacrine promotes autophagic vacuole development through LCB3 and impedes the p62 selective autophagy receptor. Quinacrine inhibits DNA damage repair and induces DNA damage, which may be associated to drug intercalation with DNA. In addition, quinacrine intercalation alters chromatin structure resulting in chromatin trapping of FACT (SSRP1/Spt16 complex). Quinacrine activates apoptotic signaling through several pathways such as inducing p53 and enhancing receptor binding of TRAIL as well as arresting cells in S phase.

fully understood. These characteristics place quinacrine in the unique position to offer anticancer activity alone or in combination with other treatments while carrying low overall treatment toxicity. Recent studies in gynecologic and breast cancer have expanded our knowledge on potential anticancer mechanisms of action associated with quinacrine treatment. These studies have shown that quinacrine is able to promote DNA damage, stimulate FACT chromatin trapping, and induce autophagy in addition to previously described mechanisms (Fig. 2). Nonetheless, the primary cytotoxic mechanism by which quinacrine exerts its anticancer effects is still not clearly identified and thus further mechanistic research is warranted. Understanding the cytotoxic selectivity of quinacrine against cancer cells may be critical for future clinical trial design and, specifically, for optimal selection of patient population and mechanistically justified combinatory treatments. This includes ongoing studies of adding quinacrine to recently approved PARP inhibitors for ovarian and breast cancers, which may have treatment potential for non-*BRCA* mutated tumors based on DNA damage repair inhibition by quinacrine. Future clinical trials are needed to prove the efficacy of quinacrine in the clinical setting as an anticancer treatment alone or in combination with systemic chemotherapy and/or targeted therapies as well as confirm its safety profile in these combinations.

Declaration of Competing Interest

The authors declare that there are no conflicts of interest.

Acknowledgements

References

[1] K. Gurova, New hopes from old drugs: revisiting DNA-binding small molecules as anticancer agents, Future Oncol. 5 (2009) 1685–1704.

[2] R. Ehsanian, C. Van Waes, S.M. Feller, Beyond DNA binding - a review of the potential mechanisms mediating quinacrine's therapeutic activities in parasitic infections, inflammation, and cancers, Cell Commun. Signaling: CCS 9 (2011) 13.

[3] W.C. Campbell, The chemotherapy of parasitic infections, J. Parasitol. 72 (1986) 45–61.

[4] R. Canete, A.A. Escobedo, M.E. Gonzalez, P. Almirall, Randomized clinical study of five days apostrophe therapy with mebendazole compared to quinacrine in the treatment of symptomatic giardiasis in children, World J. Gastroenterol. 12 (2006) 6366–6370.

[5] S.J. Lerman, R.A. Walker, Treatment of giardiasis: literature review and recommendations, Clin. Pediatr. 21 (1982) 409–414.

[6] E. Toubi, A. Kessel, I. Rosner, M. Rozenbaum, D. Paran, Y. Shoenfeld, The reduction of serum B-lymphocyte activating factor levels following quinacrine add-on therapy in systemic lupus erythematosus, Scand. J. Immunol. 63 (2006) 299–303.

[7] K.M. Stuhlmeier, C. Pollaschek, Quinacrine but not chloroquine inhibits PMA induced upregulation of matrix metalloproteinases in leukocytes: quinacrine acts at the transcriptional level through a PLA2-independent mechanism, J. Rheumatol. 33 (2006) 472–480.

[8] R. Feldmann, D. Salomon, J.H. Saurat, The association of the two antimalarials chloroquine and quinacrine for treatment-resistant chronic and subacute cutaneous lupus erythematosus, Dermatology (Basel, Switzerland) 189 (1994) 425–427.

[9] R.I. Rynes, Antimalarial drugs in the treatment of rheumatological diseases, Br. J. Rheumatol. 36 (1997) 799–805.

[10] D.J. Wallace, The use of quinacrine (Atabrine) in rheumatic diseases: a reexamination, Semin. Arthritis Rheum. 18 (1989) 282–296.

[11] S.M. Cattaneo, H.D. Sirak, K.P. Klassen, Recurrent spontaneous pneumothorax in the high-risk patient. Management with intrapleural quinacrine, J. Thorac. Cardiovasc. Surg. 66 (1973) 467–471.

[12] H.M. Janzing, A. Derom, E. Derom, C. Eeckhout, F. Derom, M.T. Rosseel, Intrapleural quinacrine instillation for recurrent pneumothorax or persistent air leak, Ann. Thorac. Surg. 55 (1993) 368–371.

[13] A.J. Larrieu, G.F. Tyers, E.H. Williams, M.J. O'Neill, J.R. Derrick, Intrapleural instillation of quinacrine for treatment of recurrent spontaneous pneumothorax, Ann. Thorac. Surg. 28 (1979) 146–150.

[14] S. Koldsland, J.L. Svennevig, G. Lehne, E. Johnson, Chemical pleurodesis in malignant pleural effusions: a randomised prospective study of mepacrine versus bleomycin, Thorax 48 (1993) 790–793.

[15] S.A. Taylor, N.S. Hooton, A.M. Macarthur, Quinacrine in the management of

ARTICLE IN PRESS

D.B. Oien, et al.   Seminars in Cancer Biology xxx (xxxx) xxx–xxx

malignant pleural effusion, Br. J. Surg. 64 (1977) 52–53.

[16] G. Hillerdal, Pleural malignancies including mesothelioma, Curr. Opin. Pulm. Med. 1 (1995) 339–343.

[17] K. Doh-Ura, T. Iwaki, B. Caughey, Lysosomotropic agents and cysteine protease inhibitors inhibit scrapie-associated prion protein accumulation, J. Virol. 74 (2000) 4894–4897.

[18] D.C. Sokal, T. Hieu do, N.D. Loan, D. Hubacher, K. Nanda, D.H. Weiner, T.H. Vach, Safety of quinacrine contraceptive pellets: results from 10-year follow-up in Vietnam, Contraception 78 (2008) 66–72.

[19] D.C. Sokal, J. Zipper, R. Guzman-Serani, T.E. Aldrich, Cancer risk among women sterilized with transcervical quinacrine hydrochloride pellets, 1977 to 1991, Fertil. Steril. 64 (1995) 325–334.

[20] A. Dabancens, D.C. Sokal, M. Pruyas, M. Rivera, J. Zipper, Prevalence and stan-dardized incidence rates of preclinical cervical pathology among 1,061 women sterilized with transcervical quinacrine hydrochloride pellets, Fertil. Steril. 64 (1995) 444–446.

[21] E. Kessel, 100,000 quinacrine sterilizations, Adv. Contracept. 12 (1996) 69–76.

[22] E. Kalogera, D. Roy, A. Khurana, S. Mondal, A.L. Weaver, X. He, S.C. Dowdy, V. Shridhar, Quinacrine in endometrial cancer: repurposing an old antimalarial drug, Gynecol. Oncol. 146 (2017) 187–195.

[23] D.B. Oien, J. Chien, TP53 mutations as a biomarker for high-grade serous ovarian cancer: are we there yet? Transl. Cancer Res. 5 (2016) S264–268.

[24] D.B. Oien, J. Chien, N. Cheng, Regulation of chemo-sensitivity in ovarian cancer via a stroma dependent gluathion pathway, Transl. Cancer Res. 5 (2016) S514–519.

[25] D.J. Klionsky, Autophagy: from phenomenology to molecular understanding in less than a decade, Nature reviews, Mol. Cell Biol. 8 (2007) 931–937.

[26] J. O'Shaughnessy, Extending survival with chemotherapy in metastatic breast cancer, Oncologist 10 (Suppl 3) (2005) 20–29.

[27] C.R. Chong, D.J. Sullivan Jr., New uses for old drugs, Nature 448 (2007) 645–646.

[28] J.K. Aronson, Old drugs—new uses, Br. J. Clin. Pharmacol. 64 (2007) 563–565.

[29] L.A. Tartaglia, Complementary new approaches enable repositioning of failed drug candidates, Expert Opin. Investig. Drugs 15 (2006) 1295–1298.

[30] E.L. Tobinick, The value of drug repositioning in the current pharmaceutical market, Drug News Perspect. 22 (2009) 119–125.

[31] S.M. Paul, D.S. Mytelka, C.T. Dunwiddie, C.C. Persinger, B.H. Munos, S.R. Lindborg, A.L. Schacht, How to improve R&D productivity: the pharmaceu-tical industry's grand challenge, nature reviews, Drug Discovery 9 (2010) 203–214.

[32] V. Prasad, S. Mailankody, Research and development spending to bring a single cancer drug to market and revenues after approval, JAMA Intern. Med. 177 (2017) 1569–1575.

[33] J.J. Hernandez, M. Pryszlak, L. Smith, C. Yanchus, N. Kurji, V.M. Shahani, S.V. Molinski, Giving drugs a second chance: overcoming regulatory and financial hurdles in repurposing approved drugs as cancer therapeutics, Front. Oncol. 7 (2017) 273.

[34] T.T. Ashburn, K.B. Thor, Drug repositioning: identifying and developing new uses for existing drugs, nature reviews, Drug Discovery 3 (2004) 673–683.

[35] J.A. DiMasi, R.W. Hansen, H.G. Grabowski, The price of innovation: new estimates of drug development costs, J. Health Econ. 22 (2003) 151–185.

[36] M.R. Hurle, L. Yang, Q. Xie, D.K. Rajpal, P. Sanseau, P. Agarwal, Computational drug repositioning: from data to therapeutics, Clin. Pharmacol. Ther. 93 (2013) 335–341.

[37] S. Kumar, A. Meuter, P. Thapa, C. Langstraat, S. Giri, J. Chien, R. Rattan, W. Cliby, V. Shridhar, Metformin intake is associated with better survival in ovarian cancer: a case-control study, Cancer 119 (2013) 555–562.

[38] C. Skriver, C. Dehlendorff, M. Borre, K. Brasso, S.B. Larsen, S.O. Dalton, M. Norgaard, A. Pottegard, J. Hallas, H.T. Sorensen, S. Friis, Use of low-dose as-pirin and mortality after prostate cancer diagnosis: a nationwide cohort study, Ann. Intern. Med. (2019).

[39] P.C. Elwood, J.E. Pickering, G. Morgan, J. Galante, A.L. Weightman, D. Morris, M. Longley, M. Mason, R. Adams, S. Dolwani, W.K.J. Chia, A. Lanas, Systematic review update of observational studies further supports aspirin role in cancer treatment: time to share evidence and decision-making with patients? PLoS One 13 (2018) e0203957.

[40] R.A. Cohen, P. Boersma, A. Vahratian, Strategies used by adults aged 18–64 to reduce their prescription drug costs, 2017, NCHS Data Brief (2019).

[41] A.L. Hopkins, J.S. Mason, J.P. Overington, Can we rationally design promiscuous drugs? Curr. Opin. Struct. Biol. 16 (2006) 127–136.

[42] A. Sivachenko, A. Kalinin, A. Yuryev, Pathway analysis for design of promiscuous drugs and selective drug mixtures, Curr. Drug Discov. Technol. 3 (2006) 269–277.

[43] P.L. de Souza, M. Castillo, C.E. Myers, Enhancement of paclitaxel activity against hormone-refractory prostate cancer cells in vitro and in vivo by quinacrine, Br. J. Cancer 75 (1997) 1593–1600.

[44] K.V. Gurova, J.E. Hill, C. Guo, A. Prokvolit, L.G. Burdelya, E. Samoylova, A.V. Khodyakova, R. Ganapathi, M. Ganapathi, N.D. Tararova, D. Bosykh, D. Lvovskiy, T.R. Webb, G.R. Stark, A.V. Gudkov, Small molecules that reactivate p53 in renal cell carcinoma reveal a NF-kappaB-dependent mechanism of p53 suppression in tumors, Proc. Natl. Acad. Sci. U. S. A. 102 (2005) 17448–17453.

[45] A. Eriksson, A. Osterroos, S. Hassan, J. Gullbo, L. Rickardson, M. Jarvius, P. Nygren, M. Fryknas, M. Hoglund, R. Larsson, Drug screen in patient cells sug-gests quinacrine to be repositioned for treatment of acute myeloid leukemia, Blood Cancer J. 5 (2015) e307.

[46] J. Friedman, L. Nottingham, P. Duggal, F.G. Pernas, B. Yan, X.P. Yang, Z. Chen, C. Van Waes, Deficient TP53 expression, function, and cisplatin sensitivity are restored by quinacrine in head and neck cancer, Clin. Cancer Res. 13 (2007)

6568–6578.

[47] J.K. Dermawan, K. Gurova, J. Pink, A. Dowlati, S. De, G. Narla, N. Sharma, G.R. Stark, Quinacrine overcomes resistance to erlotinib by inhibiting FACT, NF-kappaB, and cell-cycle progression in non-small cell lung cancer, Mol. Cancer Ther. 13 (2014) 2203–2214.

[48] L.S. Lerman, Structural considerations in the interaction of DNA and acridines, J. Mol. Biol. 3 (1961) 18–30.

[49] L.S. Lerman, The structure of the DNA-acridine complex, Proc. Natl. Acad. Sci. U. S. A. 49 (1963) 94–102.

[50] M. Aslanoglu, G. Ayne, Voltammetric studies of the interaction of quinacrine with DNA, Anal. Bioanal. Chem. 380 (2004) 658–663.

[51] S. Doglia, A. Graslund, A. Ehrenberg, Specific interactions between quinacrine and self-complementary deoxydinucleotides, Anticancer Res. 6 (1986) 1363–1368.

[52] L. Rivas, A. Murza, S. Sanchez-Cortes, J.V. Garcia-Ramos, Interaction of anti-malarial drug quinacrine with nucleic acids of variable sequence studied by spectroscopic methods, J. Biomol. Struct. Dyn. 18 (2000) 371–383.

[53] G. Baldini, S. Doglia, S. Dolci, G. Sassi, Fluorescence-determined preferential binding of quinacrine to DNA, Biophys. J. 36 (1981) 465–477.

[54] A.V. Gasparian, C.A. Burkhart, A.A. Purmal, L. Brodsky, M. Pal, M. Saranadasa, D.A. Bosykh, M. Commane, O.A. Guryanova, S. Pal, A. Safina, S. Sviridov, I.E. Koman, J. Veith, A.A. Komar, A.V. Gudkov, K.V. Gurova, Curaxins: anticancer compounds that simultaneously suppress NF-kappaB and activate p53 by targeting FACT, Sci. Transl. Med. 3 (2011) 95ra74.

[55] M. Hossain, P. Giri, G.S. Kumar, DNA intercalation by quinacrine and methylene blue: a comparative binding and thermodynamic characterization study, DNA Cell Biol. 27 (2008) 81–90.

[56] R.L. O'Brien, J.G. Olenick, F.E. Hahn, Reactions of quinine, chloroquine, and quinacrine with DNA and their effects on the DNA and RNA polymerase reactions, Proc. Natl. Acad. Sci. U. S. A. 55 (1966) 1511–1517.

[57] D.C. Sokal, A. Dabancens, R. Guzman-Serani, J. Zipper, Cancer risk among women sterilized with transcervical quinacrine in Chile: an update through 1996, Fertil. Steril. 74 (2000) 169–171.

[58] J. Zipper, V. Trujillo, 25 years of quinacrine sterilization experience in Chile: re-view of 2,592 cases, Int. J. Gynaecol. Obstet. 83 (Suppl 2) (2003) S23–29.

[59] C.W. Hays, The united states army and malaria control in world war II, Parassitologia 42 (2000) 47–52.

[60] R. Preet, P. Mohapatra, S. Mohanty, S.K. Sahu, T. Choudhuri, M.D. Wyatt, C.N. Kundu, Quinacrine has anticancer activity in breast cancer cells through in-hibition of topoisomerase activity, Int. J. Cancer 130 (2012) 1660–1670.

[61] H. Sun, J. Xiang, Q. Li, Y. Liu, L. Li, Q. Shang, G. Xu, Y. Tang, Recognize three different human telomeric G-quadruplex conformations by quinacrine, Analyst 137 (2012) 862–867.

[62] R.J. Harrison, S.M. Gowan, L.R. Kelland, S. Neidle, Human telomerase inhibition by substituted acridine derivatives, Bioorg. Med. Chem. Lett. 9 (1999) 2463–2468.

[63] J.H. Tan, L.Q. Gu, J.Y. Wu, Design of selective G-quadruplex ligands as potential anticancer agents, Mini Rev. Med. Chem. 8 (2008) 1163–1178.

[64] M.A. Read, A.A. Wood, J.R. Harrison, S.M. Gowan, L.R. Kelland, H.S. Dosanjh, S. Neidle, Molecular modeling studies on G-quadruplex complexes of telomerase inhibitors: structure-activity relationships, J. Med. Chem. 42 (1999) 4538–4546.

[65] R.D. Snyder, M.R. Arnone, Putative identification of functional interactions be-tween DNA intercalating agents and topoisomerase II using the V79 in vitro mi-cronucleus assay, Mutat. Res. 503 (2002) 21–35.

[66] G. Fox, O. Popanda, L. Edler, H.W. Thielmann, Preferential inhibition of DNA polymerases alpha, delta, and epsilon from Novikoff hepatoma cells by inhibitors of cell proliferation, J. Cancer Res. Clin. Oncol. 122 (1996) 78–94.

[67] J. Wang, J. Du, Z. Wu, Q. Jin, Quinacrine impairs enterovirus 71 RNA replication by preventing binding of polypyrimidine-tract binding protein with internal ri-bosome entry sites, PLoS One 8 (2013) e52954.

[68] S.Z. Hirschman, E. Garfinkel, Inhibition of hepatitis B DNA polymerase by inter-calating agents, Nature 271 (1978) 681–683.

[69] M.L. Seligman, H.G. Mandel, Inhibition of growth and RNA biosynthesis of Bacillus cereus by quinacrine, J. Gen. Microbiol. 68 (1971) 135–148.

[70] M. Penzo, L. Montanaro, D. Trere, M. Derenzini, The ribosome biogenesis-cancer connection, Cells 8 (2019).

[71] J.R. Mann, R.N. DuBois, Cyclooxygenase-2 and gastrointestinal cancer, Cancer J. (Sudbury, Mass.) 10 (2004) 145–152.

[72] M.I. Patel, C. Kurek, Q. Dong, The arachidonic acid pathway and its role in prostate cancer development and progression, J. Urol. 179 (2008) 1668–1675.

[73] R.L. Keith, Y.E. Miller, Lung cancer: genetics of risk and advances in chemopre-vention, Curr. Opin. Pulm. Med. 11 (2005) 265–271.

[74] P. Jimenez, A. Garcia, S. Santander, E. Piazuelo, Prevention of cancer in the upper gastrointestinal tract with COX-inhibition. Still an option? Curr. Pharm. Des. 13 (2007) 2261–2273.

[75] S. Mehta, I.T. Johnson, M. Rhodes, Systematic review: the chemoprevention of oesophageal adenocarcinoma, Aliment. Pharmacol. Ther. 22 (2005) 759–768.

[76] T.F. Borin, K. Angara, M.H. Rashid, B.R. Achyut, A.S. Arbab, Arachidonic acid metabolite as a novel therapeutic target in breast cancer metastasis, Int. J. Mol. Sci. 18 (2017).

[77] M.M. Billah, E.G. Lapetina, P. Cuatrecasas, Phospholipase A2 activity specific for phosphatidic acid. A possible mechanism for the production of arachidonic acid in platelets, J. Biol. Chem. 256 (1981) 5399–5403.

[78] M.K. Jain, B.Z. Yu, J. Rogers, G.N. Ranadive, O.G. Berg, Interfacial catalysis by phospholipase A2: dissociation constants for calcium, substrate, products, and competitive inhibitors, Biochemistry 30 (1991) 7306–7317.

[79] B.M. Loffler, E. Bohn, B. Hesse, H. Kunze, Effects of antimalarial drugs on phos-pholipase A and lysophospholipase activities in plasma membrane, mitochondrial,

microsomal and cytosolic subcellular fractions of rat liver, Biochim. Biophys. Acta 835 (1985) 448–455.

[80] C.A. Dise, J.W. Burch, D.B. Goodman, Direct interaction of mepacrine with erythrocyte and platelet membrane phospholipid, J. Biol. Chem. 257 (1982) 4701–4704.

[81] P. Mustonen, J.Y. Lehtonen, P.K. Kinnunen, Binding of quinacrine to acidic phospholipids and pancreatic phospholipase A2. Effects on the catalytic activity of the enzyme, Biochemistry 37 (1998) 12051–12057.

[82] D.F. Horrobin, M.S. Manku, M. Karmazyn, A.I. Ally, R.O. Morgan, R.A. Karmali, Quinacrine is a prostaglandin antagonist, Biochem. Biophys. Res. Commun. 76 (1977) 1188–1193.

[83] R. Zidovetzki, I.W. Sherman, P.A. Maguire, H. De Boeck, A nuclear magnetic resonance study of the interactions of the antimalarials chloroquine, quinacrine, quinine and mefloquine with lipids extracted from normal human erythrocytes, Mol. Biochem. Parasitol. 38 (1990) 33–39.

[84] A.A. Abdel-Latif, J.P. Smith, R.A. Akhtar, Studies on the mechanism of alteration by propranolol and mepacrine of the metabolism of phosphoinositides and other glycerolipids in the rabbit iris muscle, Biochem. Pharmacol. 32 (1983) 3815–3821.

[85] K. Yamada, Y. Okano, K. Miura, Y. Nozawa, A major role for phospholipase A2 in antigen-induced arachidonic acid release in rat mast cells, Biochem. J. 247 (1987) 95–99.

[86] A. Ahmed, I.T. Cameron, R.A. Ferriani, S.K. Smith, Activation of phospholipase A2 and phospholipase C by endothelin-1 in human endometrium, J. Endocrinol. 135 (1992) 383–390.

[87] E. Bugge, T.M. Gamst, A.C. Hegstad, T. Andreasen, K. Ytrehus, Mepacrine protects the isolated rat heart during hypoxia and reoxygenation—but not by inhibition of phospholipase A2, Basic Res. Cardiol. 92 (1997) 17–24.

[88] J.K. Beckman, S.M. Borowitz, I.M. Burr, The role of phospholipase A activity in rat liver microsomal lipid peroxidation, J. Biol. Chem. 262 (1987) 1479–1484.

[89] P.M. Evans, D.F. Lanham, Effects of inhibitors of arachidonic acid metabolism on intercellular adhesion of SV40-3T3 cells, Cell Biol. Int. Rep. 10 (1986) 693–698.

[90] N.P. Hurst, J.K. French, A.L. Bell, G. Nuki, M.L. O'Donnell, W.H. Betts, L.G. Cleland, Differential effects of mepacrine, chloroquine and hydroxychloroquine on superoxide anion generation, phospholipid methylation and arachidonic acid release by human blood monocytes, Biochem. Pharmacol. 35 (1986) 3083–3089.

[91] P.C. Churchill, M.C. Churchill, F.D. McDonald, Quinacrine antagonizes the effects of Na,K-ATPase inhibitors on renal prostaglandin E2 release but not their effects on renin secretion, Life Sci. 36 (1985) 277–282.

[92] A. Erman, R. Azuri, A. Raz, Prostaglandin biosynthesis in rabbit kidney: mepacrine inhibits renomedullary cyclooxygenase, Biochem. Pharmacol. 33 (1984) 79–82.

[93] A. Raz, Mepacrine blockade of arachidonate-induced washed platelet aggregation: relationship to mepacrine inhibition of platelet cyclooxygenase, Thromb. Haemost. 50 (1983) 784–786.

[94] S.L. Hofmann, S.M. Prescott, P.W. Majerus, The effects of mepacrine and p-bromophenacyl bromide on arachidonic acid release in human platelets, Arch. Biochem. Biophys. 215 (1982) 237–244.

[95] T.Y. Lot, T. Bennett, Comparison of the effects of chloroquine quinacrine and quinidine on autonomic neuroeffector mechanisms, Med. Biol. 60 (1982) 307–315.

[96] K.S. Authi, J.R. Traynor, Stimulation of polymorphonuclear leucocyte phospholipase A2 activity by chloroquine and mepacrine, J. Pharm. Pharmacol. 34 (1982) 736–738.

[97] J.T. Flynn, Inhibition of complement-mediated hepatic thromboxane production by mepacrine, a phospholipase inhibitor, Prostaglandins 33 (1987) 287–299.

[98] H. Oshima, K. Oguma, Y.C. Du, M. Oshima, Prostaglandin E2, Wnt, and BMP in gastric tumor mouse models, Cancer Sci. 100 (2009) 1779–1785.

[99] D. Kamei, M. Murakami, Y. Nakatani, Y. Ishikawa, T. Ishii, I. Kudo, Potential role of microsomal prostaglandin E synthase-1 in tumorigenesis, J. Biol. Chem. 278 (2003) 19396–19405.

[100] K. Yoshimatsu, D. Golijanin, P.B. Paty, R.A. Soslow, P.J. Jakobsson, R.A. DeLellis, K. Subbaramaiah, A.J. Dannenberg, Inducible microsomal prostaglandin E synthase is overexpressed in colorectal adenomas and cancer, Clin. Cancer Res. 7 (2001) 3971–3976.

[101] G.W. Liang, W.L. Lu, J.W. Wu, J.H. Zhao, H.Y. Hong, C. Long, T. Li, Y.T. Zhang, H. Zhang, J.C. Wang, X. Zhang, Q. Zhang, Enhanced therapeutic effects on the multi-drug resistant human leukemia cells in vitro and xenograft in mice using the stealthy liposomal vincristine plus quinacrine, Fundam. Clin. Pharmacol. 22 (2008) 429–437.

[102] D. Boscoboinik, R.M. Epand, Increased cellular internalization of amphiphiles in a multidrug-resistant CHO cell line, Biochim. Biophys. Acta 1014 (1989) 53–56.

[103] M. Inaba, E. Maruyama, Reversal of resistance to vincristine in P388 leukemia by various polycyclic clinical drugs, with a special emphasis on quinacrine, Cancer Res. 48 (1988) 2064–2067.

[104] W.T. Beck, M.C. Cirtain, C.J. Glover, R.L. Felsted, A.R. Safa, Effects of indole alkaloids on multidrug resistance and labeling of P-glycoprotein by a photoaffinity analog of vinblastine, Biochem. Biophys. Res. Commun. 153 (1988) 959–966.

[105] L. Thommesen, W. Sjursen, K. Gasvik, W. Hanssen, O.L. Brekke, L. Skattebol, A.K. Holmeide, T. Espevik, B. Johansen, A. Laegreid, Selective inhibitors of cytosolic or secretory phospholipase A2 block TNF-induced activation of transcription factor nuclear factor-kappa B and expression of ICAM-1, J. Immunol. (Baltimore, Md.: 1950) 161 (1998) 3421–3430.

[106] M. Harada, K. Morimoto, T. Kondo, R. Hiramatsu, Y. Okina, R. Muko, I. Matsuda, T. Kataoka, Quinacrine inhibits ICAM-1 transcription by blocking DNA binding of the NF-kappaB subunit p65 and sensitizes human lung adenocarcinoma A549 cells to TNF-alpha and the fas ligand, Int. J. Mol. Sci. 18 (2017).

[107] R. Belotserkovskaya, S. Oh, V.A. Bondarenko, G. Orphanides, V.M. Studitsky, D. Reinberg, FACT facilitates transcription-dependent nucleosome alteration, Science 301 (2003) 1090–1093.

[108] D. Reinberg, R.J. Sims 3rd, De FACTo nucleosome dynamics, J. Biol. Chem. 281 (2006) 23297–23301.

[109] G. Orphanides, G. LeRoy, C.H. Chang, D.S. Luse, D. Reinberg, FACT, a factor that facilitates transcript elongation through nucleosomes, Cell 92 (1998) 105–116.

[110] H.W. Chang, M.E. Valieva, A. Safina, R.V. Chereji, J. Wang, O.I. Kulaeva, A.V. Morozov, M.P. Kirpichnikov, A.V. Feofanov, K.V. Gurova, V.M. Studitsky, Mechanism of FACT removal from transcribed genes by anticancer drugs curaxins, Sci. Adv. 4 (2018) eaav2131.

[111] S. Jimeno-Gonzalez, F. Gomez-Herreros, P.M. Alepuz, S. Chavez, A gene-specific requirement for FACT during transcription is related to the chromatin organization of the transcribed region, Mol. Cell. Biol. 26 (2006) 8710–8721.

[112] D.V. Oliveira, A. Kato, K. Nakamura, T. Ikura, M. Okada, J. Kobayashi, H. Yanagihara, Y. Saito, H. Tauchi, K. Komatsu, Histone chaperone FACT regulates homologous recombination by chromatin remodeling through interaction with RNF20, J. Cell. Sci. 127 (2014) 763–772.

[113] A.T. Yarnell, S. Oh, D. Reinberg, S.J. Lippard, Interaction of FACT, SSRP1, and the high mobility group (HMG) domain of SSRP1 with DNA damaged by the anticancer drug cisplatin, J. Biol. Chem. 276 (2001) 25736–25741.

[114] S. Piquet, F. Le Parc, S.K. Bai, O. Chevallier, S. Adam, S.E. Polo, The histone chaperone FACT coordinates H2A.X-Dependent signaling and repair of DNA damage, Mol. Cell 72 (2018) 888–901 e887.

[115] D.M. Keller, H. Lu, p53 serine 392 phosphorylation increases after UV through induction of the assembly of the CK2.hSPT16.SSRP1 complex, J. Biol. Chem. 277 (2002) 50206–50213.

[116] J. Yang, X. Zhang, J. Feng, H. Leng, S. Li, J. Xiao, S. Liu, Z. Xu, J. Xu, D. Li, Z. Wang, J. Wang, Q. Li, The histone chaperone FACT contributes to DNA replication-coupled nucleosome assembly, Cell Rep. 16 (2016) 3414.

[117] K. Heo, H. Kim, S.H. Choi, J. Choi, K. Kim, J. Gu, M.R. Lieber, A.S. Yang, W. An, FACT-mediated exchange of histone variant H2AX regulated by phosphorylation of H2AX and ADP-ribosylation of Spt16, Mol. Cell 30 (2008) 86–97.

[118] J.L. Charles Richard, M.S. Shukla, H. Menoni, K. Ouararhni, I.N. Lone, Y. Roulland, C. Papin, E. Ben Simon, T. Kundu, A. Hamiche, D. Angelov, S. Dimitrov, FACT assists base excision repair by boosting the remodeling activity of RSC, PLoS Genet. 12 (2016) e1006221.

[119] C.A. Bewley, A.M. Gronenborn, G.M. Clore, Minor groove-binding architectural proteins: structure, function, and DNA recognition, Annu. Rev. Biophys. Biomol. Struct. 27 (1998) 105–131.

[120] M. Gariglio, G.G. Ying, L. Hertel, M. Gaboli, R.G. Clerc, S. Landolfo, The high-mobility group protein T160 binds to both linear and cruciform DNA and mediates DNA bending as determined by ring closure, Exp. Cell Res. 236 (1997) 472–481.

[121] S.L. Bruhn, D.E. Housman, S.J. Lippard, Isolation and characterization of cDNA clones encoding the Drosophila homolog of the HMG-box SSRP family that recognizes specific DNA structures, Nucleic Acids Res. 21 (1993) 1643–1646.

[122] E. Nesher, A. Safina, I. Aljahdali, S. Portwood, E.S. Wang, I. Koman, J. Wang, K.V. Gurova, Role of chromatin damage and chromatin trapping of FACT in mediating the anticancer cytotoxicity of DNA-Binding small-molecule drugs, Cancer Res. 78 (2018) 1431–1443.

[123] A. Safina, P. Cheney, M. Pal, L. Brodsky, A. Ivanov, K. Kirsanov, E. Lesovaya, D. Naberezhnov, E. Nesher, I. Koman, D. Wang, J. Wang, M. Yakubovskaya, D. Winkler, K. Gurova, FACT is a sensor of DNA torsional stress in eukaryotic cells, Nucleic Acids Res. 45 (2017) 1925–1945.

[124] H. Garcia, D. Fleyshman, K. Kolesnikova, A. Safina, M. Commane, G. Paszkiewicz, A. Omelian, C. Morrison, K. Gurova, Expression of FACT in mammalian tissues suggests its role in maintaining of undifferentiated state of cells, Oncotarget 2 (2011) 783–796.

[125] M.E. Hudson, I. Pozdnyakova, K. Haines, G. Mor, M. Snyder, Identification of differentially expressed proteins in ovarian cancer using high-density protein microarrays, Proc. Natl. Acad. Sci. U. S. A. 104 (2007) 17494–17499.

[126] I.E. Koman, M. Commane, G. Paszkiewicz, B. Hoonjan, S. Pal, A. Safina, I. Toshkov, A.A. Purmal, D. Wang, S. Liu, C. Morrison, A.V. Gudkov, K.V. Gurova, Targeting FACT complex suppresses mammary tumorigenesis in Her2/neu transgenic mice, Cancer Prev. Res. Phila. (Phila. Pa) 5 (2012) 1025–1035.

[127] D. Fleyshman, L. Prendergast, A. Safina, G. Paszkiewicz, M. Commane, K. Morgan, K. Attwood, K. Gurova, Level of FACT defines the transcriptional landscape and aggressive phenotype of breast cancer cells, Oncotarget 8 (2017) 20525–20542.

[128] K. Attwood, D. Fleyshman, L. Prendergast, G. Paszkiewicz, A.R. Omilian, W. Bshara, K. Gurova, Prognostic value of histone chaperone FACT subunits expression in breast cancer, Breast Cancer (Dove Med Press) 9 (2017) 301–311.

[129] S. Crawford, Is it time for a new paradigm for systemic cancer treatment? Lessons from a century of cancer chemotherapy, Front. Pharmacol. 4 (2013) 68.

[130] R. Agarwal, S.B. Kaye, Ovarian cancer: strategies for overcoming resistance to chemotherapy, Nat. Rev. Cancer 3 (2003) 502–516.

[131] J. Chien, R. Kuang, C. Landen, V. Shridhar, Platinum-sensitive recurrence in ovarian cancer: the role of tumor microenvironment, Front. Oncol. 3 (2013) 251.

[132] D.B. Oien, T. Garay, S. Eckstein, J. Chien, Cisplatin and pemetrexed activate AXL and AXL inhibitor BGB324 enhances mesothelioma cell death from chemotherapy, Front. Pharmacol. 8 (2017) 970.

[133] D.B. Oien, J. Moskovitz, Genetic regulation of longevity and age-associated diseases through the methionine sulfoxide reductase system, Biochimica et biophysica acta. Molecular basis of disease (2018).

[134] A. Khurana, D. Roy, E. Kalogera, S. Mondal, X. Wen, S. He, S. Dowdy, V. Shridhar, Quinacrine promotes autophagic cell death and chemosensitivity in ovarian cancer and attenuates tumor growth, Oncotarget 6 (2015) 36354–36369.

[135] D. Jung, A. Khurana, D. Roy, E. Kalogera, J. Bakkum-Gamez, J. Chien, V. Shridhar, Quinacrine upregulates p21/p27 independent of p53 through autophagy-mediated downregulation of p62-Skp2 axis in ovarian cancer, Sci. Rep. 8 (2018) 2487.

[136] R. Preet, S. Siddharth, S.R. Satapathy, S. Das, A. Nayak, D. Das, M.D. Wyatt, C.N. Kundu, Chk1 inhibitor synergizes quinacrine mediated apoptosis in breast cancer cells by compromising the base excision repair cascade, Biochem. Pharmacol. 105 (2016) 23–33.

[137] S. Siddharth, D. Nayak, A. Nayak, S. Das, C.N. Kundu, ABT-888 and quinacrine induced apoptosis in metastatic breast cancer stem cells by inhibiting base excision repair via adenomatous polyposis coli, DNA Repair 45 (2016) 44–55.

[138] S. Das, A. Nayak, S. Siddharth, D. Nayak, S. Narayan, C.N. Kundu, TRAIL enhances quinacrine-mediated apoptosis in breast cancer cells through induction of autophagy via modulation of p21 and DR5 interactions, Cell. Oncol. (Dordr) 40 (2017) 593–607.

[139] S. Das, N. Tripathi, R. Preet, S. Siddharth, A. Nayak, P.V. Bharatam, C.N. Kundu, Quinacrine induces apoptosis in cancer cells by forming a functional bridge between TRAIL-DR5 complex and modulating the mitochondrial intrinsic cascade, Oncotarget 8 (2017) 248–267.

[140] P. Mohapatra, R. Preet, D. Das, S.R. Satapathy, T. Choudhuri, M.D. Wyatt, C.N. Kundu, Quinacrine-mediated autophagy and apoptosis in colon cancer cells is through a p53- and p21-dependent mechanism, Oncol. Res. 20 (2012) 81–91.

[141] S. Park, A.Y. Oh, J.H. Cho, M.H. Yoon, T.G. Woo, S.M. Kang, H.Y. Lee, Y.J. Jung, B.J. Park, Therapeutic effect of quinacrine, an antiprotozoan drug, by selective suppression of p-CHK1/2 in p53-Negative malignant cancers, Mol. Cancer Res. MCR 16 (2018) 935–946.

[142] R. Preet, P. Mohapatra, D. Das, S.R. Satapathy, T. Choudhuri, M.D. Wyatt, C.N. Kundu, Lycopene synergistically enhances quinacrine action to inhibit Wnt-TCF signaling in breast cancer cells through APC, Carcinogenesis 34 (2013) 277–286.

[143] W. Wang, J.N. Gallant, S.I. Katz, N.G. Dolloff, C.D. Smith, J. Abdulghani, J.E. Allen, D.T. Dicker, B. Hong, A. Navaraj, W.S. El-Deiry, Quinacrine sensitizes hepatocellular carcinoma cells to TRAIL and chemotherapeutic agents, Cancer Biol. Ther. 12 (2011) 229–238.

[144] T.S. Jani, J. DeVecchio, T. Mazumdar, A. Agyeman, J.A. Houghton, Inhibition of NF-kappaB signaling by quinacrine is cytotoxic to human colon carcinoma cell lines and is synergistic in combination with tumor necrosis factor-related apoptosis-inducing ligand (TRAIL) or oxaliplatin, J. Biol. Chem. 285 (2010) 19162–19172.

[145] H. Yan, A. Bian, X. Gao, H. Li, Z. Chen, X. Liu, Novel applications for an established antimalarial drug: tumoricidal activity of quinacrine, Future Oncol. (Lond., Engl.) 14 (2018) 1511–1520.

[146] E. Wirawan, T. Vanden Berghe, S. Lippens, P. Agostinis, P. Vandenabeele, Autophagy: for better or for worse, Cell Res. 22 (2012) 43–61.

[147] P. Bastola, D.B. Oien, M. Cooley, J. Chien, Emerging cancer Therapeutic targets in protein homeostasis, AAPS J. 20 (2018) 94.

[148] E.J. White, V. Martin, J.L. Liu, S.R. Klein, S. Piya, C. Gomez-Manzano, J. Fueyo, H. Jiang, Autophagy regulation in cancer development and therapy, Am. J. Cancer Res. 1 (2011) 362–372.

[149] C. Peracchio, O. Alabiso, G. Valente, C. Isidoro, Involvement of autophagy in ovarian cancer: a working hypothesis, J. Ovarian Res. 5 (2012) 22.

[150] R. Safaei, B.J. Larson, T.C. Cheng, M.A. Gibson, S. Otani, W. Naerdemann, S.B. Howell, Abnormal lysosomal trafficking and enhanced exosomal export of cisplatin in drug-resistant human ovarian carcinoma cells, Mol. Cancer Ther. 4 (2005) 1595–1604.

[151] H. Yu, J. Su, Y. Xu, J. Kang, H. Li, L. Zhang, H. Yi, X. Xiang, F. Liu, L. Sun, p62/SQSTM1 involved in cisplatin resistance in human ovarian cancer cells by clearing ubiquitinated proteins, Eur. J. Cancer (Oxf. Engl. 1990) 47 (2011) 1585–1594.

[152] J. Nowak, C. Archange, J. Tardivel-Lacombe, P. Pontarotti, M.J. Pebusque, M.I. Vaccaro, G. Velasco, J.C. Dagorn, J.L. Iovanna, The TP53INP2 protein is required for autophagy in mammalian cells, Mol. Biol. Cell 20 (2009) 870–881.

[153] G. Valente, F. Morani, G. Nicotra, N. Fusco, C. Peracchio, R. Titone, O. Alabiso, R. Arisio, D. Katsaros, C. Benedetto, C. Isidoro, Expression and clinical significance of the autophagy proteins BECLIN 1 and LC3 in ovarian cancer, Biomed Res. Int. 2014 (2014) 462658.

[154] L.A. Torre, F. Bray, R.L. Siegel, J. Ferlay, J. Lortet-Tieulent, A. Jemal, Global cancer statistics, 2012, CA Cancer J. Clin. 65 (2015) 87–108.

[155] Y. Wang, Q. Bi, L. Dong, X. Li, X. Ge, X. Zhang, J. Fu, D. Wu, S. Li, Quinacrine enhances cisplatin-induced cytotoxicity in four cancer cell lines, Chemotherapy 56 (2010) 127–134.

[156] B. Jing, J. Jin, R. Xiang, M. Liu, L. Yang, Y. Tong, X. Xiao, H. Lei, W. Liu, H. Xu, J. Deng, L. Zhou, Y. Wu, Vorinostat and quinacrine have synergistic effects in T-cell acute lymphoblastic leukemia through reactive oxygen species increase and mitophagy inhibition, Cell Death Dis. 9 (2018) 589.

[157] M.R. Lobo, S.C. Green, M.C. Schabel, G.Y. Gillespie, R.L. Woltjer, M.M. Pike, Quinacrine synergistically enhances the antivascular and antitumor efficacy of cediranib in intracranial mouse glioma, Neurooncology 15 (2013) 1673–1683.

[158] A. Eriksson, E. Chantzi, M. Fryknas, P. Nygren, M. Gustafsson, M. Hoglund, R. Larsson, Towards repositioning of quinacrine for treatment of acute myeloid leukemia - Promising synergies and in vivo effects, Leuk. Res. 63 (2017) 41–46.

[159] P. Bhateja, A. Dowlati, N. Sharma, Phase I study of the combination of quinacrine and erlotinib in patients with locally advanced or metastatic non small cell lung cancer, Invest. New Drugs 36 (2018) 435–441.